



UNIVERSITÀ DEGLI STUDI DI SALERNO  
DIPARTIMENTO DI MEDICINA CHIRURGIA E  
ODONTOIATRIA “SCUOLA MEDICA  
SALERNITANA”

Corso di Dottorato di Ricerca in  
Medicina Traslazionale dello Sviluppo e  
dell’Invecchiamento Attivo

XXXIII Ciclo  
Coordinatore: Prof. Palmiero Monteleone

Functional and Metabolic Brain Correlates in  
Hearing Loss and Rehabilitation

Tutor  
Ch.mo Prof. Fabrizio Esposito

Candidata  
Sara Ponticorvo  
Matr. 8800903

Anno Accademico 2020/2021



*Alla mia mamma e al mio papà*



# Summary

|   |    |
|---|----|
| <b>Summary</b>  | 9  |
| <b>Sommario</b>   | 13 |
| <b>Chapter 1</b>  | 17 |
| Auditory Perception in Humans   | 17 |
| 1.1 Introduction  | 18 |
| 1.2 Peripheral auditory pathway   | 19 |
| 1.3 Central auditory pathway  | 21 |
| 1.4 Age-related hearing loss  | 23 |
| 1.5 Presbycusis and brain   | 25 |
| 1.6 Hearing rehabilitation  | 29 |
| <b>Chapter 2</b>  | 31 |
| Cortical pattern of reduced perfusion in hearing loss revealed by ASL-MRI | 31 |
| 2.1 Introduction  | 32 |
| 2.2 Materials and Methods   | 34 |
| 2.2.1 Subjects  | 35 |
| 2.2.3 Image analysis  | 40 |
| 2.3 Results   | 45 |
| 2.3.1 Clinical data   | 45 |
| 2.3.2 Neuroimaging data   | 46 |
| 2.4 Discussion  | 53 |

|  |    |
|--|----|
| <b>Chapter 3</b>   | 65 |
| Hearing Loss in Aging: Is the Audiogram shape linked to Auditory Cortex perfusion changes? | 65 |
| 3.1 Introduction   | 66 |
| 3.2 Materials and Methods  | 68 |
| 3.2.1 Subjects   | 68 |
| 3.2.2 MRI acquisition  | 70 |
| 3.2.3 Image analysis   | 71 |
| 3.3 Results  | 73 |
| 3.4 Discussion   | 77 |
| 3.5 Conclusion   | 82 |
| <b>Chapter 4</b>   | 83 |
| Long-range Auditory Functional Connectivity in Hearing Loss and Rehabilitation             | 83 |
| 4.1 Introduction   | 84 |
| 4.2 Materials and methods  | 86 |
| 4.2.1 Subjects   | 86 |
| 4.2.2 Neuropsychological assessment  | 89 |
| 4.2.3 Audiological assessment  | 89 |
| 4.2.4 Image acquisition and preprocessing  | 90 |
| 4.2.5 CBF Image Analysis   | 94 |
| 4.2.6 Rs-fMRI Data Analysis  | 95 |
| 4.3. Results   | 96 |

|  |     |
|--|-----|
| 4.3.1 Clinical and CBF evaluation _____  | 97  |
| 4.3.2 Seed-based Functional Connectivity _____   | 101 |
| 4.4. Discussion _____  | 105 |
| 4.4.1 Regional CBF analysis _____  | 106 |
| 4.4.2 Seed-based Functional Connectivity Analysis<br>(baseline) _____  | 107 |
| 4.4.3 Seed-based Functional Connectivity Analysis<br>(follow-up) _____   | 110 |
| 4.4.5 Study limitations _____  | 112 |
| 4.5. Conclusions _____   | 113 |
| <b>Chapter 5</b> _____   | 115 |
| Neuropsychological profile of hearing-impaired patients<br>and the effect of hearing aid on cognitive functions_ | 115 |
| 5.1 Introduction _____   | 116 |
| 5.2 Material and Methods _____   | 117 |
| 5.2.1 Patients _____   | 117 |
| 5.2.2 Statistical Analysis _____   | 119 |
| 5.3 Results _____  | 120 |
| 5.3.1 Comparison between NH and HL subjects  | 120 |
| 5.3.2 Comparison of patients with and without<br>hearing aids _____  | 122 |
| 5.4 Discussion _____   | 124 |
| 5.4.1 Comparison between healthy subjects and<br>HL-patients _____   | 124 |

|   |     |
|---|-----|
| 5.4.2 Comparison of patients with and without hearing aid _____ | 127 |
| <b>Chapter 6</b> _____  | 130 |
| Conclusions _____   | 130 |
| <b>Bibliography</b> _____                                       | 133 |
| <b>Akwnoledgeмент</b> _____                                     | 169 |

# Summary

The human auditory system serves the role of extracting information from objects in the environment engaging in analyses of the auditory world so that the listener can accomplish the goal of learning and communication. Several shreds of evidence demonstrate that disorders of one part of the auditory system often affect the function of other parts of it. This is especially apparent with regard to hyperactive disorders, but even noise-induced and age-related hearing loss (ARHL) are not isolated cochlear phenomena, but the auditory nervous system, in its different stages, is involved in these pathologic states, and consequently it is no longer valid the sharp division of disorders into peripheral and central. ARHL is one of the most common chronic health conditions affecting older adults and its high prevalence compels different research fields from audiologists, otolaryngologists, to neuroscientists, dedicated to understand the different mechanisms underlying this disorder and so that effective prevention, intervention, and rehabilitative strategies can be developed to ameliorate the quality of life of people affected. Historically, the impetus for investigations of ARHL was Professor Schuknecht's description in 1974, whose observations have underscored that ARHL is a complex phenomenon manifested in different forms among individuals. Today investigators recognize that hearing ability in advancing age results from a combination of different factors and that there is an

association with cognitive-related process disruption and brain alteration, hypothesizing the presence of a link between ARHL, cognitive impairment, and dementia. The sole possible rehabilitation process, in case of hearing deficit, is the use of a hearing aid, a device whose only charge is the amplification of the auditory input into the ear canal, but whose daily and prolonged usage and its interaction and effects on the multifactorial nature of the pathology are still unclear.

In this context, the aim of the research project reported in this thesis is the investigation about ARHL signs on the central nervous system, with additional attention to the effects of auditory rehabilitation with prolonged and continuous hearing aids usage during normal daily life. In order to address these issues, magnetic resonance imaging (MRI) was used to study the human brain in vivo and non-invasively, since it was already widely applied for the study of neurological and psychiatric disorders as well as to understand the basis of neural physiological processes and sensory perception. The first aim of this work is concentrated on the neural modification linked to ARHL in the primary auditory cortex, the entry point of the auditory signal in the central nervous system. For this purpose, in chapter 2 and chapter 3 the attention is dedicated to the analysis of the human primary auditory cortex in ARHL patients using innovative MRI methodologies to map the basal metabolic neuronal activity. Indeed, brain images of a group of ARHL patients and age- and sex-matched healthy normal hearing controls have been acquired to analyze the cerebral metabolic changes and to possible link those to the

pathological course. A local cortical hypometabolic pattern is revealed in the right primary auditory cortex that was found to be related to the audiogram steepness, that is, the difference in hearing loss relative to adjacent frequencies. Therefore, these new pieces of information were used to classify the different types of presbycusis and their relationship to different local cortical metabolic patterns in auditory cortex consequently showing how a classification based on multiple audiological features can individuate groups of patients with different hypometabolic cortical pattern and possibly different pathological etiology.

Then the second aim, presented in chapter 4 and chapter 5, is to expand the point of view from the local perspective to a more global view (on the entire brain) in a dual way: (i) combining the metabolic information with a whole brain functional connectivity analysis, to explore if and how the localized hypometabolic pattern in primary auditory cortex influences the global brain connectivity or drag a general reallocation of resources and a functional brain reorganization and (ii) using a longitudinal experimental framework, explore how all those brain changes interact when ARHL patients follow a rehabilitation period with continuous usage of hearing aids devices with an additional focus on the neuropsychological profile. In this case, the impact of HL condition (and its subsequent hearing aids mediated rehabilitation) was highlighted on the long-range neural communication between the primary auditory cortex and higher-order brain regions, suggesting that the hypoperfused early auditory cortex could be a seed place where different neuroplastic

changes originate. Together with the functional and metabolic analysis, the neuropsychological evaluation underlies the presence of an executive and attentional impairment in HL population. Therefore, it was proved for the first time, that the prolonged use of hearing aid devices, is not able to reverse the reduced activity in the primary sensory cortex, but can cause a global functional reorganization especially concentrated in the communication between the primary sensory centers and multimodal key areas of the frontal and temporal lobes as well as an improvement in visuo-spatial abilities only in patients whose hearing deficit is limited.

# Sommario

Il ruolo del sistema uditivo negli umani è quello di estrarre informazioni dall'ambiente circostante per fornire all'ascoltatore indicazioni per un'analisi del "mondo uditivo", allo scopo di imparare e comunicare. Numerose evidenze scientifiche dimostrano che un parziale malfunzionamento del sistema uditivo può avere effetto e coinvolgere funzioni svolte da altre parti di esso. Questo è osservabile in particolare nei disordini dovuti ad iperattività (i.e. acufeni), ma risulta essere altrettanto vero in caso di perdite uditive (generalmente o parziali) causate da eccessiva esposizione al rumore o legate all'invecchiamento, che in tal modo risultano essere fenomeni non unicamente legati ad un danno cocleare periferico ma piuttosto risultano coinvolgere l'intero sistema nervoso uditivo (nei suoi differenti livelli), tanto da rendere sempre meno netta la suddivisione tra patologie periferiche e centrali. L'ipoacusia dovuta all'invecchiamento (o presbiacusia) è una delle più comuni patologie degli anziani e la sua alta diffusione coinvolge attivamente differenti (e normalmente distanti) ambiti di ricerca e personalità, dagli audiologi, gli otorinolaringoiatri ai neuroscienziati, tutti dedicati alla comprensione dei diversi meccanismi coinvolti e con lo scopo di sviluppare effettive misure di prevenzione, intervento e riabilitazione per migliorare la qualità della vita delle persone affette da questo disturbo. Storicamente l'impulso allo studio approfondito della presbiacusia parte dalla descrizione fattane dal Professor

Schuknecht nel 1974, le cui osservazioni sottolineavano la complessità del fenomeno che si manifestava in forme diverse tra le persone. Oggi, gli esperti del settore riconoscono che le capacità uditive degli anziani derivano dalla combinazione di diversi fattori e che sicuramente esiste una associazione con il degrado dei processi cognitivi e delle alterazioni cerebrali, ipotizzando la presenza di un legame tra presbiacusia, declino cognitivo e demenza. L'unico processo di riabilitazione in caso di presbiacusia è l'utilizzo di una protesi uditiva, un dispositivo il cui esclusivo compito è quello di amplificare l'input sonoro all'interno del canale uditivo, ma le cui implicazioni, date da un utilizzo giornaliero e prolungato, sulla multifattorialità del disturbo sono ad oggi poco chiare.

In questo contesto, lo scopo di questo progetto di ricerca, riportato in questa tesi, è analizzare i segni di presbiacusia nel sistema nervoso centrale con una attenzione aggiuntiva agli effetti dell'utilizzo giornaliero e prolungato di protesi uditive. A questo scopo, viene suggerito l'utilizzo dell'imaging con risonanza magnetica (MRI) per studiare il cervello umano in-vivo e in modo non invasivo, considerando anche il largo utilizzo di questo strumento per lo studio di patologie neurologiche e psichiatriche, così come l'utilizzo per la ricerca di base nel capire i processi neurali fisiologici e legati alla percezione sensoriale. Il primo scopo di questo lavoro è dunque concentrato sull'analisi delle eventuali alterazioni neurali, legate alla presbiacusia e localizzate nella corteccia uditiva primaria, il punto di ingresso del segnale uditivo all'interno del sistema nervoso centrale. A questo scopo

nei capitoli 2 e 3 l'attenzione è concentrata sull'analisi della corteccia uditiva primaria umana in pazienti presbiacusici con l'utilizzo di una metodica di MRI avanzata che permette la quantificazione del metabolismo neuronale basale. Per cui, le immagini cerebrali di un gruppo di pazienti con presbiacusia e di controlli normo-udenti, in media non differenti in età e sesso, sono state acquisite per rilevare eventuali differenze in termini di metabolismo cerebrale e per associare questi cambiamenti al decorso patologico. I risultati hanno mostrato un locale ipometabolismo corticale localizzato nella corteccia uditiva primaria dell'emisfero di destra, che risulta essere correlato alla caratteristica audiologica di steepness, ossia la differenza di perdita uditiva tra due frequenze adiacenti. Visto le differenti manifestazioni cliniche di presbiacusia, questo primo risultato è stato poi utilizzato per classificare le diverse tipologie di pazienti in relazione alla diversa tipologia di pattern ipometabolico della corteccia uditiva primaria ed è stato mostrato come una classificazione basata su più caratteristiche audiologiche riesca ad individuare gruppi con diversi pattern di ipometabolismo corticale e probabilmente con patologie a differente eziologia.

Il secondo scopo, esposto nei capito 4 e 5 è quello di espandere il punto di vista da una prospettiva locale ad una globale (sull'intero sistema nervoso centrale) in due modalità: (i) combinando l'informazione metabolica con un'analisi di connettività funzionale (sull'intero cervello), al fine di esplorare se e come il pattern di ipometabolismo locale nella corteccia uditiva primaria influenza la

connettività cerebrale o stimola una riallocazione di risorse e una riorganizzazione funzionale e (ii) utilizzando un protocollo sperimentale longitudinale, esplorare come questi cambiamenti cerebrali interagiscono quando un paziente con presbiacusia segue una riabilitazione con utilizzo giornaliero e continuo di protesi uditive, con un focus addizionale sul profilo neuropsicologico. In questo caso è stato evidenziato l'impatto della condizione di presbiacusia nella comunicazione neurale ad ampio raggio tra la corteccia uditiva primaria e regioni normalmente dedicate a funzionalità di alto livello, suggerendo così che la ipoperfusione delle aree uditive primarie può essere considerata un punto di partenza, da cui hanno origine differenti tipologie di modificazioni neuroplastiche. Insieme ai cambiamenti riscontrati in termini di metabolismo e funzionalità cerebrale, le analisi neuropsicologiche hanno evidenziato un malfunzionamento nelle abilità esecutive ed attentive in pazienti presbiacusici. L'utilizzo prolungato di protesi uditive ha mostrato non causare una inversione della ipoattività della corteccia sensoriale primaria ma una riorganizzazione globale funzionale specialmente concentrata nell'alterazione della comunicazione tra i centri sensoriali primari e delle aree multimodali del lobo frontale e temporale e un concomitante, nei soli pazienti con un danno uditivo contenuto, miglioramento delle abilità visuo-spaziali.

# **Chapter 1**

## Auditory Perception in Humans

## 1.1 Introduction

The human auditory system serves the role of extracting information from objects in the environment so that the listener can accomplish the goal of learning and communication. The complexity of auditory processing derives from the need of the auditory system to localize, analyze, and interpret a sound that will be processed by the individuals through the simultaneous integration with other sensory stimuli. For a sound to be perceived it needs to travel to, and be processed by, higher-order regions in the cerebral cortex, specifically the primary auditory area and through bottom-up and top-down signaling pathways, relaying to other areas of the cerebral cortex and lower brainstem to make meaning of the information, as well as, integrate auditory and other sensory stimuli.

The first part of this complex phenomenon, namely the transmission from the environment to the central nervous system of auditory signals, occurs in a series of analysis stages that can be resumed as three big steps: (i) the transmission of acoustic waves through the external and middle ear, (ii) the reception and conversion of acoustic waves into electric impulses of the auditory nerve fibers in the inner ear (iii) auditory processing of the electric impulses in the central parts of the auditory pathway. The first two steps involve a peripheral auditory mechanism devoted to encoding sound and to the transduction of mechanical sound waves, in the form of vibrations of the propagation medium, into nerve impulses that are perceived and elaborated in the third step by the central

subcortical (auditory nerve, cochlear nuclei, midbrain, thalamus) and cortical (primary auditory cortex located in the bilateral Heschl's gyrus) auditory pathway. The central auditory pathway, in fact, extends from the medulla in the brainstem to the cerebral cortex consisting of a series of nuclei connected by fiber tracts of axons. This complex chain of nerve cells helps to process and relay auditory information, encoded in the form of nerve impulses, directly to the highest cerebral levels in the cortex. To some extent different properties of the auditory stimulus are conveyed along distinct parallel pathways, a method to separately analyze different properties of the single auditory stimulus.

## 1.2 Peripheral auditory pathway

The peripheral portion of the human auditory organ is composed of three parts: external ear, middle ear, and inner ear (Figure 1A). Acoustic waves are gathered by the concha, transmitted through the external ear canal, and amplified in the middle ear by the movement of three ossicles (malleus, incus, and stapes). The vibration of the stapes is converted to inner-ear fluid movement in its anterior-lower part, named the cochlea. The cochlea has the shape of a snail shell, with two and a half turns, and it is the place where sensory cells are located. The cochlea serves the double task of transducing sound from mechanical vibration into a code of neural impulses for the auditory nerve and of preparing the sounds for further processing in the auditory nervous system performing a

first signal analysis. Indeed, the basilar membrane, the narrow membrane at the base of the cochlea that lies near the organ of Corti, is organized tonotopically, which means that every sound frequency is analyzed in a strictly defined place. Particularly, the high frequencies sounds are analyzed in the basilar turn of the cochlea, while the low frequencies sounds are analyzed in the apical part of the cochlea. The organ of Corti, that perceives the traveling wave caused by the movement of the fluid inside the cochlea, is the location of the sensory cells, called hair cells that are organized in one row of inner hair cells, and three rows of outer hair cells. The deflection of hair cells triggers a cascade of processes eventually resulting in a release of the neurotransmitter (glutamate) into the synapse, and activation of the auditory nerve fibers. The frequency selectivity starts in the cochlea and continues in the individual nerve fibers; in fact, fibers innervating the high-frequency base of the cochlea are tuned to receive high frequencies, while those innervating the apex are tuned to low frequencies.

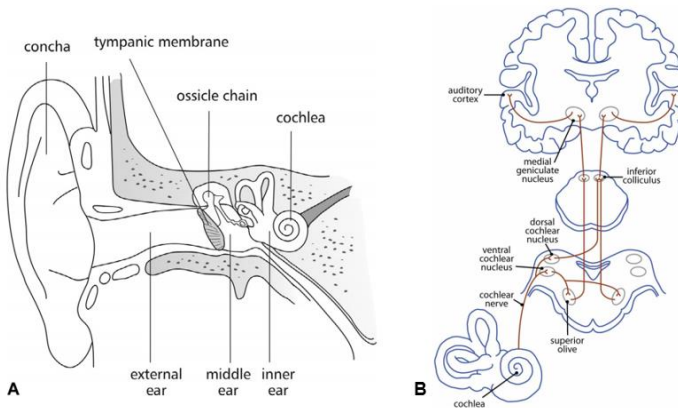


Figure 1 (A) Peripheral auditory pathway (Sliwinska-Kowalska, 2015) and (B) Central auditory pathway (Butler & Lomber, 2013).

### 1.3 Central auditory pathway

The auditory nerve terminates in the cochlear nucleus (Jones & Casseday, 1979), which is the first relay nucleus of the nervous part of the ascending auditory pathways (Figure 1B). It is located in the lower brainstem, at the pontomedullary junction on the same side as the ear from which it receives its innervations (Young & Oertel, 2004). In the cochlear nucleus, fibers of the auditory nerve contact neurons forming multiple and parallel representations of the acoustic signal. Each parallel pathway performs a different analysis of the auditory signal, thus operations like the localization of a sound source in space or the identification of a sound are separated in parallel processing in cochlear nucleus.

The cochlear nucleus anteroventral division is then the origin of pathways to the medial and lateral superior olivary complex thus the first group of nuclei that integrate information from both ears. Other pathways originate in the cochlear nucleus but bypass the superior olivary complex and cross the brain stem to terminate in the nuclei of the contralateral inferior colliculus. All the fibers of the inferior colliculus project to the ipsilateral medial geniculate body (MGB), the thalamic auditory nucleus. Whereas early views of the MGB identified it as a simple 'gateway' to the cortex, numerous studies have demonstrated that thalamic neurons in the MGB actively and dynamically shape the auditory representations that reach the cerebral cortex (Bartlett, 2013). Projections from the MGB proceed then to the primary auditory cortex (PAC) (Kaas & Hackett, 2000) located in humans along the Heschl's gyrus (HG), running from the superior temporal gyrus into the lateral sulcus. The central PAC area (core region) presents a tonotopic organization in stimuli processing with a continuous representation of frequency in a mirror symmetry along the rostral-caudal direction (Formisano et al., 2003). The central core region is surrounded by a belt region that is subsequently surrounded by a parabelt region. Each of these regions differs based on its cellular architecture, response to stimuli, as well as their input and output pathways (Hackett, 2015; Mangold & M Das, 2020). The major inputs to the core area came from the MGB, then serial connections proceed to the belt region, to finally the parabelt region. The belt and parabelt regions form connections to various auditory associated regions in the

cortex which receive complex signals from multiple sources, integrate them and provide meaningful information that can be relayed to other areas (Hackett, 2015; Musiek, 1986). Each PAC has connections with areas within the same cerebral hemisphere as well as between cerebral hemispheres. The main associated auditory areas that receive projections from the primary auditory cortex are regions of the superior temporal lobe surrounding HG, inferior parietal lobe, inferior-posterior frontal lobe, insula, amygdala, and basal ganglia. The destination of the outputs from the primary auditory cortex determines what higher-order and more complex cognitive functions take place with the incoming acoustic information. For example, auditory information traveling to the amygdala has profound impacts on the emotional and behavioral response of an individual, whereas information destined for the premotor cortex will be utilized for planning and controlling speech (Hackett, 2015; Musiek, 1986).

## 1.4 Age-related hearing loss

Around 466 million people worldwide have disabling hearing loss, and it is estimated that by 2050 over 900 million people will have disabling hearing loss (World Health Organization, 2020). Hearing loss may result from genetic causes, complications at birth, certain infectious diseases, chronic ear infections, use of drugs, exposure to excessive noise, and aging. In the latter case the World Health Organization estimates that in 2025, there will be

more than 500 million individuals who will suffer significant impairment from hearing loss related to aging. Age-related hearing loss (ARHL) or presbycusis manifests itself as a gradually progressive bilateral symmetrical hearing loss that prevalently affects mild to high frequencies (2–8 kHz). The entire phenomenon is characterized by audiometric threshold shift, but also degradation in speech understanding, and speech-perception difficulties in adverse listening conditions such as reverberant and noisy environments or speech in noise (Gates & Mills, 2005; Howarth & Shone, 2006; Lee, 2013).

The ARHL is traditionally considered caused by the loss of hair cells in the basal portion of the cochlea (Engle et al., 2013; Ramadan & Schuknecht, 1989; H. F. Schuknecht, 1955, 1964; H. F. Schuknecht & Gacek, 1993), particularly, outer hair cells are affected most and the changes begin in the basal end of the cochlea, spreading toward the apex as the condition progresses. However, the pathophysiology is not unique but can be different among different people and the first systematic analysis on ARHL is attributable to professor Schuknecht in 1974. In his seminal work professor Schuknecht (Harold F. Schuknecht, 1993) described four main types (excluding the mixed forms) of human presbycusis: (1) sensory, mainly affecting the cochlear hair cells and supporting cells, (2) neural, characterized by the loss of neurons in the cochlea, (3) metabolic, with atrophy of the stria vascularis (the secretory tissue in the lateral wall of the cochlear duct) and (4) mechanical, with the stiffening of the basilar membrane and organ of Corti. Different

types of presbycusis are found to manifest with different types of loss and then different audiogram shapes. Considering, the two most common forms, sensorial and metabolic, the former is characterized by down-sloping pure tone audiogram, while the latter presents a pantonal audiogram shape.

Yet, perception of sounds is a complex process comprising not only the inner ear but also all the nuclei of the auditory pathway and the cerebral auditory cortex as well as the interaction of the auditory cortex with other parts of the brain. In this context, it is evident that the quality of hearing depends not only on the state of the peripheral receptors but also on the integrity of the central auditory system so that any limitations in the number of receptors or their quality must influence the functions of the central auditory system (linked to a diminished input) but the central auditory system can also have its pathological evolution in terms of morphological and physiological changes induced by the biological effects of aging.

## 1.5 Presbycusis and brain

Age-related hearing deficits for most people remain a relatively unremarkable part of the aging process, but some individuals experience effort and difficulties in understanding speech, hindering communication, and socialization (Cardin, 2016). The increased listening effort may lead older adults to avoid social interaction, exacerbating loneliness and depression, and reducing

the quality of life (Rutherford et al., 2018). Recent research further shows that hearing loss is associated with cognitive decline and dementia (Livingston et al., 2017; Uchida et al., 2019). In fact, extensive pieces of evidence link midlife hearing loss to the more rapid progression of cognitive decline (Davis et al., 2016; Fortunato et al., 2016; Golub, 2017) supporting the hypothesis of an important brain involvement in the pathophysiology of ARHL. Essentially, studies examining the association between ARHL and cognitive impairment or dementia date back to at least the 1980s, but the type of association between these two phenomena is still nowadays not clear. Two possible scenarios have been proposed (Golub, 2017): a causal scenario, where ARHL causes (or increases the risk of) cognitive impairment, directly or indirectly affecting brain integrity and influencing normal brain cognition interfering in the quality of life, socialization and cognition, or decreasing the brain resources intended for understanding processes since the increased effort in the decoding stage (Tun et al., 2009).

Alternately in another type of scenario (the non-causal scenario), we can postulate that ARHL does not induce cognitive impairment, instead, there is a common etiology for the two, for example, a microvascular disease might cause ischemic injury to the cochlea and also ischemic injury to neural tissue involved in cognition.

Due to the lack of clear evidence, we are not able to individuate which of the two scenarios is true but in recent years numerous studies have focused on analyzing possible brain damages caused/linked to ARHL using

various neuroimaging methodologies. In particular, magnetic resonance imaging (MRI) is a multimodal and noninvasive tool that allows for morphological, metabolic, and functional brain monitoring and analysis. In this sense, functional analyses have investigated both the brain response to a stimulus (task-based fMRI) and the global brain connections at rest (resting-state fMRI) and its eventual pathological-related alteration in brain function of ARHL patients.

Evidence indicates that older adults with hearing loss show a series of changes in the PAC. For example, diminished grey matter (GM) volume in the primary auditory cortex was revealed in ARHL population (Alfandari et al., 2018; Husain et al., 2011; Peelle et al., 2011; Qi et al., 2019; Ren et al., 2018) and eventually linked to the level of hearing loss (HL) expressed using audiometric thresholds. One longitudinal study, with a relatively long follow-up time (~6.4 years) has been carried out providing evidence to support the idea of a causal relationship between ARHL and neural atrophy and underling the main effect concentrated in the right hemisphere (F. R. Lin et al., 2014).

Changes in white matter (WM) integrity has also been observed in middle-aged and older adults with mild to moderate hearing loss (Husain et al., 2011) and in a large dataset of elderly with moderate to severe hearing loss (Croll et al., 2020) in auditory-related areas.

Some studies have also investigated baseline neuronal metabolism using quantitative measures such as <sup>18</sup>F-fluro-deoxyglucose PET, and particularly, Verger et al. (2017) have revealed a specific pattern of decreased

regional cerebral blood flow (CBF) in the associative auditory cortex of deaf patients (mainly in the right hemisphere).

In addition to structural and metabolic changes, older adults with clinically hearing loss also display functional differences in auditory processing as revealed by fMRI studies compared to both age-matched and younger normal hearing controls. Regarding the task-based activity in response to an auditory stimulation, Profant and colleagues (Profant et al., 2015) show increased activity in the auditory cortex related to aging, even if it is not related to the hearing status. On the other hand, task-free brain activity, as measured by local parameters as regional homogeneity (ReHo) and amplitude of low-frequency fluctuations (ALFF), was found locally altered in hearing loss patients in auditory centers (Y.-C. Chen et al., 2018).

However, the perception, and, particularly, the comprehension of auditory information is strongly dependent on the integration among various brain areas. Studies have found important differences in functional connectivity among brain areas involved in auditory processing in older adults with ARHL. Specifically, findings show reduced connectivity between visual and auditory sensory cortices in ARHL (Liu et al., 2015; Puschmann & Thiel, 2016), as well as in non-sensory related brain areas such as the attention and default mode networks (Husain et al., 2014; Schmidt et al., 2013).

## 1.6 Hearing rehabilitation

Given the association between hearing loss and brain damage and/or increased rate of cognitive decline, there has been developing interest in the possible effects of hearing loss rehabilitation through hearing aids. A hearing aid is simply a microphone: sound waves strike into it, they are amplified and 'piped' into the external ear canal. The acoustic energy delivered to the ear is always greater than that received by the microphone and the battery provides the additional energy needed for the amplification.

Current research demonstrates the advantages of hearing amplification devices in at least partially restoring hearing ability and improving overall cognitive performance in older adults (Cherko et al., 2016). Several large studies show these benefits in the elderly population, with reported improvements in quality of life, general health, mental health (Boi et al., 2012), social and emotional function (Boi et al., 2012; C.D. Mulrow et al., 1992; Cynthia D. Mulrow et al., 1990; Vuorialho et al., 2006) and symptoms of depression (Cacciatore et al., 1999; Cherko et al., 2016). Recently Deal and colleagues (Deal et al., 2017) found a contribution of hearing aids in reducing the risk of dementia (even if the result did not achieve statistical significance). Few longitudinal studies have analyzed the long-term effects of daily hearing aid usage in ARHL and some of those showed unclear results. For example, hearing aid use was associated with slightly lower rates of cognitive decline and risk of incident cognitive impairment, but the results were not

statistically significant (Lee, 2013). Over a 25 years follow-up a difference was revealed in the rate of change in cognitive performances between participants with hearing loss not using hearing aids and controls but not between ARHL subjects using hearing aids and normal hearing controls (Amieva et al., 2015). Finally, at 18 months follow-up after hearing aid fitting, speech perception in quiet, listening disability, quality of life and executive functions had significantly improved in a group ARHL elderly (Sarant et al., 2020). From the neuroimaging perspective, only one study has characterized the brain changes linked to hearing aid usage by now, showing an increased fMRI activity in auditory, language, and multimodal areas in HA users using a task-based experimental design (Pereira-Jorge et al., 2018).

# Chapter 2

## Cortical pattern of reduced perfusion in hearing loss revealed by ASL-MRI

**Ponticorvo, S.**, Manara, R., Pfeuffer, J., Capiello, A., Cuoco, S., Pellecchia, M. T., Saponiero, R., Troisi, D., Cassandro, C., John, M., Scarpa, A., Cassandro, E., Di Salle, F., & Esposito, F. (2019). *Human brain mapping*, 40(8), 2475–2487.  
<https://doi.org/10.1002/hbm.24538>

## 2.1 Introduction

Pathological changes associated with HL are mainly observed in the auditory periphery, as HL typically presents an irreversible loss of sensory hair cells and neurons in the cochlea (Huang & Tang, 2010; Kidd & Bao, 2012; H. F. Schuknecht & Gacek, 1993). However, concomitant functional and structural changes along the central auditory pathway and in the cerebral cortex have been repeatedly reported in HL populations.

Recently, using  $^{18}\text{F}$ -fluro-deoxyglucose positron Emission Tomography (PET), Verger et al. (2017) have revealed a specific pattern of decreased regional cerebral blood flow (CBF), a quantitative measure of baseline neuronal metabolism, in the associative auditory cortex of HL patients (mainly in the right hemisphere). While HL is frequently caused by accumulated noise and ototoxic experiences that produce a loss of sensory cells in the cochlea (Kurabi et al., 2017), a possible reduction in the regional CBF in the auditory cortex may also indicate the presence of a vascular dysfunction, which could lead itself to neuronal deficits. In fact, because CBF is regulated according to local neuronal activity and metabolism (i.e., neurovascular coupling; Iadecola, 2017), if CBF deficiency is prior to neurodegeneration, a reduced CBF in the central auditory system of HL patients could be linked to a reduced dilatory capacity of cerebral vasculature in upregulating perfusion, with an increased risk for vascular disease and a higher vulnerability for neurological disorders in aging (Gao et al., 2013).

In the light of these evidences, it has become of outmost importance to search for functional alterations of the auditory “baseline” activation as possible early functional markers of central damage associated with HL, and to link these signs with structural and audiological measures as well as other clinical signs of neuronal degeneration. Although PET imaging provides the clinical gold standard for the absolute quantification of regional brain metabolism at baseline, analogous regional CBF images can be nowadays acquired, even during routine MRI examinations, using arterial spin labeling (ASL) techniques (Alsop et al., 2015; Detre et al., 2012; Telischak et al., 2015). Differently from PET, which requires the injection of radioactive tracers, ASL-MRI uses arterial blood water as an endogenous tracer to provide regional CBF (perfusion) measurements over the whole brain on a voxel-by-voxel basis at the same spatial resolution of BOLD-fMRI, yielding an alternative fMRI marker of the baseline neuronal metabolism of brain tissues (Telischak et al., 2015). Moreover, compared to BOLD-fMRI contrast, regional CBF mapping with ASL-MRI has a higher spatial specificity for baseline neural activity and, similar to PET, allows an absolute quantification of this parameter (J. J. Chen et al., 2015), which makes it well suited to detect early changes in neuronal function without any specific stimulation applied. For example, using ASL-MRI, Chao et al. (2010) have shown that brain hypoperfusion can predict clinical, functional, and cognitive decline, and is therefore particularly useful for an early detection of the presence of a neurodegenerative disease. Moreover, even without

any external specific acoustic stimulation (apart from the intrinsic acoustic stimulation provided by MRI scanner noise), and using the pseudocontinuous ASL (PCASL) variant, Gardumi et al. (2017) have nicely delineated an extended high-perfusion signal in the human primary auditory cortex of NH subjects, suggesting that the primary sensory areas of the auditory cortex are likely characterized by a relatively high density of microvascularization, which could in principle make the PCASL technique particularly sensitive to detect early HL-related functional changes in the primary auditory cortex. At present, due to its higher labeling efficiency, the PCASL is also the recommended ASL implementation for clinical studies (Alsop et al., 2015; Dolui et al., 2017) and can be suitably combined with a 3D readout acquisition scheme (3D-PCASL) to achieve optimal signal-to-noise ratio performances (Vidorreta et al., 2013).

The main purpose of this study was to investigate the possible relation between an early diagnosed HL condition (i.e., first symptoms reported in the first audiological examination dated back to less than a few months) and baseline perfusion of the brain. Using a clinical implementation of the 3D-PCASL on a 3T MRI scanner, the regional CBF was assessed in a group of HL patients and NH controls and the obtained perfusion measurements were related to structural MRI and audiological parameters.

## 2.2 Materials and Methods

### 2.2.1 Subjects

Thirty-one HL patients (age mean = 63.4, SD = 8.4 years, range = 47–77; 20 males) were enrolled in the study without randomization. All patients involved were at the stage of their first clinical diagnosis of HL. All of them were complaining about hypoacusia since a few months or less. None of them used hearing aids before taking part in the study. HL was evaluated with pure-tone audiometry (Davies, 2016) and audiometric thresholds for air conduction were obtained at the frequencies of 0.25, 0.5, 1, 2, 4, and 8 kHz. The measurements were carried out in a soundproof chamber using a clinical audiometer. The audiogram curves with the full frequency characterization of each patient are shown in Figure 2.1a. PTA was calculated as recommended for the classification of HLs by The Bureau International d'Audiophonologie (BIAP, 2005) for 0.5, 1, 2, and 4 kHz ([www.biap.org](http://www.biap.org)). The mean PTA of the enrolled HL patients was  $55.5 \pm 11.1$  dB in the right ear and  $53.4 \pm 10.9$  dB in the left ear. The “steepness” of the audiogram in (dB/octave) was computed for each pair of adjacent frequencies as the difference in hearing level (measured in dB) divided by the frequency difference (measured in octaves; (Koenig et al., 2006):

$$S(i) = \frac{HT(f_{i+1}) - HT(f_i)}{\log_2 f_{i+1} - \log_2 f_i}$$

Where  $HT(f_i)$  is the HL threshold in dB at the frequency  $f_i$  and  $f_i \in [0.25, 0.5, 1, 2, 4, 8]$  kHz and  $S(i)$  is the

steepness of the audiogram between frequency  $f_{i+1}$  and  $f_i$ .

Twenty-eight NH controls (age mean = 59.7, SD = 7.4 years, range = 48–78; nine males) and with no medical history of HL (or complain about their hearing) were included in the study. Figure 2b shows the mean audiogram curves (and SD bars) in the two groups in the right and left ear, respectively. No randomization was used. None of the subjects involved had any history of neurological and/or psychiatric disorders, surgical interventions in the ear, or MR contraindications. Subjects with a previous report of vascular dysfunction or with a history of stroke were not admitted to the study. As generalized microvascular alterations are to be anyway expected in these cohorts, a semiquantitative evaluation of white matter hyperintensities (a routinely used clinical marker of microvascular cerebral damage) was performed on the T2-weighted fluid attenuation inversion recovery (FLAIR) images of all individuals by two experienced neuroradiologists blinded to the group membership. The amount of these lesions was quantified separately for the deep and periventricular white matter on the four-stage Fazekas scale (Fazekas et al., 1987). A list of daily taken medications (for chronic disorders) was recorded from each subject, and thereby four major categories were individuated: hypertension, prostate, cholesterol, and heart medications. As even a simple caffeine consumption can substantially decrease ASL-derived global perfusion levels, and such decreased levels can persist for about 75 min from intake before returning to baseline (see, e.g., (Addicott et al., 2009;

Clement et al., 2018)), none of subjects was allowed to take caffeine (or any other medications) for at least 120 min before MRI scan. As all subjects were engaged in audiological and neuropsychological testing during the time between their arrival at the center and the start of the MRI scan, they could be closely and specifically monitored for this aspect. The possible effect of daily caffeine consumption was also controlled by asking for the estimated quantity of coffee as mean number of cups per day. All participants were submitted to the Montreal Cognitive Assessment (MOCA; (Nasreddine et al., 2005)) for screening of cognitive performances on the same day of (immediately before) the MRI examination. The study was carried out in accordance with The Code of Ethics of the World Medical Association (Declaration of Helsinki) for experiments involving humans and the local ethical committee approved the study. A written informed consent was signed by each participant before MRI acquisition. All the investigators knew the group allocation before (and during) the experiment and in performing the neuropsychological testing and the image data analyses (no blinding was done).

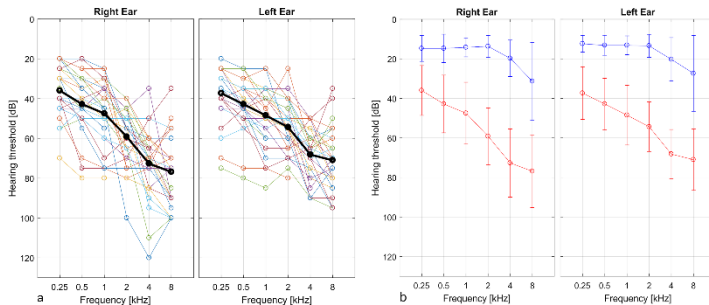


*Figure 2 (a) Hearing loss (HL) characterization of each patient in right and left ear respectively. (b) Mean and SD across HL (red) and normal hearing (NH; blue) subjects of the hearing thresholds for both ears. The thresholds were assessed at six different frequencies with pure tone audiometry.*

## 2.2.2 MRI acquisition

Brain images were acquired using a 3 T MRI scanner (Siemens MAGNETOM Skyra; Siemens Healthcare, Erlangen, Germany), equipped with a head and neck (16+4 channel) radiofrequency coil supplied by the manufacturer. The imaging protocol included the following sequences:

- 3D T1-weighted magnetization prepared rapid gradient echo (MPRAGE) sequence with repetition time (TR) = 2400 ms, echo time (TE) = 2.25 ms, resolution =  $1 \times 1 \times 1$  mm<sup>3</sup>, matrix size = 256×256, anterior–posterior phase-encoding direction, generalized autocalibrating partially parallel acquisitions (GRAPPAs) factor of 2 in phase-encoding

- direction. The MPRAGE scan was used for anatomical reference and morphometric analyses.
- A prototype 3D-PCASL sequence with TR = 4600 ms, TE = 15.6 ms, field of view 192×192 mm<sup>2</sup>; slice thickness 3 mm, resolution = 3×3×3 mm<sup>3</sup>, bolus duration 1,500 ms, postlabeling delay 1500 ms, six repetitions, M0 prescan, 42 slices, turbo factor 14, echo-planar imaging (EPI) factor 21, number of segments 6 (total acquisition time = 6 min). The 3D-PCASL sequence employs the 3D GRASE readout module and implements a pseudocontinuous labeling scheme with background suppression as described in (Dai et al., 2008, 2012; Wu et al., 2007). In each repetition of the sequence (TR), the tagging module and the EPI train causes an acoustic stimulation with a principal spectral contribution at 1 and 2 kHz (Figure 3). This series was acquired with the subject at rest with eye open.
  - 3D T2-weighted FLAIR sequence with TR = 5000 ms, TE = 387 ms, inversion time (TI) = 1800 ms, resolution = 0.6×0.6×1 mm<sup>3</sup>, matrix size = 384×384, sagittal orientation, anterior–posterior phase-encoding direction, GRAPPA factor of 2 in phase-encoding direction. The FLAIR scan was used for white matter hyperintensity analysis.

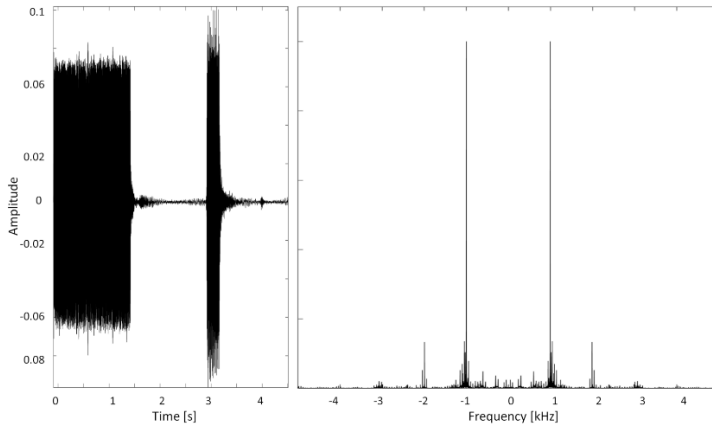


*Figure 3 3D-pseudocontinuous Arterial Spin Labeling (PCASL) acoustic stimulation in each repetition time (TR); signal in time domain (left); and frequency domain (right).*

### 2.2.3 Image analysis

Single-subject whole-brain CBF maps were calculated from the 3DPCASL raw images using the prescan M0 image and the perfusion weighted series using the calibration formula in (Alsop et al., 2015) (provided by the inline scanner software). For the group-level analysis, the single-subject CBF maps were spatially normalized using the SPM12 toolbox ([www.fil.ion.ucl.ac.uk/spm/](http://www.fil.ion.ucl.ac.uk/spm/)) running on MATLAB R2017a (The MathWorks, Inc., Natick, MA, [www.mathworks.com](http://www.mathworks.com)) to the Montreal Neurological Institute (MNI) standard template (Evans et al., 1993) using a three-step procedure: First, the control images from the 3D-PCASL series were averaged to obtain an

image with enhanced contrast, which was aligned in each subject to the corresponding anatomical 3D T1w image with an affine transformation. Second, all T1w images were segmented and normalized into a study specific template space with the nonlinear diffeomorphic DARTEL approach (John Ashburner, 2007) and then transformed to the MNI space. Third, the initial affine transformation, the DARTEL estimated nonlinear deformation fields and an isotropic 6-mm full width at half maximum (FWHM) Gaussian kernel were applied to the CBF maps of each subject. Besides CBF maps, GMV and white matter volume (WMV) maps were also obtained in the MNI space from the “unified” segmentation of T1w images (also requested by the DARTEL procedure; (J. Ashburner & Friston, 2005) by spatially smoothing (with the same isotropic 6-mm FWHM Gaussian kernel) and modulating (to compensate the effect of warping on the intensity) the spatially normalized tissue probability images in such a way to preserve the total amount of signal from each region. From this segmentation, the total intracranial volume (ICV) was also estimated for each subject using the SPM12 utility function “tissue volumes.” In addition to the absolute CBF maps, because differences in regional CBF can also be attributable to differences in tissue composition (partial volume effect), a partial volume (PV) model was also considered to separate within-voxel gray matter (GM) and white matter (WM) CBF components and to account for the spatially variable mixing of GMV and WMV at each voxel. To this purpose, a validated spatial linear regression model of GM and WM CBF components with a fixed 3D kernel of 3×3×3 voxels (Zhao

et al., 2017) was applied (on the maps already in MNI space) as described in (Asllani et al., 2008), thereby new regional CBF values could be calculated from the estimated GM CBF component. A more extended kernel of 7x7x7 voxels was also considered to verify the impact of the kernel setting on the results. For the PV corrections, single subject GM masks were obtained by applying a fixed threshold to the tissue probability maps. For GM masking, only voxels with a GM probability higher than 0.2 were selected. An analysis of covariance was performed to assess the effect of age (as continuous covariate) and group (NH vs. HL) on the size of the GM masks. In the MNI space, general linear models (for post hoc t tests) were computed voxel wise to compare GMV maps between the two groups, while accounting for total ICV, sex, and age of each subject. The resulting statistical maps (t-maps) were thresholded at  $p=0.05$  with a family wise error correction for multiple voxel-level comparisons using either the entire brain (whole brain correction) or the bilateral auditory cortex as search volume (small volume correction). For the “small volume” correction, an anatomical mask was defined on the MNI template according to a cytoarchitectonic atlas of the auditory cortex (Kim et al., 2000). Besides the anatomical masking of auditory cortical regions, this atlas provides a detailed cortical parcellation of the primary auditory areas. After spatial normalization, all individual CBF maps were imported in BrainVoyager (Brain Innovation, Maastricht, The Netherlands, [www.brainvoyager.com](http://www.brainvoyager.com)) and further transformed to the Talairach space. This step allowed the analysis and presentation of group-level CBF

data both in the volume and in the surface space on the cortical surface meshes reconstructed from the Talairach-transformed MNI template. The cortical parcellation of the primary auditory cortex was also overlaid to these meshes. In this common brain space, using BrainVoyager tools and plugins, group-level averaging, and general linear models (for post hoc t tests with correction for global CBF, age, and sex effects) were computed. The correction for global CBF was performed by first computing the mean absolute CBF over the entire brain mask in each subject and then adding the series of individual global CBF values as confound in the GLM. The t-maps resulting from the post-hoc t-tests were then applied a minimum cluster size threshold estimated with Monte Carlo simulations (Forman et al., 1995; Goebel et al., 2006). This approach allowed setting the extension of significant clusters using a nonparametric statistical approach, that is, independently of the spatial distribution of the estimated effects around each peak. In more detail, starting from either  $p=0.001$  or  $p=0.005$  as “cluster-forming” voxel-level thresholds, the threshold was first applied to all voxels; then, the minimum cluster size was set in such a way that an average of 5% false positive clusters falling within the search volume were counted in 1000 randomly generated images to which the same threshold was applied. To match the level of smoothness between the real map and the simulated maps, following the random number generation at each voxel, the resulting maps were spatially filtered with a Gaussian kernel at the FWHM initially estimated from the real map according to the 3D extension of the formula in Forman

et al. (1995). The effect size, the level of variability in each group (SD), and the % statistical power were obtained, along with the peak of the effects, as post-hoc estimates using the ClinCalc interactive web tool (<http://clincalc.com>). Besides the above described atlas from Kim et al. (2000) (here used for cortical masking and for detailed cortical parcellation of the primary auditory areas), other two atlases were imported. One, from Mutsaerts et al. (2015) with the purpose to demarcate the three main perfusion territories supplied by the anterior, middle, and posterior cerebral arteries (MCA), each divided into a proximal, an intermediate and a distal vascular territory (according to previously estimated arterial transit times). The other, the automated anatomical labeling atlas (Tzourio-Mazoyer et al., 2002) was imported and used to locate additional cortical regions beside the auditory cortex. The voxel-wise analysis (and the cluster-level correction for multiple comparisons) was replicated using a mask (the medial occipital cortex) of a cortical location potentially unaffected by HL, as searching region. Region of interest (ROI) analyses were also performed: (a) to assess the coexisting effects of HL, age, and sex on the regional CBF; (b) to assess the hemispheric laterality of the regional CBF; (c) to correlate regional CBF with structural (regional GMV) and clinical (HT, S) measures; and (d) to analyze regional CBF outside of the auditory cortex. To jointly test for the presence of age and sex effects in combination with HL-related effects, the uncorrected regional CBF values were entered into a 3-ANOVA model with age, sex, and HL specified as separate as between-

subject factors of interest. To assess the laterality, a two-way ANOVA (2-ANOVA) model with side (left, right) and HL condition, respectively, as within and between-subject factors was applied to the mean regional CBF values in the anatomically defined regions taken separately from the right (mask size 38466 mm<sup>3</sup>) and left (mask size 37368 mm<sup>3</sup>) primary auditory cortex. To investigate the correlation between regional CBF and GMV in the whole group, and the correlation between the regional CBF and the audiogram thresholds and steepness (HT, S) in the HL group, a robust (weighted) multilinear regression model was applied, after accounting for sex and age. This analysis was performed in MATLAB R2017a (The MathWorks, Inc.) with the function `robustfit` and default settings (iteratively reweighted least squares with a bisquare weighting function). Finally, to assess the local CBF alteration in a cortical area outside the auditory cortex, the mean CBF values were calculated in the medial occipital cortex (mask size 54297 mm<sup>3</sup>) and compared (both the corrected and uncorrected data for global CBF) between the groups in a 3-ANOVA with age, sex, and group as factors.

## 2.3 Results

### 2.3.1 Clinical data

According to the available audiograms, the highest steepness value was observed in the frequency range

between 2 and 4 kHz in the (relative) majority of HL patients (43.3% in the right ear, 36.7% in left ear). According to the neuropsychological testing, 29/31 HL patients were cognitively intact (MOCA total score >15.5, after correction for age and education). Two HL patients (and none of the NH controls) obtained a MOCA total score below the clinical cut-off of 15.5 and were therefore excluded from the voxel-wise group comparisons in the neuroimaging data analysis. There were no significant differences between groups in the daily amount of caffeine consumption. The use of hypertension, prostate, and heart medication was not more frequent in any of the two groups compared to the other. Cholesterol medications were more frequent in the HL group (n = 12) compared to the NH group (n = 1; chi-squared test: p = 0.007). In the semiquantitative MRI evaluation of white matter lesions, compared to the NH group, the HL group exhibited increased Fazekas scores in the deep white matter (Wilcoxon rank-sum test: p = 0.025) but not in the periventricular white matter.

### 2.3.2 Neuroimaging data

There were no significant differences between HL and NH groups in the global perfusion level (mean CBF over the whole brain) and global atrophy (mean GMV over the whole brain). Similarly, when extending the voxel-wise statistical comparisons to all brain voxels (i.e., with no anatomical mask applied); there were also no significant differences between HL and NH groups. To specifically

test for any regional effects within the entire bilateral auditory cortex, a bilateral anatomical mask was applied to restrict to search volume of voxel-wise comparisons to all primary auditory regions from both hemispheres according to the atlas parcellation. Even in this case, no clusters were found with significant regional GMV differences. In contrast, one cluster (size 327 mm<sup>3</sup>) of significant regional CBF differences emerged in the right primary auditory cortex in which HL patients exhibited a significantly reduced regional CBF in comparison to NH subjects (peak effect size: -8.2 [mL/100 g/min] corresponding to -17.2%, cluster-forming threshold  $p=0.001$ ). These regional CBF differences remained statistically significant after applying individual GM masks to the ASL images and correcting the individual CBF maps at each voxel for partial volume effects prior to recalculating the GM-specific CBF estimates for each group. There was a significant effect of age ( $p=0.0009$ ) in the size of whole GM masks but this size was not significantly different between NH and HL groups after correcting for age, nor the number of GM voxels was different across subjects in the detected cluster of reduced CBF (all voxels in this cluster had a GM probability higher than 0.2 in all subjects). After PV correction, only the GM-specific CBF estimates in this cluster, not the whole GM-specific CBF estimates, were significantly different between NH and HL groups (Table 1). Moreover, a 3-ANOVA analysis of the age- and sex-uncorrected regional CBF values confirmed a significant main effect of both HL ( $p=0.0001$ ) and age ( $p=0.0048$ ), as expected for age-related HL, but not a significant effect

of sex ( $p=0.2074$ ), ruling out that the reported HL effects could be biased by the different proportions of males and females in the two groups. The local peak of this hypoperfusion effect, corresponding to the highest regional perfusion reduction (see also Table 1) was located inside the lateral Heschl's gyrus of the right hemisphere (Figure 4). However, starting from a slightly less conservative cluster-forming voxel-level threshold ( $p=0.005$ ), the same regional effects of reduced regional CBF in HL patients emerged as two bilateral clusters in the Heschl's gyri and one additional cluster in the left superior temporal gyrus, encompassing both the proximal and the MCA perfusion territories (Figure 5).

|                             | Data                                       | NH         | HL         | Difference (p-value) |
|-----------------------------|--|------------|------------|----------------------|
| Local peak in right PAC     | CBF [ml/100g/min]                          | 47.9±9.7   | 39.7±9.3   | $p=0.0017$           |
|                             | GM CBF [ml/100g/min] (PVC kernel 3 voxels) | 131.4±29.0 | 112.4±27.3 | $p=0.013$            |
|                             | GM CBF [ml/100g/min] (PVC kernel 7 voxels) | 95.3±16.2  | 82.6±15.8  | $p=0.004$            |
| Cluster in the right PAC    | CBF [ml/100g/min]                          | 47.8±9.6   | 39.6±9.3   | $p=0.0019$           |
|                             | GM CBF [ml/100g/min] (PVC kernel 3 voxels) | 123.0±26.6 | 106.3±24.3 | $p=0.017$            |
|                             | GM CBF [ml/100g/min] (PVC kernel 7 voxels) | 97.3±17.4  | 85.2±16.9  | $p=0.01$             |
| Whole GM (individual masks) | CBF [ml/100g/min]                          | 36.6±8.1   | 33.3±8.2   | $p=0.13$             |
|                             | GM CBF [ml/100g/min] (PVC kernel 3 voxels) | 87.7±18.5  | 79.4±20.3  | $p=0.11$             |
|                             | GM CBF [ml/100g/min] (PVC kernel 7 voxels) | 79.3±17.5  | 71.7±18.9  | $p=0.12$             |

*Table 1 CBF Mean values ± standard deviation obtained from the uncorrected CBF maps and the PV corrected (kernel 3 and 7 voxels), calculated in the peak of the hypoperfused region in the right PAC, in the entire cluster, and in the whole GM. In the last column the p-values of the statistical comparison between the two groups (HL vs. NH).*

Contrariwise, no regional GMV differences emerged from the comparison between NH and HL groups over the same anatomical mask, using the same uncorrected voxel-level thresholds ( $p=0.001$  or  $p=0.005$ ) and the same minimum cluster size thresholds applied for the detection of regional CBF differences.

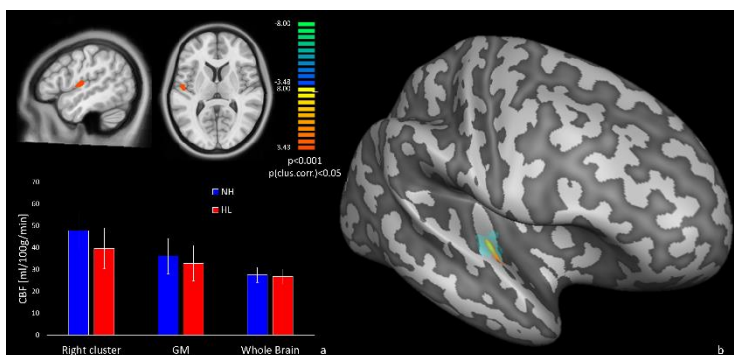


*Figure 4 (a) Statistical t-maps of the voxel-based comparison between hearing loss (HL) and normal hearing (NH;  $p < 0.05$ , cluster-level corrected for multiple comparison in the bilateral primary auditory cortex as search volume) and bar plots of the mean cerebral blood flow (CBF; PV uncorrected) with SD bars for the two groups in: (i) the significant cluster in the right primary auditory cortex, (ii) the whole GM, and (iii) the whole brain (i.e. WM + GM + CSF). (b) Projection of the significant cluster, and of the anatomical location of the lateral Heschl's gyrus, on the reconstructed surface mesh of right hemisphere of the MNI template.*

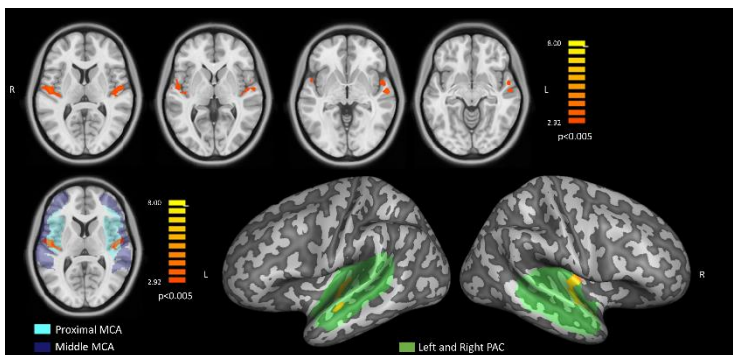
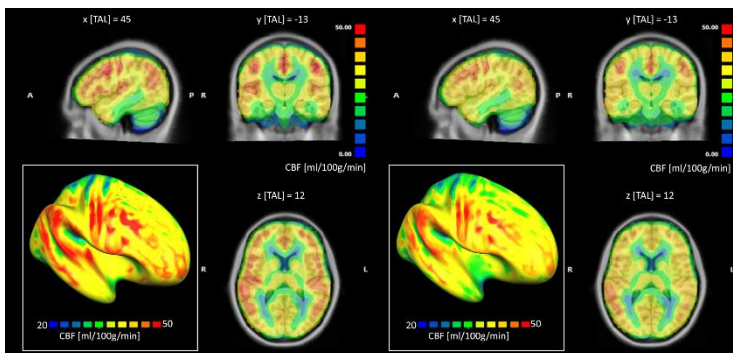


Figure 5 Upper row: statistical  $t$ -maps of the bilateral effects in the voxel-based comparison between hearing loss (HL) and normal hearing (NH;  $p < 0.005$ ). Bottom left: single slice view of the same statistical  $t$  map showing the bilateral effect with the proximal (cyan) and middle (blue) perfusion territories supplied by the middle cerebral arteries (MCAs) superimposed in transparency. Bottom right: projection of the same statistical  $t$ -map, on the MNI surface meshes with the anatomical mask of the primary auditory cortex (PAC) superimposed in green transparency.

Figure 6 displays the voxel-wise averaged whole-brain CBF maps, calculated separately for the NH ( $n = 28$ ) and HL ( $n = 29$ ) groups after spatial normalization to the common brain (MNI template) and after correcting the absolute values for the global CBF. To improve the comparative display, an identical range and pseudocolor scaling was applied to the perfusion values and the group maps were overlaid both on a triplanar volumetric view (centered at the exact peak of regional hypoperfusion) and on the reconstructed cortical surface mesh of the right hemisphere of the MNI template anatomy. In this way, the maps were further reminiscent of a spatially distributed cortical pattern of reduced perfusion levels in

the HL group, with regional effects being maximal inside, but also extending far beyond, the primary auditory cortex. Namely, the trend of reduced averaged perfusion seems to involve both secondary auditory regions (within the temporal lobe) and multiple extra-auditory regions in the parietal and prefrontal cortex. Moreover, relatively higher average CBF levels are observed in the right primary auditory cortex in both NH and HL groups in comparison to the left primary auditory cortex. Thereby, to further explore the possible “intrinsic” laterality of the regional CBF, the entire left and right auditory cortex from the same anatomical mask were also considered separately and the regional CBF values from all subjects in each group were averaged over the entire right and left auditory cortex. In this case, a statistically significant laterality effect was detected, with higher regional CBF values in the right versus left hemisphere in both HL and NH groups ( $p < 0.001$ ) and no group by side interaction ( $p > 0.05$ ). To confirm that the local CBF alteration is only confined in the auditory cortex, the whole-brain and ROI analysis were replicated in the media occipital cortex. In this case, no significant differences were found between the two groups (mean absolute CBF right: HL = 34.12 mL/100/min, NH = 37.21 mL/100 g/min; mean absolute CBF left: HL = 33.21 mL/100/min, NH = 37.00 mL/100 g/min,  $p > 0.05$ ).



*Figure 6 Group-averaged whole-brain cerebral blood flow (CBF) maps calculated after correcting the absolute values for the global CBF, for the normal hearing (NH) group (left panel) and the hearing loss (HL) group (right panel) displayed on a triplanar volumetric view after scaling between 0 and 50 mL/100 g/min. In the left-bottom inset of each panel, the same maps have been projected onto the surface mesh of the right hemisphere and rescaled between 20 and 50 mL/100 g/min.*

Finally, when extracting mean regional values from each individual in the above cluster in the right primary auditory cortex, the robust linear regression analysis highlighted a positive correlation between regional CBF and GMV (after correction for sex, age, and global values of both measures). This effect was maximally significant in the whole group of subjects ( $n = 59$ ,  $p = 0.02$ ), weakly significant in the HL group ( $n = 31$ ,  $p = 0.05$ ) and not at all significant in the NH group ( $n = 28$ ,  $p = 0.37$ ). Moreover, when considering the same regional values for all HL patients in combination with their own audiogram features, the regional CBF, but not the regional GMV, was negatively correlated with the HL steepness for both the right ( $n = 31$ ,  $r = -0.63$ ,  $p = 0.022$ ,  $r^2 = 0.21$ ) and of

the left ( $n = 31$ ,  $r = -0.71$ ,  $p = 0.015$ ,  $r^2 = 0.24$ ) ears in the 2–4 kHz interval (Figure 7), whereas no significant correlations were found with the absolute HT for any frequencies and for both ears.

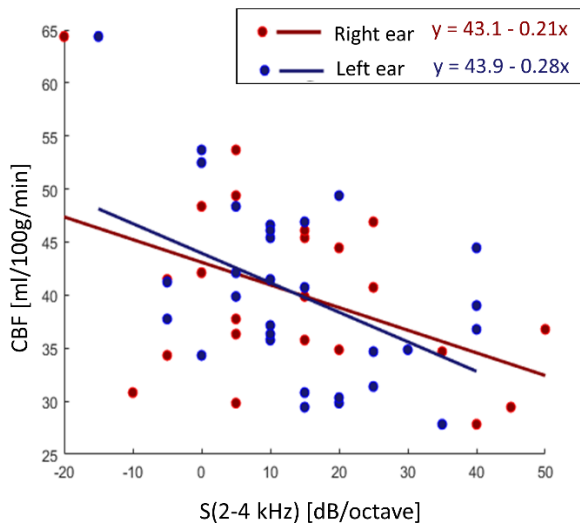


*Figure 7 Scatter plot and linear trends (and line equations) of the correlations between the audiogram steepness (2–4 kHz) and the cerebral blood flow mean value in the cluster of significant difference between normal hearing and hearing loss (HL).*

## 2.4 Discussion

The aim of the present study was to identify and characterize the possible association between HL and regional cerebral perfusion (CBF) using a clinical prototype 3D implementation of the PCASL sequence, and to possibly link such effects to structural MRI

measurements (regional GMV) and audiogram features (audiogram HL thresholds and steepness).

In other clinical applications (e.g., Alzheimer disease [AD]), areas of reduced cerebral perfusion have been detected with ASL-MRI which were largely overlapping with regions of significant hypometabolism in 18F-FDG PET study (Y. Chen et al., 2011; Verfaillie et al., 2015), thereby suggesting that ASL-MRI might provide a useful noninvasive alternative to PET imaging, to quantify regional brain metabolism in neurodegenerative diseases. In this study, the comparison between HL and NH groups, when conducted over all voxels of the auditory cortex, disclosed a significantly decreased CBF in the right primary auditory cortex, with a peak of perfusion reduction of 17.2% falling in the right lateral Heschl's gyrus, even when no significant differences were observed in the regional GMV from the same regions. Moreover, no significant local CBF depression was found when the analysis was conducted on the voxels outside the primary auditory cortex (e.g., in the visual cortex), suggesting the presence of a spatially confined phenomenon. The statistical significance of these differences was not substantially affected by the correction of partial volume effects from each individual CBF maps as calculated from the original 3D-PCASL series (with a fixed kernel of  $3 \times 3 \times 3$  or  $7 \times 7 \times 7$  voxels), nor it was biased by the different proportion of males and females in the two groups (males typically have higher HL rate than female). This distinctly suggests that the 3D-PCASL sequence has the potential to display decreased levels of functional activation or neuronal metabolism

associated with the HL condition, even when structural MRI is not providing sufficient evidence for brain atrophy and beyond the impact of partial volume and gender effects on the original ASL signal. However, larger sample sizes and long-term follow-up (e.g., 6, 12, or 24 months) studies are, respectively, needed to validate the observed hypoperfusion effects outside the primary auditory cortex and to possibly address the prognostic value of this information with respect to naturally occurring or treatment-related modifications of the HL condition. In agreement with the presented results, a recent PET study (Verger et al., 2017) conducted on late-onset deaf patients reported that the right auditory cortex was hypoperfused in HL patients, the obvious (matching) interpretation of these findings being that a functional narrowing of auditory cortical activity is occurring in association with the peripheral auditory dysfunction (Irvine & Rajan, 1996; Rajan et al., 1993). However, differently from the PET study, where the brain metabolism was also shown to increase in other regions outside the auditory cortex (especially at the vertex of the brain), our whole-brain CBF analysis did not provide evidence of CBF increase in HL patients and all statistically significant CBF alterations were strictly confined as regional effects within the primary auditory cortex (and additional trends toward possible hypoperfusion in parietal and prefrontal regions were also visible on the cortical pattern of average perfusion levels). One possible explanation of the divergent findings is that the patients involved in the PET study were all deaf for 7 years or longer whereas all patients involved in the

present study were scanned upon their very first clinical assessment for possible HL. Thus, it seems plausible that, given the early status of hearing impairment of our patients, the neuroplastic reorganization of the whole brain metabolism hypothesized previously would not be manifest yet in our sample. In addition, our MRI study involved healthy subjects that have been enrolled as control group in the same study period of HL subjects, thus minimizing the role of concomitant factors that might have affected group comparisons. This might explain the lack of hyperperfused cortical regions at the brain vertex that have been found in the PET study. On the other hand, although the selective reduction of ASL-derived perfusion levels in the primary auditory cortex persists after the correction for global CBF changes, it is not possible to exclude that some HL individuals might have confounding factors, related to a chronic pharmacological treatment or to the general vascular conditions, contributing to a more global reduction of ASL-derived perfusion levels. Indeed, we found that 12 HL subjects (vs. only one NH subject) made regular use of cholesterol medications, whereas all other types of chronic medications were balanced between groups. In addition, the size and confluence of deep, albeit not periventricular, white matter lesions were larger in HL, compared to NH, subjects. In both cases, however, it is unlikely that these factors might have biased the search for selective reduction of ASL-derived perfusion toward the primary auditory cortex. In fact, the only current evidence for ASL-derived perfusion changes in relation to the chronic use of cholesterol medication points, not to decreases, but

rather to increases in regional CBF (not in the auditory cortex) in persons at risk for AD (Carlsson et al., 2012). Moreover, recent work reported that periventricular, but not deep, white matter lesions were associated with regional cortical CBF reductions in elderly subjects at risk for cerebrovascular diseases (Bahrani et al., 2017). It should be pointed out that the ASL settings used for the present study were not optimized to provide the highest sensitivity to regional CBF changes in relation to specific perfusion territories encompassing auditory or extra-auditory regions. Indeed, the highest effects of reduced CBF were found to putatively encompass two adjacent perfusion territories (middle and proximal MCA) whereas other potentially affected (extra-auditory) regions encompass different territories (i.e., with possibly different arterial transit times). Therefore, a different postlabeling delay would have potentially increased the sensitivity of the analysis. Although we used both a labeling duration (1500 ms) and a postlabeling delay (1500 ms) shorter than the values recommended in general for clinical (2D or 3D) PCASL studies (both 1800 ms) (Alsop et al., 2015), our labeling parameters were set identically to a previous 3D-PCASL study reporting hypoperfusion areas in AD patients and specifically suggesting that a postlabeling delay of 1500 ms can be sufficient to display CBF with this ASL variant (Liu et al., 2015). Anyway, future and more advanced implementations of the same 3D-PCASL sequence, for example, allowing for multiple CBF images at different postlabeling times and the contextual estimation of the actual arterial transit times, will possibly contribute to

increase the sensitivity of whole brain CBF analyses (Johnston et al., 2015; Kramme et al., 2015).

The most significant reduction of the regional brain perfusion was confined to the right hemisphere, albeit additional effects were immediately visible within both the left and the right primary auditory cortex when slightly reducing the cluster-forming statistical threshold in the voxel-level analysis. Lateralized hypoperfusion is in line with the previous PET study (Verger et al., 2017) but also with structural morphometric findings of a lateralized atrophy in the right temporal lobe as emerging from a structural MRI follow-up of a large HL cohort (F. R. Lin et al., 2014). It should be also said, however, that, in line with our structural MRI results, at least three previous structural MRI cross-sectional studies did not report any evidence of atrophy in the temporal lobe of different HL cohorts (Alfandari et al., 2018; Boyen et al., 2013; Husain et al., 2011). A strictly related aspect, which could also at least partly explain this finding, is that the regional perfusion of the primary auditory cortex was intrinsically (and significantly) lateralized to the right hemisphere, independently of the hearing condition. A likely explanation for this lateralization is that the acoustic stimulation produced by the MRI scanner noise during the 3D-PCASL sequence, which consisted of identically repeated bursts of tonal sounds at the main frequency of 1 kHz, might have induced different baseline perfusion levels between the right and the left auditory cortex. Indeed, previous BOLD-fMRI activation studies have exhaustively demonstrated that the left auditory cortex is generally more specialized for the “temporal” processing

required for the perception of complex acoustic sounds (i.e., sounds that dynamically change their spectral features, such as, e.g., voices), whereas the right primary auditory cortex is more specialized for the “spectral” processing required for the perception of tonal stimuli (including music; (Schonwiesner et al., 2005; Sininger & de Bode, 2008; Zatorre et al., 2002). Based on this notion, the intrinsic lateralization of the regional perfusion in the primary auditory cortex (in both HL patients and NH subjects) to the right hemisphere, and, consequently, the greater size of the regional CBF alterations in HL patients (vs. NH subjects) observed in the right hemisphere, could be linked to the higher sustained functional activation elicited by the scanner acoustic noise produced by the MRI gradient system during the ASL scans. On the other hand, this explanation alone would not justify the above-mentioned homologous PET and structural MRI changes. More convincingly, it might be that the peripheral high-frequency-specific HL typically observed in aging-related HL can be related primarily to the cortical region specialized for the “spectral” processing with relative sparing of the left auditory cortex. The intrinsically activated status of the auditory cortex during the MRI scan can also explain the generally higher sensitivity of ASL techniques in these regions, compared to other brain regions. In this sense, the HL condition studied here could in principle provide a (sort of) pathological model to investigate the functional activation elicited by the MRI scanner noise in relation to the ASL sequence settings (see (Seifritz et al., 2006). However, as no significant correlations were found between the regional CBF and

the audiometric pure-tone thresholds, not even at the most stimulated frequencies (1 and 2 kHz, see Figure 3), it is also likely that the acoustic stimulation produced by the MRI scanner only contributes to the right laterality of CBF patterns (and therefore to the lateralized sensitivity of CBF analysis) according to the above described mechanisms, but not (or at least not exclusively) to the observed reduction of the regional perfusion in the primary auditory cortex of HL patients. To further investigate the nature of the reduced regional CBF in the primary auditory cortex, and to possibly highlight the structural and clinical correlates of this effect, the regional CBF values from all patients were correlated with the corresponding regional GMV measures and with the HL steepness of the audiometric curves. Although no significant GMV differences were detected between HL and NH groups, which rules out that early diagnosed HL patients were significantly more atrophic than age-matched NH subjects, and having excluded that the observed differences were substantially driven by (structural-only) partial volume effects, here we found a statistically significant positive correlation between the regional CBF and GMV values for the detected cluster of hypoperfusion in the right primary auditory cortex. This might suggest that the observed reduction of the regional CBF could still be an early sign of neuronal loss in the cerebral cortex (Madhyastha et al., 2015), rather (or more) than simply being a reduced activation response to the acoustic stimulation produced by scanner noise, which would simply mirror an (irreversible) peripheral auditory dysfunction. Moreover, when considering the

steepness of the audiograms, a significant negative correlation was found between the regional CBF values and the audiogram steepness between 2 and 4 kHz, a range of frequency that does not encompass the main harmonic of the sound produced by the MRI scanner during the 3D-PCASL scan (centered at 1 kHz). The steeply sloping high frequency loss is a highly typical audiological pattern of the age-related HL condition, which is sometimes also called “sloping” sensori-neural HL (see, e.g., (Wolak et al., 2017)). This pattern most frequently characterizes the HL impairment in the frequency interval between 2 and 4 kHz (Huang & Tang, 2010), often with a notch or dip around the 4 kHz region (H. F. Schuknecht & Gacek, 1993). A steep slope between two adjacent frequencies is therefore spotted as an audiological marker of discontinuity in the audiogram shape that can reflect corresponding discontinuities in the inner hair cells (Schecklmann et al., 2012), thereby it may represent a more specific sign of the initial (frequency selective) hearing damage. Indeed, this pattern was also characteristic of the HL patients studied here, for which the steepest slope occurred for the 2–4 kHz in the relative majority of the subjects for both ears, albeit the absolute pure tone thresholds were highly variable across subjects and between ears (and not significantly correlated with CBF). Thus, the observed patterns seem to reflect finer aspects (and provide more advanced clinical features) of the pathological HL condition, rather (or more) than displaying the simple reduction of the peripheral input at specific frequencies, thereby promoting the proposed MRI-based technique as a promising tool to detect more

fine-grained signs of the central effects of HL. In general, when functional deficits are associated with reduced local perfusion/metabolism in a brain region that is tightly linked to the affected (cognitive or sensorimotor) domain, it is not possible to mechanistically determine whether the cortical (CBF or GMV) change causes the impaired performance (as an effect of a neurovascular damage) or it is the low functional regime of the brain metabolism that triggers neuroplastic changes within the local tissue. Although we excluded from the HL group, not only subjects presenting overt dementia but also those with significant subclinical cognitive impairment (MOCA score < 15), to avoid the confounding effect of a primary diffuse (neurovascular/degenerative) cortical involvement, the possibility of a selection bias toward patients with a selective primary (neurovascular/degenerative) auditory cortex involvement cannot be ruled out completely. Therefore, the observed local perfusion/metabolism in the primary auditory cortex of the studied HL subjects could be in principle either triggered by the sensory deprivation implied by HL or vice versa. However, the most recent large-scale MRI study on cognitive aging and general cerebrovascular health conditions, using both structural and perfusion MRI with 3D PCASL, and properly accounting for age, sex, education, and occupation, as well as controlling for PET-derived global amyloid and composite tau burden as AD markers, clearly showed how systemic vascular health was associated with widespread cerebral hypoperfusion throughout the brain, whereas the regional perfusion in the primary auditory cortex (Heschl's gyrus) was not more

associated with poorer cerebrovascular and metabolic conditions than other cortical regions within the frontal, cingulate, and parietal cortex (Vemuri et al., 2018). Considering also that age-related HL is strikingly common (affecting up to 70% of normal population aged more than 70 years), the possibility of having selected a specific sample of patients with a selective primary vascular/neurodegenerative auditory cortex involvement appears unlikely. For this reason, even though a more reliable demonstration can be likely obtained only with a follow-up evaluation of samples with treated and non treated HL, our current opinion is that the observed auditory cortical hypoperfusion reflects the peripheral dysfunction.

In conclusion, this study has presented the first application of an ASL-MRI technique to the brain perfusion analysis of the HL condition. The reported cortical pattern of reduced perfusion and the observed regional effects of central hypoperfusion within the primary auditory cortex associated with an early HL condition suggests that there is a link between cortical activation and neuronal metabolism and HL even if no structural damage (atrophy) is evident. Although further technical improvements are possible, and longitudinal studies on possibly larger samples of patients are required to validate this tool for the clinical application, the reported results from the currently available implementation of the 3D-PCASL may potentially contribute novel and early functional markers of reduced central processing associated with HL. Future studies are needed to combine this information with BOLD-fMRI

activation experiments and a longitudinal investigation of the reported effects will be essential to monitor the HL condition over time in parallel with the neuropsychological outcome.

# Chapter 3

Hearing Loss in Aging:  
Is the Audiogram shape  
linked to Auditory  
Cortex perfusion  
changes?

Cassandro E., Manara R., **Ponticorvo S.**, Brotto D.,  
Cappiello A., Cuoco S., Pellecchia M.T., Cassandro C.,  
Cantone E., Scarpa A., Pfeuffer J., Di Salle F., Esposito  
F.(2020), *Submitted*.

## 3.1 Introduction

Presbycusis is the hearing loss determined by aging mechanisms affecting the inner ear (Gates & Mills, 2005). Presbycusis not only affects communicative skills, favoring social isolation and depression in the elderly, but it also might impact on cognitive functions accelerating the involutive decline of the aging brain (Gates & Mills, 2005). Recently, many audiological studies have highlighted the strong association between presbycusis and mild cognitive impairment or overt dementia suggesting a possible causal role of age-related hearing loss in cognitive deterioration and providing the rationale for investigating the brain in presbycusis (Castiglione et al., 2019; Jayakody et al., 2018; Frank R. Lin et al., 2011, 2011; Quaranta et al., 2014; Ren et al., 2019).

Right auditory cortex hypoperfusion was shown in our previous work (see Chapter 2) in early phases of presbycusis, confirming a regionally selective metabolic vulnerability associated with a peripheral loss of function (Ponticorvo et al., 2019). Accordingly, PET quantitative data revealed a decreased regional cerebral blood flow in the associative auditory cortex of presbycusis patients (mainly in the right hemisphere) (Verger et al., 2017). As a whole, literature data convergently report a profound multifaceted structural, functional and metabolic brain remodeling associated with presbycusis.

However, the term presbycusis encompasses different conditions that share a relatively advanced subject's age with a usually bilateral hearing loss, regardless of the

heterogeneous underlying pathogenesis. Schuknecht (H. F. Schuknecht, 1955) first classified presbycusis in (six) subtypes according to audiogram profile and cochlear histopathological findings: sensorial, metabolic, neural, cochlear conductive, mixed and indeterminate. Excluding the mixed and indeterminate forms, the main prototypical subtypes were the sensorial and metabolic forms, that are remarkably different in terms of pure-tone audiogram profile. The first form is characterized by down-sloping hearing loss affecting the high frequencies, while the second one presents a pantonal hearing loss. These two forms also differ regarding the underlying pathogenesis: the sensorial subtype seems to be due to the age-related loss of the outer hair cells of the basal cochlear turn, while the metabolic subtype was found to be associated to microvasculature changes with atrophy of the stria vascularis of the cochlea leading to endolymph content changes and consequently to global hearing dysfunction (H. F. Schuknecht & Gacek, 1993). While the distinctive audiological and histopathologic features of inner ear involvement in the two forms has been described by several studies, (H. F. Schuknecht, 1955; H. F. Schuknecht & Gacek, 1993) little is known about differences in the concomitant morphostructural, functional and metabolic brain involvement. The latter encompasses not only the possible impact of progressive selective or pantonal deafferentation but also a possible direct effect of the underlying pathogenic mechanisms on the central components of the auditory pathway. In this study, patients were stratified according to the audiogram profiles and both conventional and advanced MRI

quantitative analyses based on perfusion weighted imaging have been applied to allow a finer characterization of brain changes in the primary auditory cortex and possibly pave the way towards novel characterization of different forms of presbycusis.

## 3.2 Materials and Methods

### 3.2.1 Subjects

Sixty-two newly diagnosed HL patients (age range: 47-78 years, PTA>50dB) were enrolled in the MRI study. All have been complaining about HL since a few months or less. None of them had been using hearing aids before participating in the study. HL was evaluated with standard pure-tone audiometry in a soundproof chamber using a clinical audiometer: audiometric thresholds for air-conduction were obtained at the frequencies of 250, 500, 1000, 2000, 4000, and 8000 Hz. Pure Tone Average (PTA) was calculated as recommended for the classification of hearing losses by The Bureau International d'Audiophonologie (BIAP, 2005) for 0.5, 1, 2 and 4 kHz ([www.biap.org](http://www.biap.org)). In addition, the “steepness” of the audiogram in [dB/octave] was computed for each pair of adjacent frequencies as the difference in hearing level (measured in dB) divided by the frequency difference (measured in octaves) (Koenig et al., 2006). In order to independently characterize the shape of the audiogram, we first analyzed the audiograms from a

separate group of 55 HL patients (pure tone average (PTA) loss >50 dB), in the age range between 45 and 80 years, who accepted to participate to the study but later refused to proceed with (or could not successfully complete) all the required MRI scans. Using k-means clustering based on both the average pure tone loss at lower frequencies (250Hz, 500Hz, 1000Hz) and on the audiogram steepness [db/oct] at higher frequencies (1000Hz-2000Hz, 2000Hz-4000Hz), we defined two subgroups (clusters) of HL patients that we respectively labeled as low-loss-high-slope (Cluster 1: LLHS) and high-loss-low-slope (Cluster 2: HLLS) according to the audiogram centro-types. A line was traced between the two centro-types to derive a combined average loss-slope threshold for the classification of HL patients. The same audiograms centro-types were used to classify the HL patients participating in the MRI study: for each subject, the euclidean distance between patient and the centro-types was computed to assign the subject to the group wherewith it shows the minimal distance.

Thirty-two normal hearing (NH) subjects (age-range 48-78 years) with no medical history of hearing loss (or complain about their hearing) were also included in the study.

No randomization was used. None of the subjects involved had any history of neurological and/or psychiatric disorders, surgical interventions in the ear, or MR-contraindications. All participants underwent the Montreal Cognitive Assessment (MOCA (Nasreddine et al., 2005)) for evaluating cognitive performances on the same day of MRI examination.

The study was carried out in accordance with the Declaration of Helsinki for experiments involving humans and the local Ethical Committee approved the study. A written informed consent was signed by each participant before MRI acquisition.

The investigators knew the group allocation before the experiment and while performing the neuropsychological testing and the image data analyses (no blinding was done).

### 3.2.2 MRI acquisition

Brain scans were performed by means of a 3T MRI scanner (Siemens MAGNETOM Skyra, Siemens Healthcare, Erlangen, Germany), equipped with a 20-channel radio-frequency head and neck coil. The imaging protocol included the following sequences:

- 3D T1-weighted MPRAGE sequence with repetition time (TR)=2400 ms, echo-time (TE)=2.25 ms, resolution=1x1x1 mm<sup>3</sup>, matrix size=256x256, anterior-posterior phase encoding direction, GRAPPA factor of 2 in phase-encoding direction. The MPRAGE scan was used for anatomical reference and morphometric analyses.
- A prototype 3D-PCASL sequence with TR=4600 ms, TE=15.6 ms, field of view 192x192 mm<sup>2</sup>; slice thickness 3 mm, resolution=3x3x3 mm<sup>3</sup>, bolus duration 1500 ms, post-labeling delay 1500 ms, 6 repetitions, M0 prescan, 42 slices, iPAT GRAPPA 2, turbo factor 14, EPI factor 21, number of segments 6

(total acquisition time: 6 min). The 3D-PCASL sequence employs the 3D GRASE readout module and implements a pseudo-continuous labeling scheme with background suppression as described in (Dai et al., 2008, 2012; Wu et al., 2007). In each repetition of the sequence (TR), the tagging module and the EPI-train causes an acoustic stimulation with a principal spectral contribution at 1 and 2 kHz. This series was acquired with the subject at rest with eye open.

- 3D fluid FLAIR, TR/TE/TI 5000/387/1800ms; voxel-size 1x1x1 mm; echo-train length 278; field of view 230; acquisition-time 4min 32s). Axial, coronal and sagittal multiplanar reconstructions of the whole brain were obtained (slice thickness 3mm without interslice gap). The FLAIR scan was used for vascular-like lesion analysis.

### 3.2.3 Image analysis

Single-subject whole-brain CBF maps were calculated from the 3D-PCASL raw images using the prescan M0 image and the perfusion-weighted series using the calibration formula in (Alsop et al., 2015) (provided by the inline scanner software with calibration parameters:  $\lambda = 0.9$  mL/g,  $\alpha = 98\%$ ,  $T1a = 1650$  ms).

For the group-level analysis, the single-subject CBF maps were spatially normalized using the SPM12 toolbox ([www.fil.ion.ucl.ac.uk/spm/](http://www.fil.ion.ucl.ac.uk/spm/)) running on MATLAB R2017a (The MathWorks, Inc., Natick, Massachusetts, United

States, [www.mathworks.com](http://www.mathworks.com)) to the Montreal Neurological Institute (MNI) standard template (Evans et al., 1993) using a three-step procedure: First, the control images from the 3D-PCASL series were averaged to obtain an image with enhanced contrast, which was aligned in each subject to the corresponding anatomical 3D T1w image with an affine transformation. Second, all T1w images were segmented and normalized into a study specific template space with the non-linear diffeomorphic DARTEL approach (John Ashburner, 2007) and then transformed to the MNI space. Third, the initial affine transformation, the DARTEL estimated non-linear deformation fields and an isotropic 6-mm full width at half maximum (FWHM) Gaussian kernel were applied to the CBF maps of each subject.

After spatial normalization, all individual CBF maps were imported in BrainVoyager (Brain Innovation, Maastricht, The Netherlands, [www.brainvoyager.com](http://www.brainvoyager.com)) and further transformed to the Talairach space for subsequent analyses. In this common brain space, using BrainVoyager tools and plugins, group-level averaging and general linear models (for post-hoc t-tests with correction for global CBF, age and sex effects) were computed and the resulting t-maps were applied a minimum cluster size threshold estimated with Montecarlo simulations (Forman et al., 1995; Goebel et al., 2006). Particularly, Talairach-transformed CBF maps were compared between HL (sub)groups vs. NH over the entire primary auditory cortex, and average CBF data were calculated for statistically significant regional effects ( $p \leq 0.05$ , cluster-level corrected for multiple

comparisons over the bilateral primary auditory cortex, initial voxel-level p-value 0.005). To define the search region, an anatomical mask was defined based on the cytoarchitectonic atlas of the auditory cortex (Kim et al., 2000).

Parenchymal brain lesions (silent strokes and white matter lesions) were evaluated on FLAIR images; in particular, white matter lesion burden was graded according to the well-validated semi-quantitative Fazekas Score (Fazekas et al., 1987). Occurrence of Fazekas Score > 1 was compared between HL and NH with a chi-square test.

### 3.3 Results

HL patients and controls did not differ in terms of age and gender. According to the neuropsychological testing, all HL patients and NH controls were cognitively intact (MOCA total score > 15.5, after correction for age and education). No significant differences were detected in total MOCA score between HL and NH (two sample t-test,  $p > 0.05$ ).

The entire HL group ( $n=62$ ) undergoing MRI was equally stratified in LLHS ( $n=31$ ) and HLLS ( $n=31$ ) patients according to the audiogram features by applying the combined loss-slope threshold previously obtained from the independent sample of  $n=55$  HL patients (Figure 8).

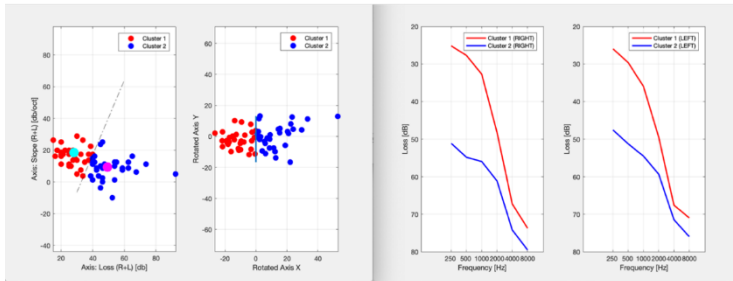


Figure 8 Left panels: Scatter plot of hearing loss at lower frequencies (Y axis) and slope at higher frequencies (X axis) of the entire sample of HL patients ( $n=62$ ) and its translated and rotated version highlighting the separation of patients in two clusters (Cluster 1: LLHS ( $n=31$ ), Cluster 2: HLLS ( $n=31$ )). The separation line was obtained from the centropypes (highlighted in cyan and violet on the plot), of the K-means clustering applied to an independent set of HL patients ( $n=55$ ). Right panels: Average audiograms of LLHS and HLLS patients for the right and left ears.

When comparing CBF maps from all HL patients (regardless of cluster membership) to NH controls over the entire primary auditory cortex, a compact area (extension =  $763 \text{ mm}^3$ , voxel-level  $p < 0.005$ , cluster-level  $p < 0.05$ ) with statistically significant CBF reduction was obtained encompassing the right transverse temporal gyrus (BA41). This regional effect was significant in both LLHS (effect size =  $-8.6\%$ ,  $p = 0.003$ ) and HLLS (effect size =  $-6.5\%$ ,  $p = 0.030$ ) patients (Figure 9).

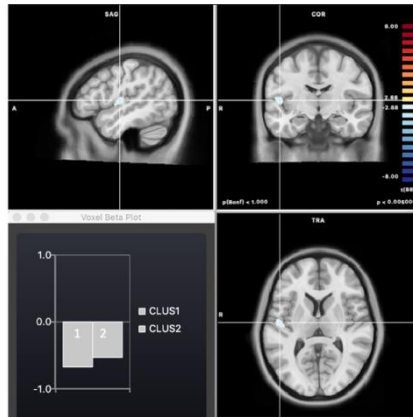


Figure 9 Cluster of reduced perfusion in the right primary auditory cortex resulting from the comparison between HL patients ( $n=62$ ) and NH controls ( $n=33$ ). The average reduction in the CBF (standardized score with respect to NH subjects) in this region is shown for LLHS (clus1) and HLLS (clus2) patients.

When comparing cluster 1 LLHS patients to NH subjects, a slightly more extended compact region (extension =  $1046 \text{ mm}^3$ , voxel-level  $p < 0.005$ , cluster-level  $p < 0.05$ ) with statistically significant CBF reduction was detected, extending from BA41 towards the boundary between BA41 and BA40. In this more extended region, a statistically significant negative correlation between the regional CBF reduction and the audiogram slopes at 2-4 KHz was observed in LLHS ( $p=0.0002$ ), but not in HLLS ( $p=0.15$ ), patients (Figure 10).

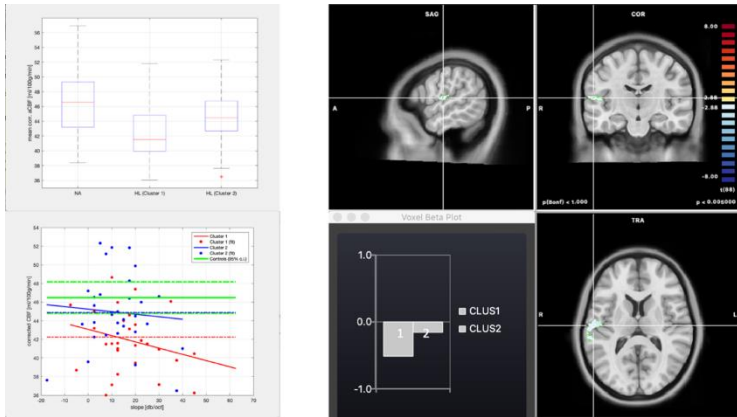
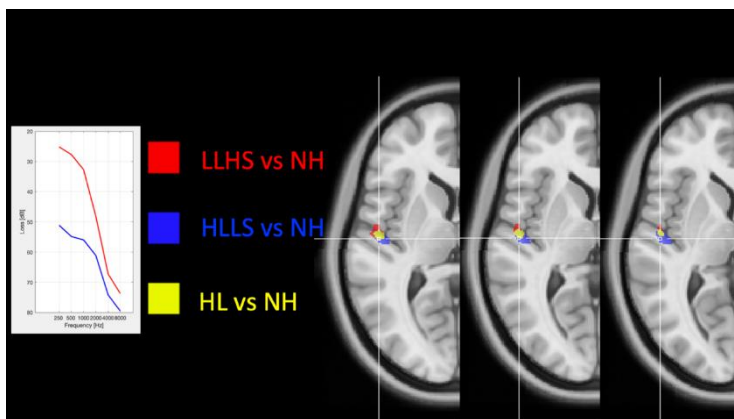


Figure 10 Cluster of reduced perfusion in the right primary auditory cortex resulting from the comparison between LLHS patients ( $n=31$ ) and NH controls ( $n=33$ ). The average reduction in the (standardized) CBF in this region is shown for LLHS (clus1) and HLLS (clus2) patients. The box plot (vs. groups) and the scatter plot (vs. slope) of the age, sex, and global CBF corrected CBF values are shown for all patients and controls with separate linear trend lines estimated for LLHS (clus1) and HLLS (clus2) patients and the 95% confidence interval for the NH subjects.

When comparing cluster 2 HLLS patients to NH subjects over the entire primary auditory cortex, a smaller region with CBF reduction was also detected (cluster size:  $399 \text{ mm}^3$ , voxel-level  $p < 0.005$ , cluster-level  $p > 0.05$ ) albeit not reaching the minimum cluster size threshold required to meet the employed criterion for the correction of multiple voxel-level comparisons. Descriptively, compared to the previous clusters, the localization of this cluster was more confined towards the transverse temporal gyrus (BA41) (Figure 11). NH, LLHS and HLLS subgroups did not differ in terms of presence and severity of cerebral

vasculopathy (Fazekas score >1 in 9/32 NH, 13/31 LLHS and 13/31 HLLS,  $p>0.5$ ).



*Figure 11 Multiple overlay of three compact regions of reduced perfusion in the right primary auditory cortex resulting from the comparison of LLHS patients ( $n=31$ ) vs. NH controls ( $n=32$ ) (red), HLLS patients ( $n=31$ ) vs. NH controls ( $n=32$ ) (blue) and all HL patients ( $n=62$ ) vs. NH controls ( $n=32$ ) (yellow).*

## 3.4 Discussion

The present non-invasive perfusion MRI study confirms, on a larger study sample compared to the previous study (Ponticorvo et al., 2019), our finding that presbycusis is associated with significant central auditory cortex hypoperfusion. These perfusion changes, observed in the right hemisphere, correlate, rather than with the absolute hearing loss, with the audiogram profile, as they are more evident in patients with a prominent 2-4 kHz frequency

slope. In addition, the audiogram profile seems to be associated with spatially distinct regions of cortical hypoperfusion, thus highlighting the heterogeneity of presbycusis not only in terms of pathogenesis but also when considering the associated brain metabolic changes.

The term presbycusis is known to encompass disparate conditions featured by different audiograms and histopathologic findings (H. F. Schuknecht & Gacek, 1993) and, most likely, a different pathogenesis. Indeed, presbycusis is generally classified into sensorial, neural, metabolic, cochlear conductive, mixed and indeterminate (H. F. Schuknecht & Gacek, 1993), although this distinction is often neglected in clinical practice and in research settings. The first (classic) four forms are characterized by different audiogram profiles: the sensorial subtype presents low-frequency sparing and high-frequency loss; the neural subtype presents loss of word discrimination in spite of a relatively preserved pure-tone audiogram; the metabolic subtype presents flat pure-tone audiogram while the cochlear conductive shows low-frequency loss and high-frequency sparing (Fetoni et al., 2011). In contrast, the pure-tone audiogram profile of the last two forms by definition results from the concomitance of different pathogenesis (mixed form) or from the impossibility to classify the hearing loss among the above-mentioned classic forms likely because of confounding factors (indeterminate form).

Actually, the cochlear conductive form existence is questioned in the literature, while, in the neural form, the pure-tone audiogram abnormalities are usually

negligible. Therefore, the audiogram prototypes of the classic forms seem to be summarized in two main pure-tone audiogram patterns that represent the ideal extremes of a continuous spectrum: the downsloping high frequency hearing loss (LLHS) and the flat pantonal hearing loss (HHLS). Accordingly, we investigated a group of 55 presbycusis patients and defined the salient audiogram features for clusterizing the spectrum of presbycusis into one of the two above mentioned prototypical shapes (either LLHS or HHLS). Subsequently, we applied this clusterization on a different cohort of presbycusis patients undergoing MRI perfusion showing that these clusters present a nonidentical regional pattern of central acoustic pathway hypoperfusion. Differences in auditory cortex hypoperfusion might either be a simple consequence of selective cortical deafferentation (due to audiogram profile differences) or highlight differences among hearing loss pathogenetic mechanisms, some of which might primarily involve the auditory cortex.

Regarding the spatially distinct cortical hypoperfusion pattern, the prevalent involvement of the lateral Heschl's gyrus in high-sloping patients is intriguing, since, in the tonotopic map, this region corresponds to the high frequencies (Formisano et al., 2003). The perfusional data seem therefore to suggest the direct role of selective deafferentation on the primary auditory cortex metabolism. On the other hand, according to our perfusion analysis, the restricted loss of the high frequencies seems to be associated with a more pronounced cortical remodeling than in patients with a

pantonal and globally more severe hearing loss. This unexpected finding unveils the complexity of the human cortex plasticity where global unisensorial deafferentation likely leads eventually to a readaptation of the cortical function and, consequently, of its metabolic demand. Ongoing studies on the auditory network connectivity at rest will possibly help to define whether the less compromised cortical perfusion in the pantonal subgroups reflects a functional remodeling of the auditory cortex.

A few satellite aspects deserve to be mentioned. Firstly, even doubling the sample size compared with the previous work of our group (Ponticorvo et al., 2019), significant perfusion changes confirmed to be restricted to the right auditory cortex. Right temporal cortex changes were observed also in previous metabolic and structural morphometric studies (F. R. Lin et al., 2014; Verger et al., 2017) confirming the higher vulnerability of the right hemisphere in age-related hearing loss. Notably, in the present study right auditory cortex hypoperfusion was more pronounced in patients with a sloping hearing loss. As the right hemisphere is mainly involved in spectral analysis (Schonwiesner et al., 2005; Siningger & de Bode, 2008; Zatorre et al., 2002), our findings seem to suggest that the selective high frequency hearing loss impacts more severely on the perfusion of the auditory cortex compared to a pantonal hearing loss. Prospective longitudinal studies will help unravel whether the increased metabolic cerebral effect of sloping hearing loss could represent a major risk factor for age-related dementia. On the other hand, the audiogram profile does

not seem to be associated with other signs of microvasculature impairment at cerebral level. In fact, the two different audiogram-related clusters showed similar microvascular white matter involvement. This seems to be in contrast with histopathologic findings that primarily distinguish the metabolic form from the sensorial form of age-related hearing loss, i.e. the intracochlear microvascular involvement with atrophy of the stria vascularis (H. F. Schuknecht & Gacek, 1993). Therefore, either the metabolic hearing loss does not primarily depend on microvasculature impairment or the microvascular involvement of the cochlea follows a different independent path than the microvascular impairment in the brain. Indeed, according to some authors both microvascular involvements might be epiphenomena of a common age-related frailty that might variably affect the neural tissue and/or the inner ear structures (Castiglione et al., 2019). Yet, the neuroradiological analysis of cerebral vasculopathies in the studied HL patients did not provide any evidence for a possible correlation between increased brain white matter changes and an audiogram profile consistent with a microvascular pathogenesis of presbycusis. This lack of correlation remarks that the link between these conditions remains elusive and further effort is needed to investigate possible common pathogenic mechanisms.

### 3.5 Conclusion

The present study shows that presbycusis is associated with metabolic perfusion changes in the brain, at least in the primary auditory cortex, with a different pattern according to the audiogram profile. Future studies will define whether presbycusis subjects with different audiogram profiles have a different outcome in terms of progressive cognitive deterioration and/or of benefit after hearing rehabilitation.

# Chapter 4

## Long-range Auditory Functional Connectivity in Hearing Loss and Rehabilitation

**Ponticorvo S.**, Manara R., Pfeuffer J., Cappiello A., Cuoco S., Pellecchia M.T., Troisi D., Scarpa A., Cassandro E., Di Salle F., Esposito F. *Brain Connectivity*. 2021 Jan 21. doi: 10.1089/brain.2020.0814. Epub ahead of print. PMID: 33478362.

## 4.1 Introduction

Age-related sensorineural hearing loss (HL) symptoms are typically ascribed to the impairment of the peripheral auditory system (i.e. outer, middle and inner ear and cranial nerves) with reduced collection, amplification and transduction of sound waves causing reduced input into the central nervous system. However, more recently, HL has been also linked to morphological (Eckert et al., 2019; Frank R. Lin et al., 2011), functional (Wolak et al., 2019; X.-M. Xu, Jiao, Tang, Lu, et al., 2019) and metabolic (Ponticorvo et al., 2019; Verger et al., 2017) changes in the central auditory pathway (i.e. subcortical nuclei and auditory cortex) resulting in reduced perception and integration of acoustic information streams (Golub, 2017).

HL patients may benefit from rehabilitation with cochlear implant and acoustic hearing aids (HA) devices. Although patients must adapt to their use (Chang et al., 2016; Dawes & Munro, 2017), these devices allow to experience significant auditory input amplification during work-related and social activities and an improvement in general hearing (Barbosa et al., 2015; Pichora-Fuller & Singh, 2006) and cognitive abilities (Amieva et al., 2015) has been previously observed in HA users. Particularly, the use of HA may improve, not only speech perception, listening abilities and quality of life (Sarant et al., 2020), but also working memory, executive functions, attention and visual learning (Anderson, 2019). Consequently, it has become crucial to address if, and eventually understand how, the prolonged exposure to HA-mediated

auditory input amplification would also trigger functional changes in the brain, both locally, within the primary auditory cortex (i.e. the cortical entry point of sensorineural signals), and globally, within the whole-brain pattern of neural communications between primary auditory and higher order brain regions. To tackle the first part of this issue (i.e. HA-mediated local functional changes), a longitudinal MRI study has recently examined HL patients undergoing HA-based auditory rehabilitation (Pereira-Jorge et al., 2018). In this work, locally increased blood oxygen level dependent (BOLD) functional MRI (fMRI) responses to naturalistic acoustic stimuli (alternating blocks of narrative listening and silence) were observed within auditory, language, and multi-sensory integration regions, after one year of HA usage. However, this study did not investigate the auditory long-range functional connectivity (FC), i.e. the functional coupling between primary auditory regions and anatomically distant brain areas throughout the whole brain.

Local functional alterations in the primary auditory cortex have been recently shown in cognitively intact HL patients (Ponticorvo et al., 2019). More specifically, using three-dimensional pseudo-continuous arterial spin labeling (3D-PCASL) MRI, a compact region in the right Heschl's gyrus (HG) was highlighted, where HL patients exhibited reduced absolute levels of cerebral blood flow (CBF), in comparison to age- and sex-matched normal hearing (NH) healthy controls. As these effects were largely confined to the primary auditory cortex, we hypothesized that a possible brain involvement in the

pathophysiology of HL, as well as subsequent HA-mediated adaptive changes, at the larger scale of whole-brain functional networks, might eventually originate from, or at least be closely linked to, this local perfusion deficit at the cortical entry point of auditory signals. To test this hypothesis, we acquired both 3D-PCASL and BOLD resting-state fMRI (rs-fMRI) data, from a larger sample of 62 HL patients, across two successive time points (at baseline and after 6 months). During the follow-up period, about half of the HL patients used an HA device during normal daily life activities. We anticipated that: (i) long-range whole-brain FC changes from a seed region of reduced perfusion in the primary auditory cortex could be associated with the general HL condition and/or its HA mediated peripheral correction, and (ii) an altered brain FC could be related to audiological and neurological features of the patients, eventually to speech recognition and cognitive abilities..

## 4.2 Materials and methods

### 4.2.1 Subjects

Eighty-seven HL patients (29 females) aged  $64.4 \pm 7.7$  years (mean  $\pm$  standard deviation) were consecutively enrolled for the study. All patients had a recent clinical diagnosis of HL (less than a month) and all of them were complaining about hearing problems for a few months or less. None of them used HA before taking part in the

study. Prior to MRI, all patients underwent audiological and neurological assessments (for details, see sections 4.2.2 and 4.2.3).

After completion of the first (baseline, t0) audiological assessment, upon HL diagnosis confirmation, the otorhinolaryngologist suggested to each patient to consider the use of a HA device albeit the patient was left free to decide about whether to use it or not, which center to refer to, and which type or model to take. 39 HL patients initially accepted to wear a HA device. During the first weeks after the enrollment, these patients had several meetings with an audioprosthesis to adapt the device to their specific needs. These patients were instructed to wear HA daily during normal activities (e.g., work-related activities, free time, social activities, etc.). Among non-users, commonly reported reasons supporting their choice included personal, social and economic issues, but also some prejudiced disappointment in HA effectiveness, which probably masked little perceived need of, or fear of social stigma associated with, this kind of prosthetics. After completion of the first neurological assessment, 4 patients were excluded due to neurological issues (2 patients were excluded for head trauma, 1 patient reported symptoms of epilepsy and 1 patient was excluded because of right maxillary malignant neoplasm). At follow-up (t1), 21 patients did not return to the planned visit and were therefore excluded from the study. In total, sixty-two HL patients (22 female) aged  $64.4 \pm 7.6$  years completed the study with a second audiological and neurological assessment and a second MRI exam. Within the final

sample, a sub-group of 31 HL patients (aged  $63.4 \pm 7.5$  years) had been effectively using a HA device daily (mean HA usage  $9.5 \pm 3.8$  hours/day, range 1-17 hours/day) (yHA group), whereas the remaining 31 patients (aged  $65.3 \pm 7.7$  years) had not (nHA group). Both patient subgroups came to the follow-up visit (t1) after a period of ~6 months ( $198 \pm 24.3$  days). Patients characteristics (age, sex, educational level) were statistically compared between the two groups (yHA vs. nHA) with two sample t-test (age, education) and chi-square test (sex). Neuropsychological (33 independent scores in total) and audiological (4 independent scores in total) clinical scores were compared at each time point (two sample t-test) and longitudinally (t0 vs. t1, paired t-test). Thirty-two normal hearing (NH) controls (22 female) aged  $59.3 \pm 7.3$  years, with no medical history of hearing loss (or complain about their hearing), were included in the study.

None of the subjects enrolled had any history of neurological and/or psychiatric disorders, surgical interventions in the ear, or MR-specific contraindications. 20/62 HL patients and 29/32 NH controls had been also included in the sample of our previous metabolic study (Ponticorvo et al., 2019).

The study was carried out in accordance with The Code of Ethics of the World Medical Association (Declaration of Helsinki) for experiments involving humans and the local ethical committee approved the study. Written informed consent was signed by each participant before MRI acquisition.

## 4.2.2 Neuropsychological assessment

All subjects underwent the Montreal Cognitive Assessment (MOCA) (Nasreddine et al., 2005) for the screening of cognitive performances. 56/62 HL patients also performed a more accurate neuropsychological battery including the Attentional Matrices (ATT) and the Trail Making Test (TMT) to investigate the attentional domain, the Rey's auditory 15-word learning test to assess verbal memory (immediate recall and delayed recall; 15-RAWLT), the Stroop Color and Word Test (SCWT), the Rey-Osterrieth Complex Figure Test memory (ROCF memory) to investigate visuospatial memory, the ROCF copy, the Raven's Progressive Matrices (RPM) and the Clock Drawing Test (CDT) to test frontal/executive functions and the Short Form 36 (SF-36), the Hearing Handicap Inventory (HHI), the Beck Depression Inventory II (BDI II) and the Dimensional Apathy Scale (DAS) to assess quality of life and levels of depression and apathy.

## 4.2.3 Audiological assessment

In both visits, HL was evaluated with pure-tone audiometry and speech audiometry. All the audiometric measurements (tonal/speech) presented here were performed in unaided conditions, i.e. without hearing aids. The audiometric thresholds for air-conduction in the pure tone audiometry were obtained at the frequencies of 0.25, 0.5, 1, 2, 4, and 8 kHz in a soundproof chamber with

headphones using a clinical audiometer. Pure tone average (PTA) was calculated as recommended by The Bureau International d'Audiophonologie ([www.biap.org](http://www.biap.org)) as average loss at 0.5, 1, 2, and 4 kHz. Patients' ability to recognize speech sounds was evaluated in 57/62 HL patients and the speech reception threshold (SRT) for disyllables was calculated. Speech audiometry was performed in a soundproof chamber with the patient wearing headphones to receive the stimuli. The standard routine entails with the examiner delivering blocks of 10 disyllabic words that the patient needs to repeat aloud. The intensity level is increased across blocks with steps of 10 dB from 10 to 100 dB and the number of correct words at each intensity is recorded. The SRT is determined as the level at which the patient is able to repeat correctly at least 50% of the words delivered (Bronkhorst & Plomp, 1989).

#### 4.2.4 Image acquisition and preprocessing

Brain images were acquired using a 3T MRI scanner (Siemens MAGNETOM Skyra, Siemens Healthcare, Erlangen, Germany), equipped with a 20-channel radio-frequency head and neck coil.

The imaging protocol included a 3D T1-weighted MPRAGE sequence with repetition time (TR)=2400 ms, echo-time (TE)=2.25 ms, resolution=1x1x1 mm<sup>3</sup>, matrix size=256x256, anterior-posterior phase encoding direction, GRAPPA factor of 2 in phase-encoding direction. A prototype 3D-PCASL sequence with

TR=4600 ms, TE=15.6 ms, field of view 192×192 mm<sup>2</sup>, resolution=3×3×3 mm<sup>3</sup>, bolus duration 1500 ms, post-labeling delay 1500 ms, 6 repetitions, M0 prescan, turbo factor 14, EPI factor 21, number of segments 6 (total acquisition time: 6 min). The 3D-PCASL sequence employs the 3D GRASE readout module and implements a pseudo-continuous labeling scheme with background suppression as described in (Dai et al., 2008, 2012; Detre et al., 2012; Wu et al., 2007). A resting-state Blood Oxygenated Level Dependent (BOLD) multi-band accelerated echo-planar (MB-EPI) fMRI sequence (rs-fMRI) (Feinberg et al., 2010; Moeller et al., 2010; J. Xu et al., 2013) with TR=1000 ms, TE=30 ms, resolution=2.5×2.5×2.5 mm<sup>3</sup>, MB factor=4, acquisition matrix=96×96, 400 dynamic volumes, anterior-posterior phase encoding direction acquisition. The MB-EPI sequence was repeated two more times with only five dynamic scans and opposite (anterior-posterior, posterior-anterior) phase encoding directions for the purpose to correct the MB-EPI images distortions (Andersson et al., 2003; Smith et al., 2004). During the 3D-PCASL and the MB-EPI the subjects were instructed to stay still and with eyes open.

Single-subject whole-brain CBF maps were calculated from the 3D-PCASL raw images using the prescan M0 image and the perfusion-weighted series in the 3D-PCASL calibration formula (Alsop et al., 2015) (as provided by the inline scanner software with calibration parameters:  $\lambda = 0.9$  mL/g,  $\alpha = 98\%$ ,  $T1a = 1650$  ms). Using BrainVoyager QX (Brain Innovation, Maastricht, The Netherlands, [www.brainvoyager.com](http://www.brainvoyager.com))

each individual rs-fMRI time series was first corrected for the different slice scan acquisition times (via trilinear/sinc interpolation) and for rigid head motion effects (via realignment of all volumes to the first). At this stage, a careful analysis of motion parameters was performed to possibly exclude subjects exhibiting excessive amounts of motion. In particular, at this stage the six estimated head motion parameter (3 translation and 3 rotation) series were considered and subjects exhibiting head translations > 3 mm and/or head rotations > 3 degrees in at least one of the scans were excluded from successive analyses. Subsequently, the image time series were first high-pass filtered (with cut-off frequency set to 0.008 Hz) and then exported to NIFTI format for geometrical distortion correction via the TOPUP tool of FSL (Andersson et al., 2003; Smith et al., 2004). Finally, to reduce the residual effects of head motion (micromotion), as well as the effects of respiratory and cardiac signals, second-order motion and physiological nuisance correction was performed using a linear regression approach. The regression model included 24 motion-related predictors (Friston et al., 1996) (6 head motion parameter time-series, their first-order derivatives and the 12 corresponding squared parameter time-series) and the mean time-courses from a white matter mask and a cerebrospinal fluid mask (as obtained from 3D-T1w spatial segmentation) as two additional predictors. In order to account for residual motion-related spikes, an additional spike-related regressor was created from the framewise displacement time-series i.e. a predictor with a value of 1 at the time points of each detected spike and

a value of 0 elsewhere (Lemieux et al., 2007; Satterthwaite et al., 2013). The framewise displacement (FD) was also used to estimate the number of potentially corrupted volumes. A spike was identified as a volume in the time series where the FD value exceeded a threshold of 0.5 mm, and the spike-corrupted volumes were calculated by taking the volume at that time point as well as the two volumes before and after this time point. At this stage, subjects for whom this percentage exceeded 50% in at least one of the two scans were also excluded from the analyses.

For the group-level analysis at  $t_0$ , the single-subject CBF maps and rs-fMRI time series were spatially normalized using the SPM12 toolbox ([www.fil.ion.ucl.ac.uk/spm/](http://www.fil.ion.ucl.ac.uk/spm/)) running on MATLAB R2019a (The MathWorks, Inc., Natick, Massachusetts, United States, [www.mathworks.com](http://www.mathworks.com)) to the Montreal Neurological Institute (MNI) standard template (Evans et al., 1993) using a two-step procedure: First, the mean control volume (for 3D-PCASL series) and the first volume (for rs-fMRI) were aligned to the corresponding anatomical 3D-T1w image with an affine transformation. Second, all T1w images were normalized with the non-linear diffeomorphic DARTEL approach (John Ashburner, 2007) and spatially smoothed with an isotropic 6-mm full width at half maximum (FWHM) Gaussian kernel. The initial affine transformation, the DARTEL estimated non-linear deformation fields, and the Gaussian kernel were also applied to the CBF maps and to the rs-fMRI time series of each subject with a final resampling at  $3 \text{ mm}^3$  and  $2 \text{ mm}^3$  voxel size respectively.

For the group-level analysis at follow-up, the two anatomical 3D-T1w volumes of each subject (t0 and t1) were combined into one 3D-T1w average volume (T1w-avg) using the intra-subject longitudinal diffeomorphic transformation as implemented in SPM12 (John Ashburner & Ridgway, 2013). Then, the single-subject CBF maps and rs-fMRI time series were first aligned to the corresponding (same session) anatomical 3D-T1w volume with an affine transformation and then to the T1w-avg volume with the nonlinear warping calculated in the longitudinal intra-subject alignment. Finally, all T1w-avg images were normalized to the MNI standard space with the same approach performed for baseline analysis and CBF maps and rs-fMRI time series were consequently resampled to the standard space at  $3 \text{ mm}^3$  and  $2 \text{ mm}^3$  voxel size respectively.

After spatial normalization, all individual CBF maps and rs-fMRI time series were imported in BrainVoyager and transformed to the Talairach space for further analysis.

#### 4.2.5 CBF Image Analysis

CBF analysis was conducted at the regional level according to previous results (Ponticorvo et al., 2019) of local hypoperfusion in the right primary auditory cortex with the peak in lateral Heschl's gyrus (right HG). Mean CBF values in right HG were extracted at t0 for HL and NH subjects and corrected with a linear regression for age, sex, and global CBF value calculated as mean value across all voxels in the brain (gray matter and white

matter). Then, the two groups were compared in a one-way analysis of variance (1-ANOVA) statistical model. In the longitudinal processing, regional CBF was extracted in HL group both at t0 and t1. Also, in this case, regional values were corrected with a linear regression model from age, sex, and global CBF confounds and then statistically compared in a two-way ANOVA model (2-ANOVA) with one within-subject factor (time: t1 vs. t0) and one between-subject factor (yHA vs. nHA).

#### 4.2.6 Rs-fMRI Data Analysis

The ROI in the right HG was used to analyze the whole brain FC using a seed-based voxel-based approach. Pearson  $r$  coefficient of correlation was calculated between the mean time series in the seed region and each voxel time-course in the brain at t0 for HL and NH subjects and, for the follow-up analysis, at t0 and t1 for both yHA and nHA subjects. The resulting  $r$  values were transformed to  $z$  scores by the Fisher's R-to-Z transformation (Fisher, 1915).

At baseline, FC  $z$ -maps were compared between HL and NH subjects in a one-way analysis of covariance (ANCOVA) as implemented in the ANCOVA module of BrainVoyager QX. In this model, group membership (HL, NH) was specified as between-subject factor and age as a continuous covariate.

In the follow-up analysis, FC  $z$ -maps of HL subjects were compared in a two-way ANCOVA model with group membership (yHA, nHA) as between-subject factor, time

(t0, t1) as within-subject factor and age as continuous covariate.

To protect against false positives and correct for multiple comparisons, only statistically significant regional effects were displayed for compact clusters surviving the joint application of a voxel- and a cluster-level threshold to the ANCOVA t/F statistics maps. These were chosen using a non-parametric randomization approach based on Monte Carlo simulations (Forman et al., 1995), as implemented in BrainVoyager (Goebel et al., 2006). Namely, an uncorrected threshold ( $p < 0.001$ ) was applied to all voxels (Eklund et al., 2016); then, the minimum cluster size was set in such a way that an average of 5% false positive clusters were counted in 10000 randomly generated images with smoothness matching to the original maps (Forman et al., 1995).

Pearson correlation coefficients were also calculated to explore the possible correlation between neural effects (regional CBF and FC) and audiological characteristics. Spearman's rank correlation coefficients ( $\rho$ ) were calculated between the variation in regional connectivity z-scores (i.e. between time points) and the corresponding variation in the neuropsychological scores, separately for yHA and nHA subgroups. For this explorative analysis, statistical significance (p-values) lower than 5% were reported without and with Bonferroni correction (for all correlation tests performed).

### 4.3. Results

### 4.3.1 Clinical and CBF evaluation

Audiological and neuropsychological characteristics of HL patients in the two subgroups at the two time points are summarized in Table 2 and Figure 12. There were no significant differences in sex, age, education, PTA and SRT between yHA and nHA subgroups ( $p>0.05$ ) in both visits, and no audiological changes were detected over time in each group between the two time points ( $p>0.05$ ). All patients were cognitively intact (total MOCA score  $\geq 15.5$ , according to the normative data of the Italian version of the MOCA, (Santangelo et al., 2015)) and no significant differences were detected in total MOCA score (after correction for age and education) between yHA and nHA ( $p>0.05$ ) in both visits, or in each group between time points ( $p>0.05$ ). No significant differences were detected between yHA and nHA both at t0 and t1 ( $p>0.05$ ) in any neuropsychological test. Significant differences between time points (t0 vs. t1) were detected, with an increase for the nHA group in 15-RAWLT immediate recall ( $p=0.018$ ) and RPM ( $p=0.0013$ ) test scores, an increase for the yHA group in 15-RAWLT delayed recall ( $p=0.0087$ ) and SF-36 sub-score of physical pain ( $p=0.017$ ) and a decrease for the yHA group in HHI ( $p=0.035$ ). However, none of these differences remained significant after Bonferroni correction for all 66 comparisons.

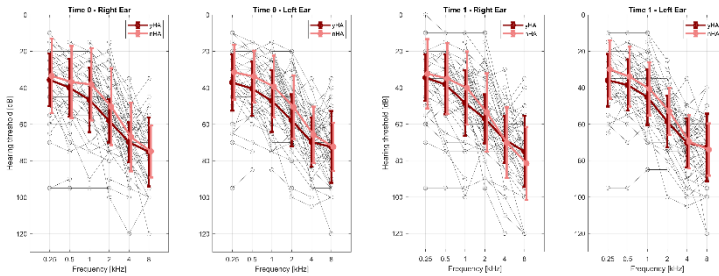


Figure 12 Hearing loss characterization of each patient (black line) in right and left ear respectively at the baseline visit ( $t_0$ ) and at the follow-up visit ( $t_1$ ). Overlaid in bold the mean lines, and standard deviation bars, hearing loss of the yHA group (dark red line), and nHA group (pink line) at each visit ( $t_0$  and  $t_1$ ). To avoid bars overlapping pink lines were shifted of 0.1 on x-axis. yHA=hearing aids users, nHA=patients not using hearing aids.

The results of the CBF analysis are shown in Figure 13. At baseline ( $t_0$ ), mean regional CBF level in right HG was significantly reduced in HL patients, compared to NH controls, after correction for age, sex, and global mean CBF level ( $t$ -value=-2.64,  $df=92$ ,  $p=0.009$ ). The mean ( $\pm$  standard deviation) CBF levels as well as the variations between time points ( $t_1-t_0$ ) in right HG are reported in Table 3 respectively for HL and NH groups. The regional follow-up CBF analysis in the right HG did not reveal any significant difference between time points ( $t_1$  vs.  $t_0$ , yHA:  $t=1.26$ ,  $df=30$ ; nHA:  $t=-0.44$ ,  $df=30$ ;  $p>0.05$ ) and between subgroups (yHA vs. nHA,  $t_0$ :  $t=-0.23$ ,  $df=60$ ;  $t_1$ :  $t=-0.43$ ,  $df=60$ ;  $p>0.05$ ).

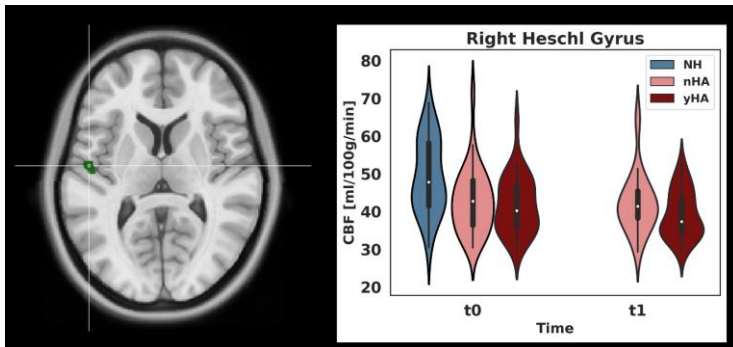


Figure 13 Left panel: Location of the right HG hypoperfused cluster (in green), superimposed on an anatomical T1w image. Right panel: Violin plots indicating median (white circle) and relative frequency distributions of the CBF levels in the right HG for the three groups (NH=blue, yHA=pink, and nHA=dark red) and the two time points (t0 and t1). HG=Heschl's gyrus, NH=normal hearing, yHA=hearing aids users, nHA=patients not using hearing aids, CBF=cerebral blood flow

|                                 | <b>yHA - t0<br/>(mean ± sd)</b> | <b>nHA - t0<br/>(mean ± sd)</b> | <b>yHA - t1<br/>(mean ± sd)</b> | <b>nHA - t1<br/>(mean ± sd)</b> |
|---------------------------------|---------------------------------|---------------------------------|---------------------------------|---------------------------------|
| PTA right ear [dB]              | 53.6 ± 10.6                     | 48.1 ± 17.7                     | 53.0 ± 11.2                     | 49.7 ± 17.2                     |
| PTA left ear [dB]               | 53.8 ± 11.9                     | 47.4 ± 13.3                     | 53.1 ± 10.7                     | 49.3 ± 11.3                     |
| SRT right ear [dB]              | 40.0 ± 17.1                     | 45.7 ± 20.8                     | 42.0 ± 14.7                     | 42.2 ± 20.7                     |
| SRT left ear [dB]               | 47.1 ± 16.4                     | 43.4 ± 18.3                     | 47.8 ± 15.5                     | 40.7 ± 14.6                     |
| Education [years]               | 10.6 ± 4.7                      | 10.8 ± 5.3                      | NA                              | NA                              |
| MOCA – total                    | 21.8 ± 3.9                      | 22.1 ± 3.6                      | 22.7 ± 3.5                      | 22.8 ± 4.2                      |
| MOCA – visuospatial ability     | 3.5 ± 0.7                       | 3.3 ± 0.8                       | 3.2 ± 1.0                       | 3.3 ± 0.7                       |
| MOCA – executive functions      | 1.6 ± 1.3                       | 1.7 ± 1.2                       | 1.7 ± 1.0                       | 1.9 ± 1.2                       |
| MOCA – language                 | 4.8 ± 1.2                       | 5.1 ± 1.0                       | 4.8 ± 1.1                       | 5.0 ± 0.9                       |
| MOCA – orientation              | 5.8 ± 0.4                       | 5.8 ± 0.5                       | 6.0 ± 0.2                       | 5.7 ± 0.9                       |
| MOCA – attention                | 4.8 ± 1.0                       | 4.7 ± 1.6                       | 5.1 ± 1.0                       | 4.9 ± 1.3                       |
| 15-RAWLT – immediate recall     | 35.8 ± 11.1                     | 34.4 ± 10.3                     | 37.1 ± 10.3                     | 38.2 ± 10.4                     |
| 15-RAWLT – delayed recall       | 6.9 ± 2.8                       | 7.2 ± 2.7                       | 8.2 ± 3.5                       | 8.1 ± 3.3                       |
| RPM                             | 27.4 ± 4.3                      | 24.5 ± 6.3                      | 26.2 ± 5.3                      | 26.9 ± 4.6                      |
| SCWT – word reading             | 55.8 ± 16.6                     | 56.4 ± 19.2                     | 57.4 ± 16.3                     | 53.1 ± 20.6                     |
| SCWT – color naming             | 41.4 ± 7.9                      | 36.8 ± 10.3                     | 41.2 ± 10.3                     | 38.5 ± 8.8                      |
| SCWT – color-word               | 18.3 ± 5.7                      | 17.2 ± 7.9                      | 19.1 ± 6.4                      | 17.5 ± 5.1                      |
| TMT – A                         | 38.0 ± 25.8                     | 31.7 ± 20.6                     | 34.6 ± 25.1                     | 34.3 ± 17.8                     |
| TMT – B                         | 95.9 ± 58.2                     | 91.5 ± 50.2                     | 95.6 ± 69.4                     | 98.4 ± 88.0                     |
| TMT – B-A                       | 61.9 ± 44.4                     | 67.1 ± 46.6                     | 65.0 ± 60.9                     | 64.4 ± 81.4                     |
| ATT                             | 47.1 ± 6.2                      | 45.4 ± 8.0                      | 43.9 ± 11.7                     | 43.8 ± 9.7                      |
| ROCF – copy                     | 31.2 ± 6.6                      | 29.8 ± 7.8                      | 30.3 ± 6.7                      | 28.4 ± 7.0                      |
| ROCF – memory                   | 14.5 ± 6.3                      | 15.5 ± 5.4                      | 18.1 ± 7.3                      | 15.8 ± 6.4                      |
| CDT                             | 9.5 ± 1.0                       | 9.2 ± 1.1                       | 9.4 ± 1.3                       | 9.4 ± 1.3                       |
| SF-36 – physical activity       | 77.0 ± 27.8                     | 73.8 ± 24.9                     | 75.5 ± 25.4                     | 72.7 ± 26.9                     |
| SF-36 – limits of physical act. | 54.9 ± 40.3                     | 58.3 ± 44.0                     | 66.3 ± 40.4                     | 61.4 ± 45.5                     |
| SF-36 – physical pain           | 51.3 ± 30.8                     | 56.4 ± 31.3                     | 63.0 ± 26.8                     | 53.5 ± 33.4                     |
| SF-36 – general health          | 49.5 ± 23.2                     | 48.2 ± 26.0                     | 46.7 ± 22.3                     | 49.3 ± 25.8                     |
| SF-36 – vitality                | 47.7 ± 24.8                     | 51.0 ± 19.9                     | 49.8 ± 22.9                     | 56.4 ± 23.6                     |
| SF-36 – social activity         | 63.6 ± 30.1                     | 57.6 ± 28.1                     | 70.9 ± 19.0                     | 61.8 ± 32.2                     |
| SF-36 – limits emotional role   | 51.3 ± 42.0                     | 61.0 ± 44.7                     | 66.6 ± 44.9                     | 66.6 ± 46.0                     |
| SF-36 – mental health           | 57.6 ± 25.7                     | 52.7 ± 22.4                     | 57.7 ± 16.9                     | 60.5 ± 22.4                     |
| HHL                             | 44.5 ± 28.6                     | 37.0 ± 28.3                     | 28.7 ± 25.1                     | 35.5 ± 31.3                     |
| BDI II                          | 8.1 ± 6.8                       | 8.3 ± 9.9                       | 7.0 ± 7.2                       | 6.6 ± 6.5                       |
| DAS – total                     | 23.1 ± 7.4                      | 19.8 ± 11.2                     | 22.1 ± 8.0                      | 22.7 ± 11.5                     |
| DAS – executive functions       | 6.8 ± 3.9                       | 6.2 ± 5.0                       | 6.5 ± 3.7                       | 6.1 ± 4.9                       |
| DAS – emotional                 | 8.7 ± 3.5                       | 6.6 ± 4.5                       | 7.2 ± 4.2                       | 9.4 ± 4.8                       |
| DAS – cognitive                 | 7.6 ± 3.9                       | 7.1 ± 5.0                       | 8.5 ± 4.5                       | 8.1 ± 5.2                       |

*Table 2 Audiological and neuropsychological characteristics of each of the two HL subgroups (yHA, nHA) at baseline (t0) and at 6-month follow-up (t1). PTA=pure tone average on four frequencies (0.5, 1, 2, 4 kHz); SRT=speech recognition threshold; yHA=hearing aids users; nHA=patients not using hearing aid; MOCA=Montreal Cognitive Assessment; ATT=Attentional Matrices; TMT=Trail Making Test; 15-RAWLT=Rey's auditory 15-word learning test; SCWT=Stroop Color and Word Test; ROCF=Rey-Osterrieth Complex Figure Test; RPM=Raven's Progressive Matrices Test; CDT=Clock Drawing Test; SF-36=Short Form 36; HHL=Hearing Handicap Inventory; BDI II=Beck Depression Inventory-II; DAS=Dimensional Apathy Scale; NA=not available.*

|              | yHA (n=31)                        | nHA (n=31)                        | NH (n=32)                         |
|--------------|-----------------------------------|-----------------------------------|-----------------------------------|
| <b>t0</b>    | Mean $\pm$ sd<br>41.76 $\pm$ 7.36 | Mean $\pm$ sd<br>42.75 $\pm$ 8.51 | Mean $\pm$ sd<br>49.28 $\pm$ 9.73 |
| <b>t1</b>    | 39.20 $\pm$ 6.29                  | 42.21 $\pm$ 7.91                  | NA                                |
| <b>t1-t0</b> | -2.56 $\pm$ 8.98                  | -0.54 $\pm$ 7.42                  | NA                                |

*Table 3 First two rows absolute mean  $\pm$  standard deviation CBF levels [ml/100g/min] in the seed region in right Heschl's gyrus for the three groups and the two time points. Third row mean ( $\pm$  standard deviation) CBF variation over time (t1-t0) for the two hearing loss sub-groups.*

### 4.3.2 Seed-based Functional Connectivity

Prior to FC group analysis, ten HL patients and two NH subjects were excluded due to either excessive rigid head motion (two HL subjects) or excessive local motion (8 HL and 2 NH subjects), in at least one session, thereby, whole-brain FC group analyses were performed on 52 HL (25 yHA, 27 nHA) patients and 30 NH subjects.

At baseline, the whole brain ANCOVA of FC z-maps (with seed region in the right HG) revealed a significant negative connectivity (anti-correlation) in HL patients, compared to NH controls (see Table 4 for details), with peaks in the right precuneus and right cerebellum crus I (Figure 14). Within the whole HL group, the mean regional FC in the precuneus was found to negatively correlate with the mean PTA (Pearson  $r=-0.28$ ,  $p=0.04$ ) and the mean SRT (Pearson  $r=-0.32$ ,  $p=0.027$ ) from the right ear (supplementary figure 2). In addition, the right

HG-Precuneus FC was negatively correlated with the BDI II score (Spearman  $\rho=-0.33$ ,  $p=0.032$ ) and with the performance at the executive sub-test of the DAS (Spearman  $\rho=-0.31$ ,  $p=0.049$ ), albeit none of these correlations remained significant after correction for multiple comparisons.

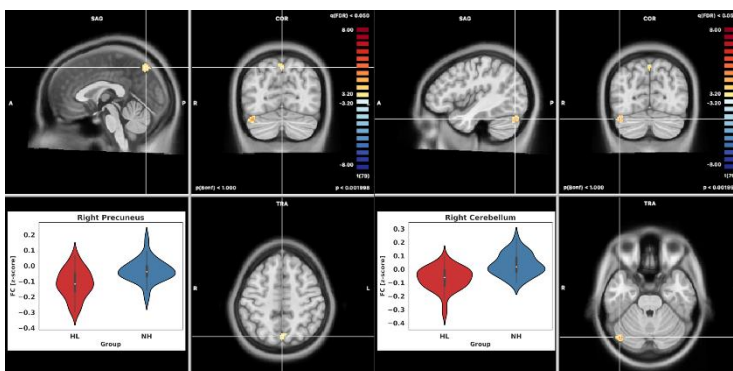


Figure 14 T-maps of the statistical comparison at baseline between HL and NH and violin plots with median (white circle) and relative frequency distribution of the functional connectivity in the two detected clusters for the two groups (HL=red, NH=blue).

| Label  | Peak Coordinate<br>[x, y, z] | Peak<br>p-value | Peak Statistics      |
|--|------------------------------|-----------------|----------------------|
| <b>Baseline (t0) analysis, HL vs. NH</b>                                       |                              |                 |                      |
| Right Precuneus  | [1, -67, 50]                 | p<0.001         | t=4.05, df=79        |
| Right Cerebellum (crus I)  | [41, -69, -22]               | p<0.001         | t=5.31, df=79        |
| <b>Follow-up analysis, interaction group (yHA vs. nHA) by time (t0 vs. t1)</b> |                              |                 |                      |
| Right Superior Frontal Gyrus   | [7, -3, 68]                  | p<0.001         | F=29.49, df = (1,50) |
| Right Middle Temporal Gyrus  | [55, -69, 18]                | p<0.001         | F=15.88, df = (1,50) |

*Table 4 Results of the functional connectivity analysis. First column: Peak location region label; Second column: spatial coordinate (TAL) of the peak location; Third column: p-value of the statistical comparison respectively between groups (HL vs. NH) for the baseline analysis and in the interaction group (yHA vs. nHA) by time (t0 vs. t1) for the follow-up analysis; Fourth column: details of the statistics in the peak with respectively the t-value and the degree of freedom in the baseline analysis and the F-value and the degree of freedom in the follow-up analysis for the interaction contrast. HL=hearing loss, yHA=hearing aids users, nHA=patients not using hearing aids, NH=normal hearing, df=degree of freedom.*

At follow-up, the FC analysis revealed two clusters with significant time by HA use interaction effects (Figure 15). These were located in the right superior frontal gyrus (SFG) and in the right middle temporal gyrus (MTG) (cluster-level corrected, minimum cluster size 96 mm<sup>3</sup>, see Table 4 for details).

In the right SFG cluster, a significant positive difference in the regional FC z-score between t0 and t1 was observed in the comparison between yHA and nHA groups. This was due to a statistically significant increase in the yHA group (one-sample t-test on delta values, t1-

t0,  $p < 0.001$ ) and a statistically significant decrease in the nHA (one-sample t-test on delta values,  $t_1 - t_0$ ,  $p < 0.001$ ). For the yHA group, but not for the nHA group, a significant positive correlation was observed between the variation in the regional FC score (between time points) and the variation in the MOCA score for the executive domain (Spearman  $\rho = 0.72$ ,  $p = 0.00012$ , corrected for multiple comparison on all 66 performed tests) (Figure 16). A similar regional effect was observed, albeit with opposite polarity, in right MTG. For this region, none of the correlation tests with audiological characteristics and neuropsychological performances was statistically significant for any of the two HL subgroups. For both SFG and MFG, no significant correlations were found between the regional FC z-scores and the mean HA usage (hours/day).

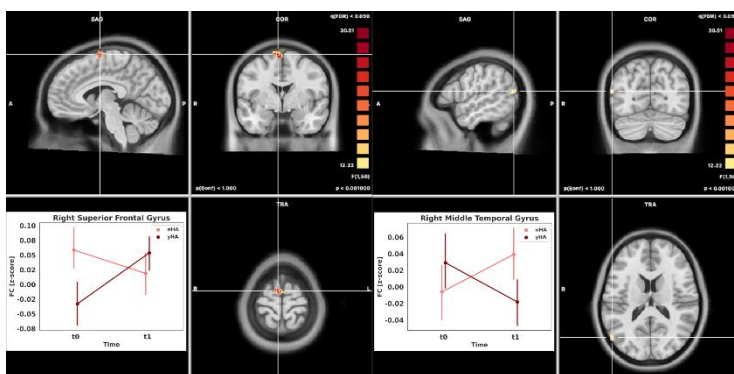


Figure 15 F-maps of the interaction contrast (time by HA) in the longitudinal analysis 2-ANOVA,  $p < 0.05$  after correction for multiple comparison (cluster-forming threshold  $p < 0.001$ ). Left panel: Mean connectivity values (and confidence intervals at 95% of the value

distribution bars) for the two groups (yHA=dark red line, and nHA=pink line) in the clusters of significant interaction in the two time points.

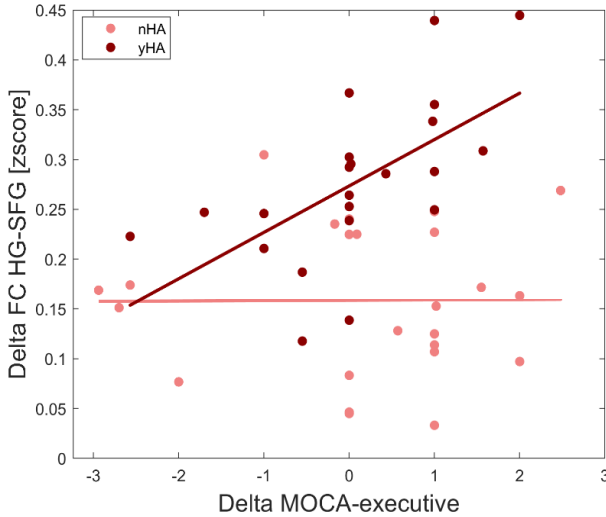


Figure 16. Scatter plots (with linear trend lines) of the functional connectivity HG-SFG change ( $t1-t0$ ) and the MOCA-executive score change ( $t1-t0$ ) and in the two groups (nHA=pink, yHA=dark red). HG=Heschl's gyrus, SFG=superior frontal gyrus, yHA=patients hearing aids users, nHA=patients not using hearing aids.

## 4.4. Discussion

This study builds up on previous ASL-MRI findings showing that, in the absence of cognitive impairment, HL is associated with neural tissue hypoperfusion (i.e. reduced CBF) within the primary auditory cortex (Ponticorvo et al., 2019). By seeding whole-brain FC analyses in the (hypoperfused and therefore potentially

damaged) cortical entry point of the auditory system, here we aimed at (i) exploring long-range auditory FC changes associated with HL and its peripheral correction via the usage of a HA device and (ii) relating such possible neural effects with audiological deficits and neuropsychological performances.

#### 4.4.1 Regional CBF analysis

First of all, the CBF analysis at baseline (t0) extended to an enlarged sample of HL patients, confirms the previous observation of reduced neuronal metabolism in the right HG. Moreover, as no longitudinal CBF changes (t0 vs. t1) were found significant in the right HG, we also added that, for at least six months, HL-related hypoperfusion in the right HG was neither reversed or worsened, regardless of hearing rehabilitation by means of HA. This was in line with the audiological condition of the HL patients, as neither PTA or SRT was significantly changed between time points in both yHA and nHA patients.

According to normative data (Clement et al., 2018), mean CBF levels across the whole gray matter are expected to be decreased by normal aging at the rate of 0.31 ml/100g/min per year. With these premises, we already expected that pure age-related decrease in CBF levels would be negligible during the 6-month follow-up period, at least if compared to any clinically meaningful pathophysiological effects. On the other hand, two previous studies reported a SRT improvement in HL patients using a HA device, respectively after twelve and eighteen months (Pereira-Jorge et al., 2018; Sarant et al., 2020).

Thus, although none of these studies included a control cohort (i.e. HL patients not using a HA device) or CBF measurements, we can not exclude that the 6-month follow-up period might have been just too short to disclose any significant changes in the clinical conditions, as well as in the local perfusion of the primary auditory cortex, of the HL patients. Notwithstanding these findings, it remains plausible that the plain sensory input amplification provided by an HA device, is simply not able to reverse the central metabolic damage and future studies are needed to possibly address this aspect as well as the lack of systematic behavioural changes associated with the experience of HA fitting.

#### 4.4.2 Seed-based Functional Connectivity Analysis (baseline)

The seed-based whole-brain FC analysis at baseline (t0) revealed two regions with significantly negative (i.e. anti-correlation) effects in the comparison between HL and NH groups, which were located in the precuneus and in the cerebellum.

It is well established that the active human brain is intrinsically organized into task-positive and task-negative functional networks (Smith et al., 2009) and that, in the resting state, signal fluctuations in task-positive regions are dynamically anti-correlated with signal fluctuations in task-negative regions (Fox et al., 2005). Particularly, signal changes within a sensory network are found anti-correlated with signal changes within a cognitive network (Zhu et al., 2016) reflecting the

(average) amount of mutual inhibitory synchronization between remotely communicating neural populations (Deco et al., 2011).

Among task-negative regions, the precuneus is often targeted as the central hub of the default mode network (DMN) (Raichle et al., 2001). The DMN plays a pivotal role in the neural control of intrinsic cognitive processes, such as consciousness, autobiographical memory, and internal (self-directed) attention (see, e.g., (Mak et al., 2017) for review). Thus, the emerging anti-correlation between the right HG and precuneus may indicate that the chronic state of reduced cortical input from the auditory pathway, as induced by the HL condition, abnormally increases the level of mutual inhibitory influence between the auditory and the DMN system, specifically via the (hypoactive) right HG. In this way, the intrinsic neural processes handled by the DMN would be directly impacted by the loss of sensory information along the auditory pathway.

An impact of the HL condition on the DMN has been already highlighted in previous works (Schmidt et al., 2013; Wang et al., 2014; Zhang et al., 2015), and an altered FC in the precuneus has been previously shown, either as a within-network effect, i.e. secondary to disruption of the whole DMN (Y.-C. Chen et al., 2018; Husain et al., 2014; Schmidt et al., 2013) or as a between-network effect, i.e. secondary to disruption of the coupling between the DMN and the dorsal attention network (DAN) (Rosemann & Thiel, 2019). Particularly, the latter study reported a significant correlation between DMN-DAN FC and listening effort in a sample of 19 HL patients.

However, no previous FC study highlighted a direct neural link between the auditory function and (any nodes of) the DMN, in association with the HL condition. Therefore, seeding whole-brain FC analyses from such a specific region in the primary auditory cortex (possibly damaged according to the CBF analysis), might have been crucial to more directly probing into the long-range communication mechanism by which HL affects the brain. Indeed, this neural effect was found to significantly correlate with the audiological deficit, both at the pure tone level (PTA) and at the speech recognition level (SRT), implying that, the more severe the clinical HL condition is, the more (aberrant) negative coupling occurs between the early auditory cortex and the DMN.

Albeit only explorative, we also observed that this negative FC effect was correlated with two neuropsychological measures: BDI II and DAS-es. These measures respectively reflect mood depression and apathy and may therefore indicate a modified mental state (Beck et al., 1961). Particularly, the DAS-es measure is associated with impaired planning, attention or organization (Radakovic & Abrahams, 2014). Thus, the lack of complete information from the auditory environment, by chronically inducing an aberrant coupling between the primary auditory cortex and the DMN, may eventually lead to increased risk of depression and cognitive impairment in HL patients, as already postulated in the current literature (Rutherford et al., 2018).

An altered FC at baseline ( $t_0$ ) was also unveiled between the right HG and the right posterolateral portion (crus I) of

the cerebellum. This was not surprising as (i) previous task-based fMRI studies had shown already that functional activity in right cerebellum (crus I/II) is normally elicited during phonological processing and language comprehension (King et al., 2019; Lesage et al., 2017) and (ii) Xu and colleagues (X.-M. Xu, Jiao, Tang, Zhang, et al., 2019) had pointed out the role of HL in the disruption of the auditory cerebellar-cerebral communication. Thus, our results would confirm the presence of long-range FC changes in the auditory cerebellar-cerebral communication, but also add that this alteration may be vehicled by a damaged cortical center.

#### 4.4.3 Seed-based Functional Connectivity Analysis (follow-up)

In the longitudinal FC analysis (t0 vs. t1), two compact clusters were detected in which a time by HA use interaction was statistically significant in the HL cohort. More specifically, the FC of the right HG was found to be increased in the right SFG and decreased in the right MTG, in the yHA (vs. nHA) group, at 6-month follow-up. In the context of large-scale (task-positive) functional networks, the SFG plays an essential role in combining information from external inputs with the (intermediate) product of cognitive operations, thus enabling the necessary neural control on cognitive processing (Kamigaki, 2019). In this way, the SFG contributes to a number of executive functions, including working memory (du Boisgueheneuc et al., 2006; Owen, 2000; Owen et al., 1998; Petrides, 2000), and modulates external

attention (Fox et al., 2006). In chronic HL patients, Xu and colleagues (X.-M. Xu, Jiao, Tang, Lu, et al., 2019) reported a reduced FC in the SFG (at baseline), albeit from a seed located in the anterior insula. However, no previous studies observed longitudinal changes in the whole-brain FC of the primary auditory cortex, before vs. after a period of HA usage. Here we show that: (i) using a seed in the right HG, the FC is not significantly altered at baseline, but can be longitudinally increased, in the SFG, of HL patients, (ii) this neural effect only occurs in HL patients employing a HA device for 6 months, and (iii) this FC change positively correlate with an improvement in the executive function, as indexed by the MOCA item which specifically evaluates this cognitive performance. Altogether, these findings may suggest that auditory input amplification could help HL patients to more efficiently allocate neural resources for cognitive tasks (Anderson, 2019) by up-regulating the long-range FC between right HG and SFG.

It is noteworthy that a different coupling of the auditory cortex with SFG between yHA and nHA HL patients existed before the intervention. While no prior hypotheses were formulated for the comparison of whole-brain FC patterns at baseline between yHA and nHA groups, and none of the investigated parameters (both clinical and neuropsychological) explain this difference, it is possible that such preexisting difference might be due to an unmatching of the two subgroups in the absence of randomization and that this aspect might have weakened the observed neural and behavioral changes after hearing aid fitting.

The observed increase in the HG-SFG FC of yHA HL patients was mirrored by a parallel increase in the HG-MTG FC of nHA HL patients. The MTG is located at the junction between temporal and occipital cortex and can be activated during audio-visual integration tasks (Naumer et al., 2009), including, e.g., language perception (Nakamura et al., 2005). Notably, the MTG is significantly activated in deaf individuals engaged in interpreting sign language (Trumpp & Kiefer, 2018). Thereby, our data might suggest that the use of HA, and the consequential improved sensory input, may lead to a decreased need for yHA, compared to nHA, patients, of extra audio-visual integration of the auditory input in order to improve understanding and communication.

Finally, none of these FC changes correlated with the mean daily HA usage (in hours), suggesting that other variables, including, e.g., the acoustic characteristics of the living environment or the content of auditory stimulations (e.g. music, speech, noise) might eventually contribute to the full experience (and therefore the overall effectiveness) of the HA amplification.

#### 4.4.5 Study limitations

Even though this was the first fMRI study reporting long-range auditory FC changes in an HL population undergoing a period of HA mediated rehabilitation, there were two limitations to consider: First, the longitudinal part of the study did not include a NH control arm, thereby the follow-up analysis lacks an external normative control on age-related neural effects. However, according to

literature, possible within-subject (healthy) aging neural effects would be likely negligible within a time window of 6 months. Second, HL patients were left free to use (or not) a HA device, and not (randomly) assigned to a yHA or nHA subgroup. Moreover, yHA patients were referred to the HA centre of their convenience, and not to a unique centre (nor this choice was oriented towards a specific HA type or model), thereby we cannot exclude that, taken together, these choices might have introduced a bias between the resulting subgroups. Nonetheless, we observed no significant differences in all clinical scores between yHA and nHA subgroups at baseline, indicating that this subdivision did not result in a bias with respect to any of the monitored variables. Thus, although additional (unknown) factors, other than the experience of hearing aid fitting, might have also changed differently between yHA and nHA groups, the HA experience was the only known factor in this longitudinal study.

## 4.5. Conclusions

In conclusion, this study highlighted an impact of the HL condition (and its subsequent HA mediated rehabilitation) on the long-range neural communication between the primary auditory cortex and higher-order brain regions, suggesting that the hypoperfused early auditory cortex could be a seed place where different (maladaptive or protective) neuroplastic changes in the whole-brain FC originate. These FC effects highlighted a mechanism of long-range neural communication which could eventually explain the audiological and neurological course of HL.



# Chapter 5

## Neuropsychological profile of hearing- impaired patients and the effect of hearing aid on cognitive functions

Cuoco S., Cappiello A., Scarpa A., Troisi D., Autuori M.,  
**Ponticorvo S.**, Manara R., Esposito F., Santangelo G.,  
Barone P., Cassandro E., Pellecchia M.T. (2020)  
*Submitted*

## 5.1 Introduction

As underlined in the previous chapters of this thesis, it is of utmost importance to understand the link between reduced auditory input due to a hearing impairment and the declines in cognitive function in older adults (Wong et al., 2014). Indeed, in chapter 4 it has been shown recent results of a global brain involvement in the pathophysiology of HL even outside of the primary auditory processing, and the different evolution when a rehabilitation strategy is performed. HL patients showed a greater risk of developing dementia and a global decrease of cognitive performances (Gates et al., 2010; Golub, 2017; Frank R. Lin et al., 2011). Attention and processing speed are the most affected functions in HL patients, that appear to need more resources to complete the tasks (Taljaard et al., 2016), but also auditory-verbal memory is affected (Shahidipour et al., 2013). Various hypotheses have been proposed to explain cognitive decline associated with hearing impairment. Usually, HL seems to speed up cognitive decline through the combination of social and sensory isolation and through an increased cognitive load (Hardy et al., 2016). Indeed, peripheral HL is associated with structural and functional brain alterations, consistent with more demanding listening and a reduction of cognitive reserve (Hardy et al., 2016).

Comprehensive hearing rehabilitative interventions, that incorporate the use of sensory aids and rehabilitative counseling to maximize the audibility of speech signals and reduce the cognitive load, provide increased auditory

stimulation, and promote social engagement. However, only few studies have investigated the effects of hearing rehabilitative interventions on cognitive decline. Specifically, the tests used so far to measure cognitive deficits in HL patients are very heterogeneous and only recently more complete neuropsychological batteries have been used on large samples (Sarant et al., 2020; Taljaard et al., 2016). Differences in administered tests, sample selection variables, and protocols for the use of aids also led to heterogeneous results (Bernabei et al., 2014; Guglielmi et al., 2020; Luan et al., 2019; Sarant et al., 2020; Taljaard et al., 2016)

Therefore, following the extra-auditory investigations the research exposed in this chapter is bidirectional: (i) comprehensively investigate the neuropsychological profile of patients with HL at baseline (t0) and (ii) to compare the neuropsychological profiles of patients with and without hearing aid at 6 months follow-up (t1).

## 5.2 Material and Methods

### 5.2.1 Patients

Fifty-six consecutive patients with a diagnosis of HL and 40 normal hearing subjects (NH), matched for age and education, were recruited. Inclusion criteria were the following: patients older than 55 years without dementia, which was evaluated by Montreal Cognitive Assessment (MOCA) (correct score < 15.5). Exclusion criteria of recruitment in the study were the following: (i) stroke or

other neurological disorders, (ii) global cognitive impairment, (iii) major psychiatric disorders, (iv) other causes of hearing loss different from presbycusis (e.g., conductive hearing loss), (v) patients using hearing aids and (vi) other causes of significant disability.

All the audiological evaluations were carried out by an experienced audiologist in a double wall soundproof room. Air conduction pure tone audiometric hearing thresholds were evaluated at 0.125, 0.25, 0.5, 1, 2, 3, 4, 6 and 8 kHz for each subject in both ears using a clinical audiometer. The Pure Tone Average (PTA) for each subject in both ears and hearing impairment was ranked based on PTA as mild, moderate, severe, or profound as follows: mild loss, 26-40 dB; moderate loss, 41-70 dB; and severe loss, 71-90 dB, profound, 90+ (Clark, 1981). Given the reduced sample size of the PTA-groups, also divided between with and without aids, we have combined the profound and severe patients in one group. Twenty-five patients accepted to use hearing aid. Neuropsychological and emotional-behavioral examination was repeated in patients with and without hearing aids at 6-months follow-up. The neuropsychological battery included the Montreal Cognitive Assessment (MOCA) and its sub-components, to investigate the global cognitive state. The Digit Cancellation Test (DCT) and the Trail Making Test (TMT) were administered in order to investigate the attentional domain, The Rey's auditory 15-word learning test to assess verbal immediate recall and verbal delayed recall (15-RAWLT) and the Rey-Osterrieth Complex Figure Test memory (ROCF memory) to investigate visuospatial

memory. The frontal/executive domain was investigated by the ROCF copy, the Raven's Progressive Matrices (RPM) and the Clock Drawing Test (CDT). In order to investigate the quality of life and the presence of emotional disorders, such as depression and apathy, Short Form 36 (SF-36), Beck Depression Inventory II (BDI II; cut-off >12) and Dimensional Apathy Scale (DAS) were administered.

### 5.2.2 Statistical Analysis

Normality test was conducted for demographic, neuropsychological and behavioral variables. Patients were compared with NH for demographic and neuropsychological data at baseline by Mann-Whitney U-test.

We assessed the relationship between depression and quality of life (QoL) at baseline in HL patients by Spearman's correlation analysis. Changes in neuropsychological and behavioral scores between t1 and t0 were calculated ( $\Delta = t1 - t0$ ) and compared between patients with and without hearing aids using Mann-Whitney's U-test. We also used the Mann-Whitney's U-test to compare neuropsychological and behavioral parameters at baseline and changes at follow-up between HL patients with and without hearing aid divided according to the level of hearing impairment.

## 5.3 Results

### 5.3.1 Comparison between NH and HL subjects

HL patients and NH did not differ for age ( $p=0.405$ ) and education ( $p=0.749$ ), (see Table 5 for more details)

A significant difference was found between the two groups in the following tests: MOCA-total score ( $p=0.004$ ), MOCA-executive functions ( $p=0.009$ ), MOCA-attention ( $p=0.009$ ), 15 RAWLT verbal immediate recall ( $p=0.010$ ), 15 RAWLT verbal delayed recall ( $p=0.010$ ), RPM ( $p=0.001$ ), SF-36 physical role functioning ( $p=0.043$ ), SF-36 bodily pain ( $p=0.004$ ), SF-36 general health perception ( $p=0.001$ ), SF-36 vitality ( $p=0.001$ ), SF-36 social role functioning ( $p=0.005$ ), SF-36 emotional role functioning ( $p=0.011$ ) and SF-36 mental health ( $p=0.000$ ), with all average values resulting higher in NH compared to patients. Trends towards significance were also found on the MOCA language subtest ( $p=0.062$ ) and BDI-II scale ( $p = 0.064$ ) with a higher score on the MOCA language sub-score and a lower score on the BDI-II scale in NH compared to HL patients (Table 5). Specifically, 26% of HL patients showed a BDI-II score higher than 12 as compared to 8% of NH ( $p=0.077$ ). Significant negative correlations were found between BDI-II and eight domains of the SF-36: physical function ( $r=-0.362$ ,  $p=0.007$ ), role limitations due to physical problems ( $r=-0.490$ ,  $p<0.001$ ), social functioning ( $r=-0.426$ ,  $p=0.001$ ), bodily pain ( $r=-0.515$ ,  $p<0.001$ ), general mental health

perception( $r=-0.492$ ,  $p<0.001$ ), role limitations due to emotional problems ( $r=-.0438$ ,  $p=0.001$ ), emotional wellbeing ( $r=-0.492$ ,  $p<0.001$ ), and general health perception ( $r=-0.525$ ,  $p<0.001$ ).

|  | HL patients<br>(N=56)<br>Median ± IQR | HC<br>(N=40)<br>Median ± IQR | p-value |
|--|---------------------------------------|------------------------------|---------|
| Age, years U                                     | 64.26±7.97                            | 63.22±6.33                   | 0.405   |
| Age of education                                 | 10.92±4.87                            | 11.27±4.69                   | 0.749   |
| RPM  | 25.60±6.05                            | 29.94±6.34                   | 0.001   |
| MOCA-total                                       | 21.05±4.6                             | 23.67±3.45                   | 0.004   |
| MOCA-visuospatial                                | 3.19±0.81                             | 3.45±0.71                    | 0.113   |
| MOCA-executive                                   | 1.80±1.25                             | 2.47±1.19                    | 0.009   |
| MOCA-language                                    | 4.60±1.30                             | 5.10±1.03                    | 0.062   |
| MOCA-orientation                                 | 5.78±0.45                             | 5.92±0.26                    | 0.095   |
| MOCA-attention                                   | 4.66±1.5                              | 5.40±0.92                    | 0.009   |
| 15-RAWTL   | 33.26±11.11                           | 38.97±10.03                  | 0.010   |
| 15- RAWTL  | 6.41±2.83                             | 8.00±3.05                    | 0.010   |
| ROCF memory                                      | 13.21±6.55                            | 13.77±6.21                   | 0.652   |
| ROCF copy  | 29.49±7.30                            | 32.10±4.55                   | 0.170   |
| CDT  | 11.01±13.54                           | 9.55±0.98                    | 0.406   |
| TMT-A  | 48.92±27.04                           | 48.57±14.88                  | 0.298   |
| TMT-B  | 144.41±74.08                          | 124.37±42.70                 | 0.407   |
| TMT-B-A  | 98.56±56.22                           | 76.40±37.65                  | 0.083   |
| Odct   | 49.07±8.30                            | 50.56±7.01                   | 0.493   |
| BDI-II   | 8.83±8.89                             | 4.84±4.73                    | 0.064   |
| DAS-Total  | 21.21±9.77                            | 18.69±7.96                   | 0.231   |
| DAS-Executive                                    | 6.28±4.72                             | 5.00±4.58                    | 0.174   |
| DAS-Emotional                                    | 7.67±4.08                             | 6.73±3.56                    | 0.275   |
| DAS-initiation                                   | 7.26±4.57                             | 6.96±4.34                    | 0.940   |
| Sf-36 Physical function                          | 74.73±25.46                           | 79.20±29.70                  | 0.190   |
| Sf-36 Role limitations due to physical problems  | 55.03±40.76                           | 73.95±37.93                  | 0.043   |
| Sf-36 Bodily pain                                | 52.10±31.57                           | 73.95±23.25                  | 0.004   |
| Sf-36 General health perception                  | 47.67±23.48                           | 65.41±17.49                  | 0.001   |
| Sf-36 Emotional wellbeing                        | 49.55±23.10                           | 66.45±14.48                  | 0.001   |
| Sf-36 Social functioning                         | 63.75±28.93                           | 84.62±19.25                  | 0.005   |
| Sf-36 Role limitations due to emotional problems | 59.96±42.36                           | 84.62±31.12                  | 0.011   |
| Sf-36 General mental health perception           | 55.74±23.82                           | 74.91±13.12                  | 0.000   |

Table 5 Demographic, neuropsychological and behavioral features in HL patients and NH controls at baseline ( $t_0$ ).

### 5.3.2 Comparison of patients with and without hearing aids

At baseline patients not accepting HA showed higher average values on the DAS-Total ( $p=0.016$ ) and the DAS-emotional ( $p=0.048$ ) scores as compared to patients accepting HA. There was also a trend for the RPM ( $p = 0.053$ ) to be lower at t0 in patients with HA than patients without. Significantly different changes (t1-t0) were found between patients with and without HA on the RPM ( $p = 0.002$ ), the ROCF ( $p=0.032$ ), the DAS-Total ( $p=0.016$ ) and DAS-emotional ( $p=0.048$ ). In particular, patients with HA improved on the ROCF and the DAS and worsened on the RPM, as compared to patients without (Table 6).

At baseline patients with mild HL showed lower scores on spatio-temporal orientation subtest of MOCA ( $p=0.015$ ) than patients with moderate HL. No other significant differences in cognitive or behavioral parameters were found at baseline among patients with mild, moderate, or severe-profound HL. Among patients with mild HL, patients with HA significantly improved on the CDT ( $p=0.039$ ) and the MOCA visuo-spatial subtest ( $p=0.037$ ) as compared to patients without hearing aid. Among patients with moderate HL patients with HA showed a trend towards a significant improvement on ROCF memory ( $p=0.065$ ), but worsened on RPM as compared to patients without hearing aid ( $p=0.038$ ). Among patients with severe-profound HL, patients with HA significantly improved on DAS ( $p=0.032$ ), while worsening on RPM ( $0.027$ ) as compared to patients without hearing aid (Table 7).

|   | HL patients<br>with HA<br>(N=25) | HL patients<br>Without HA<br>(N=31) | p-value |
|---|----------------------------------|-------------------------------------|---------|
|   | Median ± IQR                     | Median ± IQR                        |         |
| <b>Age, years</b>                                       | 62.64±7.89                       | 65.58±7.93                          | 0.168   |
| <b>Age of education</b>                                 | 10.80±4.83                       | 11.00±4.98                          | 0.822   |
| <b>MOCA-total</b>                                       | -0.08±2.98                       | 0.06±3.39                           | 0.941   |
| <b>MOCA-visuospatial</b>                                | -0.08±0.99                       | 0.00±0.73                           | 0.942   |
| <b>MOCA-executive</b>                                   | 0.20±0.91                        | 0.32±1.24                           | 0.317   |
| <b>MOCA-language</b>                                    | -0.25±0.80                       | 0.00±1.15                           | 0.236   |
| <b>MOCA-orientation</b>                                 | 0.00±0.50                        | 0.00±1.00                           | 0.504   |
| <b>MOCA-attention</b>                                   | 0.28±0.97                        | 0.03±1.07                           | 0.217   |
| <b>15-RAWTL</b>   | 1.80±8.39                        | 3.35±6.87                           | 0.525   |
| <b>15-RAWTL</b>   | 1.20±1.82                        | 0.80±2.54                           | 0.893   |
| <b>ROCF memory</b>                                      | 4.54±8.27                        | 0.22±6.12                           | 0.032   |
| <b>ROCF copy</b>  | -0.62±3.76                       | -0.50±3.70                          | 0.698   |
| <b>RPM</b>  | -2.04±6.42                       | 1.58±3.42                           | 0.002   |
| <b>CDT</b>  | 0.00±1.00                        | -3.16±18.25                         | 0.962   |
| <b>TMT-A</b>  | -1.64±18.11                      | 3.74±16.54                          | 0.158   |
| <b>TMT-B</b>  | 0.92±56.88                       | 4.03±62.17                          | 0.828   |
| <b>TMT B-A</b>  | 1.12±65.11                       | -1.62±59.54                         | 0.362   |
| <b>Odct</b>   | 1.16±12.53                       | -1.22±6.87                          | 0.980   |
| <b>BDI-II</b>   | -2.91±9.13                       | -1.90±9.61                          | 0.518   |
| <b>DAS-Total</b>  | 14.29±19.32                      | 0.31±25.98                          | 0.016   |
| <b>DAS-executive</b>                                    | 0.33±5.08                        | -0.44±4.21                          | 0.222   |
| <b>DAS-emotional</b>                                    | -1.37±3.93                       | 1.82±5.55                           | 0.048   |
| <b>DAS-initiation</b>                                   | 0.95±4.81                        | 0.72±5.33                           | 0.693   |
| <b>Sf-36 Physical function</b>                          | -3.80±23.64                      | -5.96±33.07                         | 0.712   |
| <b>Sf-36 Role limitations due to physical problems</b>  | 8.08±40.33                       | -2.41±50.56                         | 0.636   |
| <b>Sf-36 Bodily pain</b>                                | 9.52±32.14                       | -4.22±35.82                         | 0.077   |
| <b>Sf-36 General health perception</b>                  | -3.32±22.18                      | -2.25±18.44                         | 0.954   |
| <b>Sf-36 Emotional wellbeing</b>                        | -1.4±27.21                       | 1.61±21.77                          | 0.690   |
| <b>Sf-36 Social functioning</b>                         | 4.84±33.82                       | -2.77±32.16                         | 0.310   |
| <b>Sf-36 Role limitations due to emotional problems</b> | 6.80±50.02                       | 0.09±53.06                          | 0.647   |
| <b>Sf-36 General mental health perception</b>           | -2.00±30.73                      | 2.32±22.71                          | 0.707   |

Table 6 Delta ( $\Delta$ ) values for neuropsychological and behavioral variables in HL patients with and without HA

| <i>MILD HL</i>             |                              |                                    |                |
|----------------------------|------------------------------|------------------------------------|----------------|
|                            | <b>HL with HA<br/>(N=4)</b>  | <b>HL without HA<br/>(N=6)</b>     | <b>p-value</b> |
| <i>MOCA-visuo-spatial</i>  | 0.5                          | -0.5                               | 0.037          |
| <i>CDT</i>                 | 1                            | -1.66                              | 0.039          |
| <i>MODERATE HL</i>         |                              |                                    |                |
|                            | <b>HL with HA<br/>(N=6)</b>  | <b>HL without<br/>HA<br/>(N=5)</b> | <b>p-value</b> |
| <i>RPM</i>                 | -1                           | 1.05                               | 0.038          |
| <i>ROCF memory</i>         | 6.11                         | -0.15                              | 0.065          |
| <i>SEVERE- PROFOUND HL</i> |                              |                                    |                |
|                            | <b>HL with HA<br/>(N=13)</b> | <b>HL without HA<br/>(N=20)</b>    | <b>p-value</b> |
| <i>RPM</i>                 | -5.8                         | 3.2                                | 0.027          |
| <i>DAS-Total</i>           | 25.33                        | -12.2                              | 0.032          |

*Table 7 Significant differences in Delta values for neuropsychological and behavioral variables in HL patients with and without HA divided according to the severity of HL.*

## 5.4 Discussion

### 5.4.1 Comparison between healthy subjects and HL-patients

The epidemiological evidence suggests a relationship between HL and cognitive function in adults over the age of 60, but there are still few studies on cognitive profile of HL patients (Sarant et al., 2020; Taljaard et al., 2016). This study was aimed to comprehensively evaluate the cognitive and behavioral features of subjects with HL compared with normal hearing and to assess the effect of hearing aids, used for 6 months, on cognitive and behavioral tests.

HL patients, compared with NH, showed worse performances on tests assessing the cognitive state, such as the MOCA test, and in particular the attention and executive function subtests influenced the overall score. These data are in line with previous studies that reported a relationship between hearing impairment and multiple domain cognitive deficits, with attention and executive functions mostly involved (Gusseklou et al., 2005; Tay et al., 2006). Indeed, a recent study suggested that impaired cochlear amplification mechanism could lead to cognitive deficits; in fact, HL patients with greater impaired cochlear amplification mechanism also had shown greater cerebral atrophy in the cingulate and parahippocampal cortex (Belkhiria et al., 2019), inefficient modulation of salience network, that could contribute to cognitive and emotional deficits (X.-M. Xu, Jiao, Tang, Lu, et al., 2019). On the other hand, our data are not consistent with a recent cross-sectional study, that found no significant differences in neuropsychological performance with the exception of planning skills, however this study assessed a smaller group of patients and a lower number of neuropsychological tests, mostly different from ours were used to assess patients (Loughrey et al., 2019). As compared to other recent studies, we administered a more comprehensive neuropsychological battery investigating the domains of memory, attention and executive functions in a larger sample, thus possibly explaining some discrepancies in the results.

As regards the domain of memory, we found that HL patients performed worse than NH on tasks assessing

learning and recall of verbal material. This result is in line with previous studies (Guglielmi et al., 2020; Frank R. Lin et al., 2011; Shahidipour et al., 2013) showing lower performances in long-term memory and learning. And reporting a strong association between sensory deficit and performance on tests investigating verbal auditory memory suggesting that the extra efforts required to achieve perceptual success in a hearing impaired listener may affect processing resources usually available for encoding the speech content in memory (Shahidipour et al., 2013). Even if, we did not use linguistic tasks (in order to reduce vocal stimuli), we suggest that hearing impairment may affect the association of phonological inputs, determining difficulty in accessing semantic memory and reducing the coding of information from long-term memory (Guglielmi et al., 2020).

In the behavioral-emotional variables, as expected, HL patients showed a worse quality of life compared to NH (physical and emotional, pain, vitality, general health and mental health domains); moreover, we found a trend towards a significant difference also in BDI-II, assessing cognitive and somatic-affective symptoms of depression, with a higher score for patients than NH. Previously Polku et al. (2018) found that the perceived hearing difficulty factors, was significantly associated with poorer scores on the total quality of life, and Hyams et al. (2018) showed that subjects without HA had significantly poorer quality of life index than hearing-impaired with aids and NH.

Both cross-sectional and longitudinal studies indicate that HL is related to increased depressive symptoms, although the strength of the association varies across

studies. Several methodological differences may explain this heterogeneity, but overall the evidence clearly points to an association between HL and reactive depressive symptoms, confirmed in our study by a trend difference between HL patients and NH on depression but not on apathy scale (Cosh et al., 2019).

#### 5.4.2 Comparison of patients with and without hearing aid

At baseline HL patients that refused the hearing aids were more apathetic, mostly on the emotional domain of apathy, than those who accepted the rehabilitation. Furthermore, at baseline, patients who accepted the HA have a better performance on abstract logical reasoning. At follow-up, patients with HA worsened on abstract logical reasoning and improved on long-term spatial memory and apathy as compared to patients not wearing HA. To explain these results, we suggest that since HL leads to a progressive disuse of long-term memory (Rönnerberg et al., 2011, 2014), which is compensated by a strengthening of executive functions, patients without HA may have needed more executive resources, such as logical reasoning, to compensate for long-term memory loss. Moreover, the different change at follow-up in abstract logical reasoning might also be explained according to the hypothesis of relocation of cognitive resources, suggesting that in HL there is a concomitant increased engagement of short-term memory and executive functions (Loughrey et al., 2019).

Our patients with hearing aids showed an improvement in long-term spatial memory, that can be explained according to the hypothesis of information degradation. Indeed, since HL increases the cognitive load in the auditory processing of information thus compromising the perception phase, it is supposed that other brain networks are recruited to overcome such difficulties (Merten et al., 2020). According to this hypothesis, the effects of hearing impairment on cognitive networks may be extensive, but also temporary and reversible, thus suggesting that a longer follow-up of our patients would be needed to evaluate the long-term effects.

Since the association between HL and cognitive deficits may have different pathogenic mechanisms, also the effects of hearing aids on cognition could have different explanations. Indeed, the literature on the use of hearing aids gave mixed results; some studies found an improved cognitive performance after HA use (Dawes et al., 2015; Deal et al., 2015; Mahmoudi et al., 2019; Sarant et al., 2020; Taljaard et al., 2016), while other studies found no effect on cognition and cognitive decline (Frank R. Lin et al., 2011; Saunders et al., 2018; Valentijn et al., 2005). Indeed, Taljaard et al. (2016) performed a systematic review with meta-analysis including 33 studies, and reported that hearing impairment seemed to negatively affect all cognitive domains, while any type of hearing intervention significantly improved cognition, but they also suggested that their results were not conclusive, due to differences among studies, small sample sizes, and the failure to control for premorbid and other health factors in most studies.

In our study, among patients with mild HL, patients with HA significantly improved on the CDT and visuo-spatial subtest of MOCA as compared to patients without HA; both investigating the visuo-spatial abilities. This finding suggests that mild HL responds well to HL treatment on a short-term follow-up. On the other hand, among patients with moderate or severe-profound HL, abstract logical reasoning tended to worsen in patients with HA as compared to patients without, suggesting that patients without rehabilitation may have needed more executive resources, as already discussed for the whole sample. However, our subgroups were too small to draw firm conclusions, and we can only speculate that long-term HL treatment in mild HL patients could favor a lower cognitive decline over time.

In conclusion, due to the prominent cognitive and social consequences HL should be considered a social emergency. Due to the increasing prevalence of HL, associated with increasing age of the population, research into the mechanistic pathways linking HL with dementia and the potential of rehabilitative strategies to mitigate this association is warranted. An extensive interdisciplinary collaboration among audiologists, neurologists and neuropsychologists is deserved for future studies.

# Chapter 6

## Conclusions

The presented thesis has dug into the pathophysiological brain changes related to sensory deprivation or deterioration, particularly related to the aging of the auditory system.

The first part focused on the evaluation of the auditory processes in normal hearing subjects and on the quantification of brain damages located in the primary sensory cortical center in hearing loss patients; then in the second part, the analysis is extended from the local sensory center to a more global view on the entire brain functioning investigating on long-range brain connections and cognitive profiles.

More in details, in the first section, initially a description of the state of the art about what is known regarding auditory signal processing in human in both peripheral and central pathway, is presented, along with the state of the art of neuroimaging investigations in case of age-related hearing deficit and rehabilitation. Then a quantification of brain damage is presented, in the age-related hearing loss population in terms of an alteration

of basal neuronal metabolism exclusively located in the primary auditory cortex. This result presents the first application of a novel ASL-MRI technique to report a cortical pattern of reduced perfusion in this particular pathological early condition suggesting the presence of a link between cortical activation and neuronal metabolism and hearing loss even if no structural damage in terms of atrophy is present. This result is crucial in demonstrating that brain involvement in the early hearing deficit is mostly related to the hearing deprivation due to the peripheral damage. Additionally, the relation between perfusion deficit and audiogram steepness may support the hypothesis that the variation of the pure tone loss on the frequencies is a most suitable feature for patient's characterization than absolute loss (e.g. PTA) and, consequently more appropriate for categorization. On this assumption, the second main finding of the thesis is the innovative patient's classification, based not on the absolute mean loss but on the combination of two audiogram features, the average pure tone loss at lower frequencies and the steepness at higher frequencies. Importantly, the novel characterization, it is shown to reflect in a different hypometabolic pattern and can probably be useful to individuate pathologic conditions with different etiology or time course.

Finally, the third main finding has been the individuation of a global brain reorganization in terms of functional connectivity changes comparing to normal hearing subjects and in the case of hearing aids rehabilitation. Indeed, long-range neural communication between the hyperperfused primary auditory cortex and higher-order

brain regions was revealed suggesting that the hypoperfused auditory cortex could be a seed place where different neuroplastic changes originate and influence the neuronal communication with multimodal and high order regions outside the primary sensory centers. Besides, the longitudinal investigation allows revealing that while the basal metabolic activity is not restored by the introduction of a rehabilitation device, the functional connections can be influenced by their continuous usage which can suggest the urgency of the audiological and neuroimaging community to more deeply investigate their use and their effects on brain function with longer longitudinal studies and differential cohorts of subjects.

# Bibliography

- Addicott, M. A., Yang, L. L., Peiffer, A. M., Burnett, L. R., Burdette, J. H., Chen, M. Y., Hayasaka, S., Kraft, R. A., Maldjian, J. A., & Laurienti, P. J. (2009). The Effect of Daily Caffeine Use on Cerebral Blood Flow: How Much Caffeine can we Tolerate? *Human Brain Mapping*, *30*(10), 3102–3114. <https://doi.org/10.1002/hbm.20732>
- Alfandari, D., Vriend, C., Heslenfeld, D. J., Versfeld, N. J., Kramer, S. E., & Zekveld, A. A. (2018). Brain Volume Differences Associated With Hearing Impairment in Adults. *Trends in Hearing*, *22*, 2331216518763689. <https://doi.org/10.1177/2331216518763689>
- Alsop, D. C., Detre, J. A., Golay, X., Guenther, M., Hendrikse, J., Hernandez-Garcia, L., Lu, H., MacIntosh, B. J., Parkes, L. M., Smits, M., van Osch, M. J. P., Wang, D. J. J., Wong, E. C., & Zaharchuk, G. (2015). Recommended Implementation of Arterial Spin-Labeled Perfusion MRI for Clinical Applications: A Consensus of the ISMRM Perfusion Study Group and the European Consortium for ASL in Dementia. *Magnetic Resonance in Medicine*, *73*(1), 102–116. <https://doi.org/10.1002/mrm.25197>

- Amieva, H., Ouvrard, C., Giulioli, C., Meillon, C., Rullier, L., & Dartigues, J.-F. (2015). Self-Reported Hearing Loss, Hearing Aids, and Cognitive Decline in Elderly Adults: A 25-Year Study. *Journal of the American Geriatrics Society*, *63*(10), 2099–2104.  
<https://doi.org/10.1111/jgs.13649>
- Anderson, S. (2019). Neural and Cognitive Benefits of Hearing Aid Use. *The Hearing Journal*, *72*(3), 10.  
<https://doi.org/10.1097/01.HJ.0000554350.61446.37>
- Andersson, J. L. R., Skare, S., & Ashburner, J. (2003). How to correct susceptibility distortions in spin-echo echo-planar images: Application to diffusion tensor imaging. *NeuroImage*, *20*(2), 870–888. [https://doi.org/10.1016/S1053-8119\(03\)00336-7](https://doi.org/10.1016/S1053-8119(03)00336-7)
- Ashburner, J., & Friston, K. J. (2005). Unified segmentation. *Neuroimage*, *26*(3), 839–851.  
<https://doi.org/10.1016/j.neuroimage.2005.02.018>
- Ashburner, John. (2007). A fast diffeomorphic image registration algorithm. *Neuroimage*, *38*(1), 95–113.  
<https://doi.org/10.1016/j.neuroimage.2007.07.007>
- Ashburner, John, & Ridgway, G. R. (2013). Symmetric Diffeomorphic Modeling of Longitudinal Structural MRI. *Frontiers in Neuroscience*, *6*.  
<https://doi.org/10.3389/fnins.2012.00197>

- Asllani, I., Borogovac, A., & Brown, T. R. (2008). Regression Algorithm Correcting for Partial Volume Effects in Arterial Spin Labeling MRI. *Magnetic Resonance in Medicine*, 60(6), 1362–1371. <https://doi.org/10.1002/mrm.21670>
- Bahrani, A. A., Powell, D. K., Yu, G., Johnson, E. S., Jicha, G. A., & Smith, C. D. (2017). White Matter Hyperintensity Associations with Cerebral Blood Flow in Elderly Subjects Stratified by Cerebrovascular Risk. *Journal of Stroke & Cerebrovascular Diseases*, 26(4), 779–786. <https://doi.org/10.1016/j.jstrokecerebrovasdis.2016.10.017>
- Barbosa, M. R., Medeiros, D. de S., Rossi-Barbosa, L. A. R., Silveira, M. F., Martins, A. M. E. de B. L., & Caldeira, A. P. (2015). Self-perception of the hearing-impaired elderly before and after hearing-aid fittings. *Geriatrics & Gerontology International*, 15(8), 977–982. <https://doi.org/10.1111/ggi.12376>
- Bartlett, E. L. (2013). The organization and physiology of the auditory thalamus and its role in processing acoustic features important for speech perception. *Brain and Language*, 126(1), 29–48. <https://doi.org/10.1016/j.bandl.2013.03.003>
- Beck, A. T., Ward, C. H., Mendelson, M., Mock, J., & Erbaugh, J. (1961). An Inventory for Measuring Depression. *Archives of General Psychiatry*, 4(6), 561–571. <https://doi.org/10.1001/archpsyc.1961.01710120031004>

- Belkhiria, C., Vergara, R. C., San Martín, S., Leiva, A., Marcenaro, B., Martinez, M., Delgado, C., & Delano, P. H. (2019). Cingulate Cortex Atrophy Is Associated With Hearing Loss in Presbycusis With Cochlear Amplifier Dysfunction. *Frontiers in Aging Neuroscience*, *11*, 97.  
<https://doi.org/10.3389/fnagi.2019.00097>
- Bernabei, R., Bonuccelli, U., Maggi, S., Marengoni, A., Martini, A., Memo, M., Pecorelli, S., Peracino, A. P., Quaranta, N., Stella, R., Lin, F. R., & participants in the Workshop on Hearing Loss and Cognitive Decline in Older Adults. (2014). Hearing loss and cognitive decline in older adults: Questions and answers. *Aging Clinical and Experimental Research*, *26*(6), 567–573.  
<https://doi.org/10.1007/s40520-014-0266-3>
- Boi, R., Racca, L., Cavallero, A., Carpaneto, V., Racca, M., Acqua, F. D., Ricchetti, M., Santelli, A., & Odetti, P. (2012). Hearing loss and depressive symptoms in elderly patients. *Geriatrics & Gerontology International*, *12*(3), 440–445.  
<https://doi.org/10.1111/j.1447-0594.2011.00789.x>
- Boyen, K., Langers, D. R. M., de Kleine, E., & van Dijk, P. (2013). Gray matter in the brain: Differences associated with tinnitus and hearing loss. *Hearing Research*, *295*, 67–78.  
<https://doi.org/10.1016/j.heares.2012.02.010>
- Bronkhorst, A. W., & Plomp, R. (1989). Binaural speech intelligibility in noise for hearing-impaired listeners. *Journal of the Acoustical Society of*

- America*, 86(4), 1374–1383.  
<https://doi.org/10.1121/1.398697>
- Butler, B. E., & Lomber, S. G. (2013). Functional and structural changes throughout the auditory system following congenital and early-onset deafness: Implications for hearing restoration. *Frontiers in Systems Neuroscience*, 7.  
<https://doi.org/10.3389/fnsys.2013.00092>
- Cacciatore, F., Napoli, C., Abete, P., Marciano, E., Triassi, M., & Rengo, F. (1999). Quality of Life Determinants and Hearing Function in an Elderly Population: Osservatorio Geriatrico Campano Study Group. *Gerontology*, 45(6), 323–328.  
<https://doi.org/10.1159/000022113>
- Cardin, V. (2016). Effects of Aging and Adult-Onset Hearing Loss on Cortical Auditory Regions. *Frontiers in Neuroscience*, 10.  
<https://doi.org/10.3389/fnins.2016.00199>
- Carlsson, C. M., Xu, G., Wen, Z., Barnet, J. H., Blazel, H. M., Chappell, R. J., Stein, J. H., Asthana, S., Sager, M. A., Alsop, D. C., Rowley, H. A., Fain, S. B., & Johnson, S. C. (2012). Effects of Atorvastatin on Cerebral Blood Flow in Middle-Aged Adults at Risk for Alzheimer's Disease: A Pilot Study. *Current Alzheimer Research*, 9(8), 990–997.
- Castiglione, A., Casa, M., Gallo, S., Sorrentino, F., Dhima, S., Cilia, D., Lovo, E., Gambin, M., Previato, M., Colombo, S., Caserta, E., Gheller, F., Giacomelli, C., Montino, S., Limongi, F., Brotto, D., Gabelli, C., Trevisi, P., Bovo, R., &

- Martini, A. (2019). Correspondence Between Cognitive and Audiological Evaluations Among the Elderly: A Preliminary Report of an Audiological Screening Model of Subjects at Risk of Cognitive Decline With Slight to Moderate Hearing Loss. *Frontiers in Neuroscience*, *13*, 1279. <https://doi.org/10.3389/fnins.2019.01279>
- Chang, Y.-S., Choi, J., Moon, I. J., Hong, S. H., Chung, W.-H., & Cho, Y.-S. (2016). Factors associated with self-reported outcome in adaptation of hearing aid. *Acta Oto-Laryngologica*, *136*(9), 905–911. <https://doi.org/10.3109/00016489.2016.1170201>
- Chao, L. L., Buckley, S. T., Kornak, J., Schuff, N., Madison, C., Yaffe, K., Miller, B. L., Kramer, J. H., & Weiner, M. W. (2010). ASL Perfusion MRI Predicts Cognitive Decline and Conversion From MCI to Dementia. *Alzheimer Disease & Associated Disorders*, *24*(1), 19–27. <https://doi.org/10.1097/WAD.0b013e3181b4f736>
- Chen, J. J., Jann, K., & Wang, D. J. J. (2015). Characterizing Resting-State Brain Function Using Arterial Spin Labeling. *Brain Connectivity*, *5*(9), 527–542. <https://doi.org/10.1089/brain.2015.0344>
- Chen, Y., Wolk, D. A., Eddin, J. S. R., Korczykowski, M., Martinez, P. M., Pvlusiek, E. S., Newberg, A. B., Julin, P., Arnold, S. E., Greenberg, J. H., & Detre, J. A. (2011). Voxel-level comparison of arterial spin-labeled perfusion MRI and FDG-PET in Alzheimer disease. *Neurology*, *77*(22),

- 1977–1985.  
<https://doi.org/10.1212/WNL.0b013e31823a0ef7>
- Chen, Y.-C., Chen, H., Jiang, L., Bo, F., Xu, J.-J., Mao, C.-N., Salvi, R., Yin, X., Lu, G., & Gu, J.-P. (2018). Presbycusis Disrupts Spontaneous Activity Revealed by Resting-State Functional MRI. *Frontiers in Behavioral Neuroscience*, *12*, 44. <https://doi.org/10.3389/fnbeh.2018.00044>
- Cherko, M., Hickson, L., & Bhutta, M. (2016). Auditory deprivation and health in the elderly. *Maturitas*, *88*, 52–57.  
<https://doi.org/10.1016/j.maturitas.2016.03.008>
- Clark, J. G. (1981). Uses and abuses of hearing loss classification. *ASHA*, *23*(7), 493–500.
- Clement, P., Mutsaerts, H.-J., Václavů, L., Ghariq, E., Pizzini, F. B., Smits, M., Acou, M., Jovicich, J., Vanninen, R., Kononen, M., Wiest, R., Rostrup, E., Bastos-Leite, A. J., Larsson, E.-M., & Achten, E. (2018). Variability of physiological brain perfusion in healthy subjects – A systematic review of modifiers. Considerations for multi-center ASL studies. *Journal of Cerebral Blood Flow & Metabolism*, *38*(9), 1418–1437.  
<https://doi.org/10.1177/0271678X17702156>
- Cosh, S., Helmer, C., Delcourt, C., Robins, T. G., & Tully, P. J. (2019). Depression in elderly patients with hearing loss: Current perspectives. *Clinical Interventions in Aging*, *14*, 1471–1480.  
<https://doi.org/10.2147/CIA.S195824>
- Croll, P. H., Vernooij, M. W., Reid, R. I., Goedegebure, A., Power, M. C., Rigtters, S. C., Sharrett, A. R.,

- de Jong, R. J. B., Mosley, T. H., de Groot, M., Lin, F. R., & Deal, J. A. (2020). Hearing loss and microstructural integrity of the brain in a dementia-free older population. *Alzheimer's & Dementia*, *n/a*(*n/a*).  
<https://doi.org/10.1002/alz.12151>
- Dai, W., Garcia, D., de Bazelaire, C., & Alsop, D. C. (2008). Continuous Flow-Driven Inversion for Arterial Spin Labeling Using Pulsed Radio Frequency and Gradient Fields. *Magnetic Resonance in Medicine*, *60*(6), 1488–1497.  
<https://doi.org/10.1002/mrm.21790>
- Dai, W., Robson, P. M., Shankaranarayanan, A., & Alsop, D. C. (2012). Reduced resolution transit delay prescan for quantitative continuous arterial spin labeling perfusion imaging. *Magnetic Resonance in Medicine*, *67*(5), 1252–1265.  
<https://doi.org/10.1002/mrm.23103>
- Davies, R. A. (2016). Audiometry and other hearing tests. In J. M. Furman & T. Lempert (Eds.), *Neuro-Otology* (Vol. 137, pp. 157–176).  
<https://doi.org/10.1016/B978-0-444-63437-5.00011-X>
- Davis, A., McMahon, C. M., Pichora-Fuller, K. M., Russ, S., Lin, F., Olusanya, B. O., Chadha, S., & Tremblay, K. L. (2016). Aging and Hearing Health: The Life-course Approach. *The Gerontologist*, *56*(Suppl\_2), S256–S267.  
<https://doi.org/10.1093/geront/gnw033>
- Dawes, P., Cruickshanks, K. J., Fischer, M. E., Klein, B. E. K., Klein, R., & Nondahl, D. M. (2015).

- Hearing-aid use and long-term health outcomes: Hearing handicap, mental health, social engagement, cognitive function, physical health, and mortality. *International Journal of Audiology*, 54(11), 838–844.  
<https://doi.org/10.3109/14992027.2015.1059503>
- Dawes, P., & Munro, K. J. (2017). Auditory Distraction and Acclimatization to Hearing Aids. *Ear and Hearing*, 38(2), 174–183.  
<https://doi.org/10.1097/AUD.0000000000000366>
- Deal, J. A., Betz, J., Yaffe, K., Harris, T., Purchase-Helzner, E., Satterfield, S., Pratt, S., Govil, N., Simonsick, E. M., & Lin, F. R. (2017). Hearing Impairment and Incident Dementia and Cognitive Decline in Older Adults: The Health ABC Study. *The Journals of Gerontology Series A: Biological Sciences and Medical Sciences*, 72(5), 703–709.  
<https://doi.org/10.1093/gerona/glw069>
- Deal, J. A., Sharrett, A. R., Albert, M. S., Coresh, J., Mosley, T. H., Knopman, D., Wruck, L. M., & Lin, F. R. (2015). Hearing impairment and cognitive decline: A pilot study conducted within the atherosclerosis risk in communities neurocognitive study. *American Journal of Epidemiology*, 181(9), 680–690.  
<https://doi.org/10.1093/aje/kwv333>
- Deco, G., Jirsa, V. K., & McIntosh, A. R. (2011). Emerging concepts for the dynamical organization of resting-state activity in the brain. *Nature Reviews Neuroscience*, 12(1), 43–56.  
<https://doi.org/10.1038/nrn2961>

- Detre, J. A., Rao, H., Wang, D. J. J., Chen, Y. F., & Wang, Z. (2012). Applications of arterial spin labeled MRI in the brain. *Journal of Magnetic Resonance Imaging*, *35*(5), 1026–1037. <https://doi.org/10.1002/jmri.23581>
- Dolui, S., Vidorreta, M., Wang, Z., Nasrallah, I. M., Alavi, A., Wolk, D. A., & Detre, J. A. (2017). Comparison of PASL, PCASL, and Background-Suppressed 3D PCASL in Mild Cognitive Impairment. *HUMAN BRAIN MAPPING*, *38*(10), 5260–5273. <https://doi.org/10.1002/hbm.23732>
- du Boisgueheneuc, F., Levy, R., Volle, E., Seassau, M., Duffau, H., Kinkingnehun, S., Samson, Y., Zhang, S., & Dubois, B. (2006). Functions of the left superior frontal gyrus in humans: A lesion study. *Brain*, *129*(12), 3315–3328. <https://doi.org/10.1093/brain/awl244>
- Eckert, M. A., Vaden, K. I., & Dubno, J. R. (2019). Age-Related Hearing Loss Associations With Changes in Brain Morphology. *Trends in Hearing*, *23*, 2331216519857267. <https://doi.org/10.1177/2331216519857267>
- Eklund, A., Nichols, T. E., & Knutsson, H. (2016). Cluster failure: Why fMRI inferences for spatial extent have inflated false-positive rates. *Proceedings of the National Academy of Sciences*, *113*(28), 7900–7905. <https://doi.org/10.1073/pnas.1602413113>
- Engle, J. R., Tinling, S., & Recanzone, G. H. (2013). Age-Related Hearing Loss in Rhesus Monkeys Is Correlated with Cochlear Histopathologies.

- PLOS ONE*, 8(2), e55092.  
<https://doi.org/10.1371/journal.pone.0055092>
- Evans, A., Collins, D., Mills, S., Brown, E., Kelly, R., & Peters, T. (1993). 3d Statistical Neuroanatomical Models from 305 Mri Volumes. In L. A. Klaisner (Ed.), *Nuclear Science Symposium & Medical Imaging Conference, Vols 1-3: 1993 Ieee Conference Record* (pp. 1813–1817).  
<https://doi.org/10.1109/NSSMIC.1993.373602>
- Fazekas, F., Chawluk, J., Alavi, A., Hurtig, H., & Zimmerman, R. (1987). Mr Signal Abnormalities at 1.5-T in Alzheimer Dementia and Normal Aging. *American Journal of Roentgenology*, 149(2), 351–356.  
<https://doi.org/10.2214/ajr.149.2.351>
- Feinberg, D. A., Moeller, S., Smith, S. M., Auerbach, E., Ramanna, S., Glasser, M. F., Miller, K. L., Ugurbil, K., & Yacoub, E. (2010). Multiplexed Echo Planar Imaging for Sub-Second Whole Brain fMRI and Fast Diffusion Imaging. *PLOS ONE*, 5(12), e15710.  
<https://doi.org/10.1371/journal.pone.0015710>
- Fetoni, A. R., Picciotti, P. M., Paludetti, G., & Troiani, D. (2011). Pathogenesis of presbycusis in animal models: A review. *Experimental Gerontology*, 46(6), 413–425.  
<https://doi.org/10.1016/j.exger.2010.12.003>
- Fisher, R. A. (1915). Frequency Distribution of the Values of the Correlation Coefficient in Samples from an Indefinitely Large Population.

- Biometrika*, 10(4), 507–521. JSTOR.  
<https://doi.org/10.2307/2331838>
- Forman, S., Cohen, J., Fitzgerald, M., Eddy, W., Mintun, M., & Noll, D. (1995). Improved Assessment of Significant Activation in Functional Magnetic-Resonance-Imaging (fmri)—Use of a Cluster-Size Threshold. *Magnetic Resonance in Medicine*, 33(5), 636–647.  
<https://doi.org/10.1002/mrm.1910330508>
- Formisano, E., Kim, D. S., Di Salle, F., van de Moortele, P. F., Ugurbil, K., & Goebel, R. (2003). Mirror-symmetric tonotopic maps in human primary auditory cortex. *Neuron*, 40(4), 859–869.  
[https://doi.org/10.1016/s0896-6273\(03\)00669-x](https://doi.org/10.1016/s0896-6273(03)00669-x)
- Fortunato, S., Forli, F., Guglielmi, V., De Corso, E., Paludetti, G., Berrettini, S., & Fetoni, A. R. (2016). A review of new insights on the association between hearing loss and cognitive decline in ageing. *Acta Otorhinolaryngologica Italica*, 36(3), 155–166.  
<https://doi.org/10.14639/0392-100X-993>
- Fox, M. D., Corbetta, M., Snyder, A. Z., Vincent, J. L., & Raichle, M. E. (2006). Spontaneous neuronal activity distinguishes human dorsal and ventral attention systems. *Proceedings of the National Academy of Sciences*, 103(26), 10046–10051.  
<https://doi.org/10.1073/pnas.0604187103>
- Fox, M. D., Snyder, A. Z., Vincent, J. L., Corbetta, M., Essen, D. C. V., & Raichle, M. E. (2005). The human brain is intrinsically organized into dynamic, anticorrelated functional networks.

- Proceedings of the National Academy of Sciences*, 102(27), 9673–9678.  
<https://doi.org/10.1073/pnas.0504136102>
- Friston, K. J., Williams, S., Howard, R., Frackowiak, R. S., & Turner, R. (1996). Movement-related effects in fMRI time-series. *Magnetic Resonance in Medicine*, 35(3), 346–355.  
<https://doi.org/10.1002/mrm.1910350312>
- Gao, Y.-Z., Zhang, J.-J., Liu, H., Wu, G.-Y., Xiong, L., & Shu, M. (2013). Regional Cerebral Blood Flow and Cerebrovascular Reactivity in Alzheimer's Disease and Vascular Dementia Assessed by Arterial Spin-labeling Magnetic Resonance Imaging. *Current Neurovascular Research*, 10(1), 49–53.  
<https://doi.org/10.2174/156720213804806016>
- Gardumi, A., Ivanov, D., Havlicek, M., Formisano, E., & Uludag, K. (2017). Tonotopic Maps in Human Auditory Cortex Using Arterial Spin Labeling. *Human Brain Mapping*, 38(3), 1140–1154.  
<https://doi.org/10.1002/hbm.23444>
- Gates, G. A., Gibbons, L. E., McCusry, S. M., Crane, P. K., Feeney, M. P., & Larson, E. B. (2010). Executive Dysfunction and Presbycusis in Older Persons With and Without Memory Loss and Dementia. *Cognitive and Behavioral Neurology*, 23(4), 218–223.  
<https://doi.org/10.1097/WNN.0b013e3181d748d7>

- Gates, G. A., & Mills, J. H. (2005). Presbycusis. *The Lancet*, 366(9491), 1111–1120.  
[https://doi.org/10.1016/S0140-6736\(05\)67423-5](https://doi.org/10.1016/S0140-6736(05)67423-5)
- Goebel, R., Esposito, F., & Formisano, E. (2006). Analysis of Functional Image Analysis Contest (FIAC) data with BrainVoyager QX: From single-subject to cortically aligned group general linear model analysis and self-organizing group independent component analysis. *Human Brain Mapping*, 27(5), 392–401.  
<https://doi.org/10.1002/hbm.20249>
- Golub, J. S. (2017). Brain changes associated with age-related hearing loss. *Current Opinion in Otolaryngology & Head and Neck Surgery*, 25(5), 347–352.  
<https://doi.org/10.1097/MOO.0000000000000387>
- Guglielmi, V., Marra, C., Picciotti, P. M., Masone Iacobucci, G., Giovannini, S., Quaranta, D., Anzivino, R., Paludetti, G., & Conti, G. (2020). Does Hearing Loss in the Elderly Individuals Conform to Impairment of Specific Cognitive Domains? *Journal of Geriatric Psychiatry and Neurology*, 33(4), 231–240.  
<https://doi.org/10.1177/0891988719874117>
- Gussekloo, J., de Craen, A. J. M., Oduber, C., van Boxtel, M. P. J., & Westendorp, R. G. J. (2005). Sensory impairment and cognitive functioning in oldest-old subjects: The Leiden 85+ Study. *The American Journal of Geriatric Psychiatry: Official Journal of the American Association for Geriatric*

- Psychiatry*, 13(9), 781–786.  
<https://doi.org/10.1176/appi.ajgp.13.9.781>
- Hackett, T. A. (2015). Anatomic organization of the auditory cortex. *Handbook of Clinical Neurology*, 129, 27–53. <https://doi.org/10.1016/B978-0-444-62630-1.00002-0>
- Hardy, C. J. D., Marshall, C. R., Golden, H. L., Clark, C. N., Mummery, C. J., Griffiths, T. D., Bamiou, D.-E., & Warren, J. D. (2016). Hearing and dementia. *Journal of Neurology*, 263(11), 2339–2354. <https://doi.org/10.1007/s00415-016-8208-y>
- Howarth, A., & Shone, G. R. (2006). Ageing and the auditory system. *Postgraduate Medical Journal*, 82(965), 166–171.  
<https://doi.org/10.1136/pgmj.2005.039388>
- Huang, Q., & Tang, J. (2010). Age-related hearing loss or presbycusis. *European Archives of Oto-Rhino-Laryngology*, 267(8), 1179–1191.  
<https://doi.org/10.1007/s00405-010-1270-7>
- Husain, F. T., Carpenter-Thompson, J. R., & Schmidt, S. A. (2014). The effect of mild-to-moderate hearing loss on auditory and emotion processing networks. *Frontiers in Systems Neuroscience*, 8, 10. <https://doi.org/10.3389/fnsys.2014.00010>
- Husain, F. T., Medina, R. E., Davis, C. W., Szymko-Bennett, Y., Simonyan, K., Pajor, N. M., & Horwitz, B. (2011). Neuroanatomical changes due to hearing loss and chronic tinnitus: A combined VBM and DTI study. *Brain Research*, 1369, 74–88.  
<https://doi.org/10.1016/j.brainres.2010.10.095>

- Hyams, A. V., Hay-McCutcheon, M., & Scogin, F. (2018). Hearing and quality of life in older adults. *Journal of Clinical Psychology, 74*(10), 1874–1883. <https://doi.org/10.1002/jclp.22648>
- Iadecola, C. (2017). The Neurovascular Unit Coming of Age: A Journey through Neurovascular Coupling in Health and Disease. *Neuron, 96*(1), 17–42. <https://doi.org/10.1016/j.neuron.2017.07.030>
- Irvine, D. R. F., & Rajan, R. (1996). Injury- and use-related plasticity in the primary sensory cortex of adult mammals: Possible relationship to perceptual learning. *Clinical and Experimental Pharmacology and Physiology, 23*(10–11), 939–947. <https://doi.org/10.1111/j.1440-1681.1996.tb01146.x>
- Jayakody, D. M. P., Friedland, P. L., Martins, R. N., & Sohrabi, H. P. (2018). Impact of Aging on the Auditory System and Related Cognitive Functions: A Narrative Review. *FRONTIERS IN NEUROSCIENCE, 12*. <https://doi.org/10.3389/fnins.2018.00125>
- Johnston, M. E., Lu, K., Maldjian, J. A., & Jung, Y. (2015). Multi-TI Arterial Spin Labeling MRI with Variable TR and Bolus Duration for Cerebral Blood Flow and Arterial Transit Time Mapping. *IEEE Transactions on Medical Imaging, 34*(6), 1392–1402. <https://doi.org/10.1109/TMI.2015.2395257>
- Jones, D. R., & Casseday, J. H. (1979). Projections of auditory nerve in the cat as seen by anterograde transport methods. *Neuroscience, 4*(9), 1299–

1313. [https://doi.org/10.1016/0306-4522\(79\)90158-1](https://doi.org/10.1016/0306-4522(79)90158-1)

- Kaas, J. H., & Hackett, T. A. (2000). Subdivisions of auditory cortex and processing streams in primates. *Proceedings of the National Academy of Sciences of the United States of America*, *97*(22), 11793–11799.  
<https://doi.org/10.1073/pnas.97.22.11793>
- Kamigaki, T. (2019). Prefrontal circuit organization for executive control. *Neuroscience Research*, *140*, 23–36.  
<https://doi.org/10.1016/j.neures.2018.08.017>
- Kidd, A. R., & Bao, J. (2012). Recent Advances in the Study of Age-Related Hearing Loss: A Mini-Review. *Gerontology*, *58*(6), 490–496.  
<https://doi.org/10.1159/000338588>
- Kim, J. J., Crespo-Facorro, B., Andreasen, N. C., O’Leary, D. S., Zhang, B. Q., Harris, G., & Magnotta, V. A. (2000). An MRI-based parcellation method for the temporal lobe. *Neuroimage*, *11*(4), 271–288.  
<https://doi.org/10.1006/nimg.2000.0543>
- King, M., Hernandez-Castillo, C. R., Poldrack, R. A., Ivry, R. B., & Diedrichsen, J. (2019). Functional boundaries in the human cerebellum revealed by a multi-domain task battery. *Nature Neuroscience*, *22*(8), 1371–1378.  
<https://doi.org/10.1038/s41593-019-0436-x>
- Koenig, O., Schaette, R., Kempter, R., & Gross, M. (2006). Course of hearing loss and occurrence of

- tinnitus. *Hearing Research*, 221(1–2), 59–64.  
<https://doi.org/10.1016/j.heares.2006.07.007>
- Kramme, J., Gregori, J., Diehl, V., Madai, V. I., von Samson-Himmelstjerna, F. C., Lentschig, M., Sobesky, J., & Guenther, M. (2015). Improving perfusion quantification in arterial spin labeling for delayed arrival times by using optimized acquisition schemes. *Zeitschrift Fur Medizinische Physik*, 25(3), 221–229.  
<https://doi.org/10.1016/j.zemedi.2014.07.003>
- Kurabi, A., Keithley, E. M., Housley, G. D., Ryan, A. F., & Wong, A. C.-Y. (2017). Cellular mechanisms of noise-induced hearing loss. *Hearing Research*, 349, 129–137.  
<https://doi.org/10.1016/j.heares.2016.11.013>
- Lee, K.-Y. (2013). Pathophysiology of age-related hearing loss (peripheral and central). *Korean Journal of Audiology*, 17(2), 45–49.  
<https://doi.org/10.7874/kja.2013.17.2.45>
- Lemieux, L., Salek-Haddadi, A., Lund, T. E., Laufs, H., & Carmichael, D. (2007). Modelling large motion events in fMRI studies of patients with epilepsy. *Magnetic Resonance Imaging*, 25(6), 894–901.  
<https://doi.org/10.1016/j.mri.2007.03.009>
- Lesage, E., Hansen, P. C., & Miall, R. C. (2017). Right Lateral Cerebellum Represents Linguistic Predictability. *Journal of Neuroscience*, 37(26), 6231–6241.  
<https://doi.org/10.1523/JNEUROSCI.3203-16.2017>

- Lin, F. R., Ferrucci, L., An, Y., Goh, J. O., Doshi, J., Metter, E. J., Davatzikos, C., Kraut, M. A., & Resnick, S. M. (2014). Association of hearing impairment with brain volume changes in older adults. *NeuroImage*, *90*, 84–92.  
<https://doi.org/10.1016/j.neuroimage.2013.12.059>
- Lin, Frank R., Thorpe, R., Gordon-Salant, S., & Ferrucci, L. (2011). Hearing Loss Prevalence and Risk Factors Among Older Adults in the United States. *Journals of Gerontology Series A-Biological Sciences and Medical Sciences*, *66*(5), 582–590.  
<https://doi.org/10.1093/gerona/glr002>
- Liu, B., Feng, Y., Yang, M., Chen, J., Li, J., Huang, Z., & Zhang, L. (2015). Functional Connectivity in Patients With Sensorineural Hearing Loss Using Resting-State MRI. *American Journal of Audiology*, *24*(2), 145–152.  
[https://doi.org/10.1044/2015\\_AJA-13-0068](https://doi.org/10.1044/2015_AJA-13-0068)
- Livingston, G., Sommerlad, A., Orgeta, V., Costafreda, S. G., Huntley, J., Ames, D., Ballard, C., Banerjee, S., Burns, A., Cohen-Mansfield, J., Cooper, C., Fox, N., Gitlin, L. N., Howard, R., Kales, H. C., Larson, E. B., Ritchie, K., Rockwood, K., Sampson, E. L., ... Mukadam, N. (2017). Dementia prevention, intervention, and care. *The Lancet*, *390*(10113), 2673–2734.  
[https://doi.org/10.1016/S0140-6736\(17\)31363-6](https://doi.org/10.1016/S0140-6736(17)31363-6)
- Loughrey, D. G., Mihelj, E., & Lawlor, B. A. (2019). Age-related hearing loss associated with altered

- response efficiency and variability on a visual sustained attention task. *Neuropsychology, Development, and Cognition. Section B, Aging, Neuropsychology and Cognition*, 1–25.  
<https://doi.org/10.1080/13825585.2019.1704393>
- Luan, Y., Wang, C., Jiao, Y., Tang, T., Zhang, J., & Teng, G.-J. (2019). Dysconnectivity of Multiple Resting-State Networks Associated With Higher-Order Functions in Sensorineural Hearing Loss. *Frontiers in Neuroscience*, 13, 55.  
<https://doi.org/10.3389/fnins.2019.00055>
- Mahmoudi, E., Basu, T., Langa, K., McKee, M. M., Zazove, P., Alexander, N., & Kamdar, N. (2019). Can Hearing Aids Delay Time to Diagnosis of Dementia, Depression, or Falls in Older Adults? *Journal of the American Geriatrics Society*, 67(11), 2362–2369.  
<https://doi.org/10.1111/jgs.16109>
- Mak, L. E., Minuzzi, L., MacQueen, G., Hall, G., Kennedy, S. H., & Milev, R. (2017). The Default Mode Network in Healthy Individuals: A Systematic Review and Meta-Analysis. *Brain Connectivity*, 7(1), 25–33.  
<https://doi.org/10.1089/brain.2016.0438>
- Mangold, S. A., & M Das, J. (2020). Neuroanatomy, Cortical Primary Auditory Area. In *StatPearls*. StatPearls Publishing.  
<http://www.ncbi.nlm.nih.gov/books/NBK554521/>
- Merten, N., Fischer, M. E., Tweed, T. S., Breteler, M. M. B., & Cruickshanks, K. J. (2020). Associations of Hearing Sensitivity, Higher-Order Auditory

- Processing, and Cognition Over Time in Middle-Aged Adults. *The Journals of Gerontology. Series A, Biological Sciences and Medical Sciences*, 75(3), 545–551.  
<https://doi.org/10.1093/gerona/glz189>
- Michels, T. C., Duffy, M. T., & Rogers, D. J. (2019). Hearing Loss in Adults: Differential Diagnosis and Treatment. *American Family Physician*, 100(2), 98–108.
- Moeller, S., Yacoub, E., Olman, C. A., Auerbach, E., Strupp, J., Harel, N., & Uğurbil, K. (2010). Multiband multislice GE-EPI at 7 tesla, with 16-fold acceleration using partial parallel imaging with application to high spatial and temporal whole-brain fMRI. *Magnetic Resonance in Medicine*, 63(5), 1144–1153.  
<https://doi.org/10.1002/mrm.22361>
- Mulrow, C.D., Tuley, M. R., & Aguilar, C. (1992). Sustained Benefits of Hearing Aids. *Journal of Speech, Language, and Hearing Research*, 35(6), 1402–1405.  
<https://doi.org/10.1044/jshr.3506.1402>
- Mulrow, Cynthia D., Aguilar, C., Endicott, J. E., Tuley, M. R., Velez, R., Charlip, W. S., Rhodes, M. C., Hill, J. A., & DeNino, L. A. (1990). Quality-of-Life Changes and Hearing Impairment. *Annals of Internal Medicine*, 113(3), 188–194.  
<https://doi.org/10.7326/0003-4819-113-3-188>
- Musiek, F. E. (1986). Neuroanatomy, neurophysiology, and central auditory assessment. Part II: The cerebrum. *Ear and Hearing*, 7(5), 283–294.

<https://doi.org/10.1097/00003446-198610000-00001>

- Mutsaerts, H. J. M. M., van Dalen, J. W., Heijtel, D. F. R., Groot, P. F. C., Majoie, C. B. L. M., Petersen, E. T., Richard, E., & Nederveen, A. J. (2015). Cerebral Perfusion Measurements in Elderly with Hypertension Using Arterial Spin Labeling. *Plos One*, *10*(8), e0133717.  
<https://doi.org/10.1371/journal.pone.0133717>
- Nakamura, K., Dehaene, S., Jobert, A., Le Bihan, D., & Kouider, S. (2005). Subliminal convergence of Kanji and Kana words: Further evidence for functional parcellation of the posterior temporal cortex in visual word perception. *Journal of Cognitive Neuroscience*, *17*(6), 954–968.  
<https://doi.org/10.1162/0898929054021166>
- Nasreddine, Z. S., Phillips, N. A., Bedirian, V., Charbonneau, S., Whitehead, V., Collin, I., Cummings, J. L., & Chertkow, H. (2005). The montreal cognitive assessment, MoCA: A brief screening tool for mild cognitive impairment. *Journal of the American Geriatrics Society*, *53*(4), 695–699. <https://doi.org/10.1111/j.1532-5415.2005.53221.x>
- Naumer, M. J., Doehrmann, O., Müller, N. G., Muckli, L., Kaiser, J., & Hein, G. (2009). Cortical plasticity of audio-visual object representations. *Cerebral Cortex (New York, N.Y.: 1991)*, *19*(7), 1641–1653. <https://doi.org/10.1093/cercor/bhn200>
- Owen, A. M. (2000). The role of the lateral frontal cortex in mnemonic processing: The contribution of

- functional neuroimaging. *Experimental Brain Research*, 133(1), 33–43.  
<https://doi.org/10.1007/s002210000398>
- Owen, A. M., Stern, C. E., Look, R. B., Tracey, I., Rosen, B. R., & Petrides, M. (1998). Functional organization of spatial and nonspatial working memory processing within the human lateral frontal cortex. *Proceedings of the National Academy of Sciences*, 95(13), 7721–7726.  
<https://doi.org/10.1073/pnas.95.13.7721>
- Peelle, J. E., Troiani, V., Grossman, M., & Wingfield, A. (2011). Hearing loss in older adults affects neural systems supporting speech comprehension. *The Journal of Neuroscience: The Official Journal of the Society for Neuroscience*, 31(35), 12638–12643.  
<https://doi.org/10.1523/JNEUROSCI.2559-11.2011>
- Pereira-Jorge, M. R., Andrade, K. C., Palhano-Fontes, F. X., Diniz, P. R. B., Sturzbecher, M., Santos, A. C., & Araujo, D. B. (2018). *Anatomical and Functional MRI Changes after One Year of Auditory Rehabilitation with Hearing Aids* [Research Article]. *Neural Plasticity*; Hindawi.  
<https://doi.org/10.1155/2018/9303674>
- Petrides, M. (2000). Dissociable roles of mid-dorsolateral prefrontal and anterior inferotemporal cortex in visual working memory. *The Journal of Neuroscience: The Official Journal of the Society for Neuroscience*, 20(19), 7496–7503.

- Pichora-Fuller, M. K., & Singh, G. (2006). Effects of age on auditory and cognitive processing: Implications for hearing aid fitting and audiologic rehabilitation. *Trends in Amplification, 10*(1), 29–59.  
<https://doi.org/10.1177/108471380601000103>
- Polku, H., Mikkola, T. M., Rantakokko, M., Portegijs, E., Törmäkangas, T., Rantanen, T., & Viljanen, A. (2018). Hearing and Quality of Life Among Community-Dwelling Older Adults. *The Journals of Gerontology. Series B, Psychological Sciences and Social Sciences, 73*(3), 543–552.  
<https://doi.org/10.1093/geronb/gbw045>
- Ponticorvo, S., Manara, R., Pfeuffer, J., Cappiello, A., Cuoco, S., Pellecchia, M. T., Saponiero, R., Troisi, D., Cassandro, C., John, M., Scarpa, A., Cassandro, E., Di Salle, F., & Esposito, F. (2019). Cortical pattern of reduced perfusion in hearing loss revealed by ASL-MRI. *Human Brain Mapping, 40*(8), 2475–2487.  
<https://doi.org/10.1002/hbm.24538>
- Profant, O., Tintěra, J., Balogová, Z., Ibrahim, I., Jilek, M., & Syka, J. (2015). Functional changes in the human auditory cortex in ageing. *PloS One, 10*(3), e0116692.  
<https://doi.org/10.1371/journal.pone.0116692>
- Puschmann, S., & Thiel, C. M. (2016). Changed crossmodal functional connectivity in older adults with hearing loss. *Cortex; a Journal Devoted to the Study of the Nervous System and Behavior,*

86, 109–122.

<https://doi.org/10.1016/j.cortex.2016.10.014>

Qi, R., Su, L., Zou, L., Yang, J., & Zheng, S. (2019). Altered Gray Matter Volume and White Matter Integrity in Sensorineural Hearing Loss Patients: A VBM and TBSS Study. *Otology & Neurotology: Official Publication of the American Otological Society, American Neurotology Society [and] European Academy of Otology and Neurotology*, 40(6), e569–e574.

<https://doi.org/10.1097/MAO.0000000000002273>

Quaranta, N., Coppola, F., Casulli, M., Barulli, M. R., Barulli, O., Panza, F., Lanza, F., Tortelli, R., Capozzo, R., Leo, A., Tursi, M., Grasso, A., Solfrizzi, V., Sobbà, C., & Logroscino, G. (2014). The prevalence of peripheral and central hearing impairment and its relation to cognition in older adults. *Audiology & Neuro-Otology*, 19 Suppl 1, 10–14. <https://doi.org/10.1159/000371597>

Radakovic, R., & Abrahams, S. (2014). Developing a new apathy measurement scale: Dimensional Apathy Scale. *Psychiatry Research*, 219(3), 658–663.

<https://doi.org/10.1016/j.psychres.2014.06.010>

Raichle, M. E., MacLeod, A. M., Snyder, A. Z., Powers, W. J., Gusnard, D. A., & Shulman, G. L. (2001). A default mode of brain function. *Proceedings of the National Academy of Sciences*, 98(2), 676–682. <https://doi.org/10.1073/pnas.98.2.676>

Rajan, R., Irvine, D., Wise, L., & Heil, P. (1993). Effect of Unilateral Partial Cochlear Lesions in Adult Cats

- on the Representation of Lesioned and Unlesioned Cochleas in Primary Auditory-Cortex. *Journal of Comparative Neurology*, 338(1), 17–49. <https://doi.org/10.1002/cne.903380104>
- Ramadan, H. H., & Schuknecht, H. F. (1989). Is there a conductive type of presbycusis? *Otolaryngology-Head and Neck Surgery: Official Journal of American Academy of Otolaryngology-Head and Neck Surgery*, 100(1), 30–34. <https://doi.org/10.1177/019459988910000105>
- Ren, F., Luo, J., Ma, W., Xin, Q., Xu, L., Fan, Z., Ai, Y., Zhao, B., Gao, F., & Wang, H. (2019). Hearing Loss and Cognition Among Older Adults in a Han Chinese Cohort. *Frontiers in Neuroscience*, 13. <https://doi.org/10.3389/fnins.2019.00632>
- Ren, F., Ma, W., Li, M., Sun, H., Xin, Q., Zong, W., Chen, W., Wang, G., Gao, F., & Zhao, B. (2018). Gray Matter Atrophy Is Associated With Cognitive Impairment in Patients With Presbycusis: A Comprehensive Morphometric Study. *Frontiers in Neuroscience*, 12. <https://doi.org/10.3389/fnins.2018.00744>
- Rönnerberg, J., Danielsson, H., Rudner, M., Arlinger, S., Sternäng, O., Wahlin, A., & Nilsson, L.-G. (2011). Hearing loss is negatively related to episodic and semantic long-term memory but not to short-term memory. *Journal of Speech, Language, and Hearing Research: JSLHR*, 54(2), 705–726. [https://doi.org/10.1044/1092-4388\(2010/09-0088\)](https://doi.org/10.1044/1092-4388(2010/09-0088))

- Rönnerberg, J., Hygge, S., Keidser, G., & Rudner, M. (2014). The effect of functional hearing loss and age on long- and short-term visuospatial memory: Evidence from the UK biobank resource. *Frontiers in Aging Neuroscience*, *6*, 326. <https://doi.org/10.3389/fnagi.2014.00326>
- Rosemann, S., & Thiel, C. M. (2019). The effect of age-related hearing loss and listening effort on resting state connectivity. *Scientific Reports*, *9*. <https://doi.org/10.1038/s41598-019-38816-z>
- Rutherford, B. R., Brewster, K., Golub, J. S., Kim, A. H., & Roose, S. P. (2018). Sensation and psychiatry: Linking age-related hearing loss to late-life depression and cognitive decline. *American Journal of Psychiatry*, *175*(3), 215–224. Scopus. <https://doi.org/10.1176/appi.ajp.2017.17040423>
- Santangelo, G., Siciliano, M., Pedone, R., Vitale, C., Falco, F., Bisogno, R., Siano, P., Barone, P., Grossi, D., Santangelo, F., & Trojano, L. (2015, April). *Normative data for the Montreal Cognitive Assessment in an Italian population sample*. *Neurological Sciences : Official Journal of the Italian Neurological Society and of the Italian Society of Clinical Neurophysiology*; *Neurol Sci*. <https://doi.org/10.1007/s10072-014-1995-y>
- Sarant, J., Harris, D., Busby, P., Maruff, P., Schembri, A., Lemke, U., & Launer, S. (2020). The Effect of Hearing Aid Use on Cognition in Older Adults: Can We Delay Decline or Even Improve Cognitive Function? *Journal of Clinical Medicine*, *9*(1), 254. <https://doi.org/10.3390/jcm9010254>

- Satterthwaite, T. D., Elliott, M. A., Gerraty, R. T., Ruparel, K., Loughead, J., Calkins, M. E., Eickhoff, S. B., Hakonarson, H., Gur, R. C., Gur, R. E., & Wolf, D. H. (2013). An improved framework for confound regression and filtering for control of motion artifact in the preprocessing of resting-state functional connectivity data. *NeuroImage*, *64*, 240–256.  
<https://doi.org/10.1016/j.neuroimage.2012.08.052>
- Saunders, G. H., Odgear, I., Cosgrove, A., & Frederick, M. T. (2018). Impact of Hearing Loss and Amplification on Performance on a Cognitive Screening Test. *Journal of the American Academy of Audiology*, *29*(7), 648–655.  
<https://doi.org/10.3766/jaaa.17044>
- Schecklmann, M., Vielsmeier, V., Steffens, T., Landgrebe, M., Langguth, B., & Kleinjung, T. (2012). Relationship between Audiometric Slope and Tinnitus Pitch in Tinnitus Patients: Insights into the Mechanisms of Tinnitus Generation. *Plos One*, *7*(4), e34878.  
<https://doi.org/10.1371/journal.pone.0034878>
- Schmidt, S. A., Akrofi, K., Carpenter-Thompson, J. R., & Husain, F. T. (2013). Default mode, dorsal attention and auditory resting state networks exhibit differential functional connectivity in tinnitus and hearing loss. *PloS One*, *8*(10), e76488.  
<https://doi.org/10.1371/journal.pone.0076488>

- Schonwiesner, M., Rubsamen, R., & von Cramon, D. Y. (2005). Hemispheric asymmetry for spectral and temporal processing in the human antero-lateral auditory belt cortex. *European Journal of Neuroscience*, 22(6), 1521–1528.  
<https://doi.org/10.1111/j.1460-9568.2005.04315.x>
- Schuknecht, H. F. (1955). Presbycusis. *The Laryngoscope*, 65(6), 402–419.  
<https://doi.org/10.1288/00005537-195506000-00002>
- Schuknecht, H. F. (1964). FURTHER OBSERVATIONS ON THE PATHOLOGY OF PRESBYCUSIS. *Archives of Otolaryngology (Chicago, Ill.: 1960)*, 80, 369–382.  
<https://doi.org/10.1001/archotol.1964.00750040381003>
- Schuknecht, H. F., & Gacek, M. R. (1993). Cochlear pathology in presbycusis. *The Annals of Otology, Rhinology, and Laryngology*, 102(1 Pt 2), 1–16.  
<https://doi.org/10.1177/00034894931020S101>
- Schuknecht, Harold F. (1993). *Pathology of the Ear*. Lea & Febiger.
- Seifritz, E., Di Salle, F., Esposito, F., Herdener, M., Neuhoff, J. G., & Scheffler, K. (2006). Enhancing BOLD response in the auditory system by neurophysiologically tuned fMRI sequence. *Neuroimage*, 29(3), 1013–1022.  
<https://doi.org/10.1016/j.neuroimage.2005.08.029>

- Shahidipour, Z., Geshani, A., Jafari, Z., Jalaie, S., & Khosravifard, E. (2013). Auditory Memory deficit in Elderly People with Hearing Loss. *Iranian Journal of Otorhinolaryngology*, *25*(72), 169–176.
- Sininger, Y. S., & de Bode, S. (2008). Asymmetry of temporal processing in listeners with normal hearing and unilaterally deaf subjects. *Ear and Hearing*, *29*(2), 228–238.  
<https://doi.org/10.1097/AUD.0b013e318164537b>
- Sliwiska-Kowalska, M. (2015). Hearing. *Handbook of Clinical Neurology*, *131*, 341–363.  
<https://doi.org/10.1016/B978-0-444-62627-1.00018-4>
- Smith, S. M., Fox, P. T., Miller, K. L., Glahn, D. C., Fox, P. M., Mackay, C. E., Filippini, N., Watkins, K. E., Toro, R., Laird, A. R., & Beckmann, C. F. (2009). Correspondence of the brain's functional architecture during activation and rest. *Proceedings of the National Academy of Sciences*, *106*(31), 13040–13045.  
<https://doi.org/10.1073/pnas.0905267106>
- Smith, S. M., Jenkinson, M., Woolrich, M. W., Beckmann, C. F., Behrens, T. E. J., Johansen-Berg, H., Bannister, P. R., De Luca, M., Drobnjak, I., Flitney, D. E., Niazy, R. K., Saunders, J., Vickers, J., Zhang, Y., De Stefano, N., Brady, J. M., & Matthews, P. M. (2004). Advances in functional and structural MR image analysis and implementation as FSL. *NeuroImage*, *23*, S208–S219.

<https://doi.org/10.1016/j.neuroimage.2004.07.05>

1

- Taljaard, D. S., Olaithe, M., Brennan-Jones, C. G., Eikelboom, R. H., & Bucks, R. S. (2016). The relationship between hearing impairment and cognitive function: A meta-analysis in adults. *Clinical Otolaryngology: Official Journal of ENT-UK; Official Journal of Netherlands Society for Oto-Rhino-Laryngology & Cervico-Facial Surgery*, *41*(6), 718–729.  
<https://doi.org/10.1111/coa.12607>
- Tay, T., Wang, J. J., Kifley, A., Lindley, R., Newall, P., & Mitchell, P. (2006). Sensory and cognitive association in older persons: Findings from an older Australian population. *Gerontology*, *52*(6), 386–394. <https://doi.org/10.1159/000095129>
- Telischak, N. A., Detre, J. A., & Zaharchuk, G. (2015). Arterial Spin Labeling MRI: Clinical Applications in the Brain. *Journal of Magnetic Resonance Imaging*, *41*(5), 1165–1180.  
<https://doi.org/10.1002/jmri.24751>
- Trumpp, N. M., & Kiefer, M. (2018). Functional reorganization of the conceptual brain system after deafness in early childhood. *PLoS ONE*, *13*(7).  
<https://doi.org/10.1371/journal.pone.0198894>
- Tun, P. A., McCoy, S., & Wingfield, A. (2009). Aging, hearing acuity, and the attentional costs of effortful listening. *Psychology and Aging*, *24*(3), 761–766. <https://doi.org/10.1037/a0014802>

- Tzourio-Mazoyer, N., Landeau, B., Papathanassiou, D., Crivello, F., Etard, O., Delcroix, N., Mazoyer, B., & Joliot, M. (2002). Automated anatomical labeling of activations in SPM using a macroscopic anatomical parcellation of the MNI MRI single-subject brain. *Neuroimage*, *15*(1), 273–289.  
<https://doi.org/10.1006/nimg.2001.0978>
- Uchida, Y., Sugiura, S., Nishita, Y., Saji, N., Sone, M., & Ueda, H. (2019). Age-related hearing loss and cognitive decline—The potential mechanisms linking the two. *Auris Nasus Larynx*, *46*(1), 1–9.  
<https://doi.org/10.1016/j.anl.2018.08.010>
- Valentijn, S. A. M., van Boxtel, M. P. J., van Hooren, S. A. H., Bosma, H., Beckers, H. J. M., Ponds, R. W. H. M., & Jolles, J. (2005). Change in sensory functioning predicts change in cognitive functioning: Results from a 6-year follow-up in the maastricht aging study. *Journal of the American Geriatrics Society*, *53*(3), 374–380.  
<https://doi.org/10.1111/j.1532-5415.2005.53152.x>
- Vemuri, P., Lesnick, T. G., Przybelski, S. A., Graff-Radford, J., Reid, R. I., Lowe, V. J., Zuk, S. M., Senjem, M. L., Schwarz, C. G., Gunter, J. L., Kantarci, K., Machulda, M. M., Mielke, M. M., Petersen, R. C., Knopman, D. S., & Jack, C. R. (2018). Development of a cerebrovascular magnetic resonance imaging biomarker for cognitive aging. *Annals of Neurology*, *84*(5), 705–716. <https://doi.org/10.1002/ana.25346>

- Verfaillie, S. C. J., Adriaanse, S. M., Binnewijzend, M. A. A., Benedictus, M. R., Ossenkuppele, R., Wattjes, M. P., Pijnenburg, Y. A. L., van der Flier, W. M., Lammertsma, A. A., Kuijer, J. P. A., Boellaard, R., Scheltens, P., van Berckel, B. N. M., & Barkhof, F. (2015). Cerebral perfusion and glucose metabolism in Alzheimer's disease and frontotemporal dementia: Two sides of the same coin? *European Radiology*, *25*(10), 3050–3059. <https://doi.org/10.1007/s00330-015-3696-1>
- Verger, A., Roman, S., Chaudat, R.-M., Felician, O., Ceccaldi, M., Didic, M., & Guedj, E. (2017). Changes of metabolism and functional connectivity in late-onset deafness: Evidence from cerebral F-18-FDG-PET. *Hearing Research*, *353*, 8–16. <https://doi.org/10.1016/j.heares.2017.07.011>
- Vidorreta, M., Wang, Z., Rodriguez, I., Pastor, M. A., Detre, J. A., & Fernandez-Seara, M. A. (2013). Comparison of 2D and 3D single-shot ASL perfusion fMRI sequences. *Neuroimage*, *66*, 662–671. <https://doi.org/10.1016/j.neuroimage.2012.10.087>
- Vuorialho, A., Karinen, P., & Sorri, M. (2006). Effect of hearing aids on hearing disability and quality of life in the elderly: Efecto de los auxiliares auditivos (AA) en la discapacidad auditiva y la calidad de vida de los ancianos. *International Journal of Audiology*, *45*(7), 400–405. <https://doi.org/10.1080/14992020600625007>

- Wang, X., Fan, Y., Zhao, F., Wang, Z., Ge, J., Zhang, K., Gao, Z., Gao, J.-H., Yang, Y., Fan, J., Zou, Q., & Liu, P. (2014). Altered Regional and Circuit Resting-State Activity Associated with Unilateral Hearing Loss. *PLOS ONE*, *9*(5), e96126. <https://doi.org/10.1371/journal.pone.0096126>
- Wolak, T., Ciesla, K., Lorens, A., Kochanek, K., Lewandowska, M., Rusiniak, M., Pluta, A., Wojcik, J., & Skarzynski, H. (2017). Tonotopic organisation of the auditory cortex in sloping sensorineural hearing loss. *Hearing Research*, *355*, 81–96. <https://doi.org/10.1016/j.heares.2017.09.012>
- Wolak, T., Cieśła, K., Pluta, A., Włodarczyk, E., Biswal, B., & Skarżyński, H. (2019). Altered Functional Connectivity in Patients With Sloping Sensorineural Hearing Loss. *Frontiers in Human Neuroscience*, *13*, 284. <https://doi.org/10.3389/fnhum.2019.00284>
- Wong, L. L. N., Yu, J. K. Y., Chan, S. S., & Tong, M. C. F. (2014). Screening of cognitive function and hearing impairment in older adults: A preliminary study. *BioMed Research International*, *2014*, 867852. <https://doi.org/10.1155/2014/867852>
- Wu, W.-C., Fernandez-Seara, M., Detre, J. A., Wehrli, F. W., & Wang, J. (2007). A theoretical and experimental investigation of the tagging efficiency of pseudocontinuous arterial spin labeling. *Magnetic Resonance in Medicine*, *58*(5), 1020–1027. <https://doi.org/10.1002/mrm.21403>

- Xu, J., Moeller, S., Auerbach, E. J., Strupp, J., Smith, S. M., Feinberg, D. A., Yacoub, E., & Uğurbil, K. (2013). Evaluation of slice accelerations using multiband echo planar imaging at 3T. *NeuroImage*, *83*, 991–1001. <https://doi.org/10.1016/j.neuroimage.2013.07.055>
- Xu, X.-M., Jiao, Y., Tang, T.-Y., Lu, C.-Q., Zhang, J., Salvi, R., & Teng, G.-J. (2019). Altered Spatial and Temporal Brain Connectivity in the Salience Network of Sensorineural Hearing Loss and Tinnitus. *Frontiers in Neuroscience*, *13*. <https://doi.org/10.3389/fnins.2019.00246>
- Xu, X.-M., Jiao, Y., Tang, T.-Y., Zhang, J., Lu, C.-Q., Luan, Y., Salvi, R., & Teng, G.-J. (2019). Dissociation between Cerebellar and Cerebral Neural Activities in Humans with Long-Term Bilateral Sensorineural Hearing Loss. *Neural Plasticity*, *2019*, 8354849. <https://doi.org/10.1155/2019/8354849>
- Young, E. D., & Oertel, D. (2004). Cochlear Nucleus. The Synaptic Organisation of the Brain. In *The Synaptic Organization of the Brain*. Oxford University Press. <https://jhu.pure.elsevier.com/en/publications/cochlear-nucleus-4>
- Zatorre, R. J., Belin, P., & Penhune, V. B. (2002). Structure and function of auditory cortex: Music and speech. *Trends in Cognitive Sciences*, *6*(1), 37–46. [https://doi.org/10.1016/S1364-6613\(00\)01816-7](https://doi.org/10.1016/S1364-6613(00)01816-7)

- Zhang, J., Chen, Y.-C., Feng, X., Yang, M., Liu, B., Qian, C., Wang, J., Salvi, R., & Teng, G.-J. (2015). Impairments of thalamic resting-state functional connectivity in patients with chronic tinnitus. *European Journal of Radiology*, *84*(7), 1277–1284.  
<https://doi.org/10.1016/j.ejrad.2015.04.006>
- Zhao, M. Y., Mezue, M., Segerdahl, A. R., Okell, T. W., Tracey, I., Xiao, Y., & Chappell, M. A. (2017). A systematic study of the sensitivity of partial volume correction methods for the quantification of perfusion from pseudo-continuous arterial spin labeling MRI. *Neuroimage*, *162*, 384–397.  
<https://doi.org/10.1016/j.neuroimage.2017.08.072>
- Zhu, H., Zhou, P., Alcauter, S., Chen, Y., Cao, H., Tian, M., Ming, D., Qi, H., Wang, X., Zhao, X., He, F., Ni, H., & Gao, W. (2016). Changes of intranetwork and internetwork functional connectivity in Alzheimer's disease and mild cognitive impairment. *Journal of Neural Engineering*, *13*(4), 046008.  
<https://doi.org/10.1088/1741-2560/13/4/046008>

# Akwnowledgement

Un ringraziamento speciale a chi tra tutte le persone incrociate per brevi e lunghi periodi, ha lasciato un segno e mi ha aiutato a proseguire.

Prima di tutti, il Professore Fabrizio Esposito, che mi ha insegnato tutto quello che so, e mi ha accompagnato e guidato. Lo ringrazio per aver sempre sostenuto il mio lavoro e per aver creduto in me. Ringrazio il Prof. Francesco di Salle, per aver supportato lo sviluppo di questo progetto nella sua integrità. Allo stesso modo ringrazio il Prof. Renzo Manara, per aver condiviso con me le sue conoscenze, e i lunghi pomeriggi in risonanza, e per i numerosi scambi di idee fondamentali per la mia crescita.

Ringrazio poi Anto, che mi ha affiancato lungo tutto il percorso, come guida professionale e in cui ho trovato un'amica, che anche quando un oceano ci separava mi ha aiutato e sostenuto. Ringrazio Andrea, che mi ha supportato nei momenti di eccessivo sconforto o eccessiva eccitazione. Ringrazio Silvia e Shalom che mi hanno accolto nella loro famiglia professionale e personale, e che spero di rincontrare presto.

Ringrazio la mia grande famiglia, mio fratello e Monika per avermi sempre supportato e la mia nonna che è tanto orgogliosa di me.

Infine, il ringraziamento più importante va ai miei genitori. In un percorso così lungo e faticoso, ricco di momenti di sconforto e difficoltà, non avrei potuto sperare in un

supporto migliore che quello che mi hanno dato loro, la mia mamma e il mio papà. Loro mi hanno insegnato a credere in me e ad essere libera, e senza di loro tutto questo lavoro (e questi anni) non sarebbero mai stati possibili.

Sara